Western Graduate&PostdoctoralStudies

12-10-2014 12:00 AM

Treatment of Synthetic Oil Sands Tailing Water with Activated Carbon

Alfredo Martinez Iglesias, *The University of Western Ontario*

Supervisor: Dr Madhumita Ray, *The University of Western Ontario*
A thesis submitted in partial fulfillment of the requirements for the Master of Engineering
Science degree in Chemical and Biochemical Engineering
© Alfredo Martinez Iglesias 2014

Recommended Citation

TREATMENT OF SYNTHETIC OIL SANDS TAILING WATER WITH ACTIVATED CARBON

(Thesis format: Monograph)

By

Alfredo <u>Martinez-Iglesias</u>

Graduate Program in Chemical and Biochemical Engineering

A thesis submitted in partial fulfillment
of the requirements for the degree of
Masters of Engineering Science

The School of Graduate and Postdoctoral Studies
The University of Western Ontario
London, Ontario, Canada

Abstract

The extraction of bitumen from the Canadian tar sands has thus far generated approximately 840 billion liters of oil sands process affected water (OSPW) that is currently being stored in containment ponds. OSPW is known to be acutely toxic to various organisms, due to the presence of naphthenic acids (NAs). The scale and sheer volume of OSPW being stored in tailing ponds have generated serious public concerns. Many emerging technologies have been investigated as treatment options for OSPW reclamation. This work studied the feasibility of using granular activated carbon (GAC) to adsorb several naphthenic acids in a model solution of OSPW in a batch adsorption process. The effect of process pH on both competitive and single solute adsorption was studied at equilibrium (i.e. isotherms) and transient conditions (i.e. kinetics). The adsorption results for the multi-component solution were compared to those for single compound adsorption. The model compounds selected for this work were 1,4-cylochexanedicarboxylic acid, 2-naphthoic acid, and diphenylacetic acid. GAC showed good adsorption capacity for all three model compounds and the adsorption was significantly affected by the solution pH. Maximum adsorption occurred at pH 4, and adsorption decreased with increasing pH. For multi-component adsorption it was found that at pH 8 the overall capacity increased and the time constant decreased as compared to the single compound results. Additionally it was found that 1,4-cyclohexanedicarboxylic acid exhibited cooperative adsorption, adhering to an S-class isotherm profile. The other two model compounds demonstrated conventional isotherm profiles, either L or H-class. It was found that cooperative adsorption could be hindered in multi-component adsorption due to solute competition. This was observed at all pH investigated other than pH 8 and 9. This finding is promising, as the pH range in which cooperative adsorption took place corresponds to the tailing water pH. The point of zero charge was found to be a significant factor; as the pH of the system approached the pH_{pzc} the adsorbent performance decreased. The findings of this work show promising results regarding the use of GAC for naphthenic acids removal from water.

Keywords
Naphthenic acids, model compounds, oil sand process affected water, tailing ponds, tailings, tar sands, adsorption, kinetics, isotherms, granular activated carbon, activated carbon.

Acknowledgments

I would like to thank Dr. Madhumita B. Ray and Dr. Chunbao Xu for their gracious support, patience and guidance throughout the course of my thesis.

Thank you to Hojatallah Seyedy Niasar, who worked closely with me on this project, helping me to discuss and think through the work. Thanks to Clayton Stanlick for his technical help, encouragement and late night discussions. A special thanks to Cristina Banu for her patience and willingness to lend an open ear to my frustrations and provide valuable feedback.

Nothing is achieved or created in isolation. The notion of taking sole credit for ones thoughts and behaviour ignores this principle. Like scientific knowledge, human development is a collective process that evolves. So I thank all those who have been a part of my life and as such have shaped my thoughts and behaviour.

Table of Contents

Abbreviations

ACN	acetonitrile
AEOSTO	acid extractable oil sand tailing organics
CLA	composite liquid adsorption
CSS	cycle steam stimulation
CT	composite tailings
ERCB	Alberta energy resources conservation board
FFT	fluid fine tailings
GAC	granular activated carbon
HPLC	high performance liquid chromatography
MFT	mature fine tailings
MW	molecular weight
NA	naphthenic acid
NAFC	naphthenic acid fraction compounds
NOM	naturally occurring organic mater
NORMS	naturally occurring radioactive minerals
NST	non-segregating tailings
OSPW	oil sands process affected water
OSTWAEO	oil sands tailings water acid-extractable organics
PAH	polycyclic aromatic hydrocarbon
PFO	pseudo-first order
PH$_{pzc}$	pH resulting in the point of zero charge
PSO	pseudo-second order
PTFE	polytetrafluoroethylene
pzc	point of zero charge
SAGD	steam assisted gravity drainage
SSA	solid solute adsorption
TDS	total disolved solids
TOC	total organic carbon
VAPEX	vapor extraction process
VPA	vapor or gas phase adsorption

List of Symbols

a_i	single-component liquid-phase adsorption isotherm parameters of the i_{th} adsorbate
b	adsorption affinity coefficient
b_i	single-component liquid-phase adsorption isotherm parameters of the i_{th} adsorbate
C	bulk concentration of the adsorbate within the liquid system
c_i	concentration of the i_{th} adsorbate in the solution
C_o	initial solute concentration
C_e	equilibrium solute concentration
k_d	desorption rate constant
K_f	Freundlich constant
k_2	pseudo-second-order rate constant of sorption
m	adsorbent mass
n	nonlinear index
q	amount of adsorbate per unit mass of adsorbent
q_e	equilibrium adsorption capacity
q_m	maximum adsorption capacity
q_o	amount of adsorbate initially retained by adsorbent
q_t	mass of adsorbate per unit mass of adsorbent at time t
R_L	separation factor
R^2	coefficient of determination
SSE	sum of the square error
SS_{yy}	total variation in y
T	temperature
t_{50}	half time
t	time
τ	time constant
θ	surface coverage fraction
V	volume of solution
v_d	desorption rate
χ^2	nonlinear chi-square test

Table of Figures

List of Tables

Chapter 1: Introduction

1.1 Background and Motivation

The global demand for energy has more than doubled since the 1980s. The increased price of fossil fuels has led to the utilization of once prohibitively expensive fossil fuel deposits including: deep sea oil and gas, shale, and tar sand deposits. The development of these unconventional fossil fuel sources has turned Canada into the country with the third largest oil reserves in the world; with 173 billion barrels of oil that are presently economically viable for production. The Canadian tar, or oil sand deposits, constitute approximately 97% of Canada's total reserves [1]. Tar sand deposits, including uneconomical sources, represent a potential reserve of 1.7 to 2.5 trillion barrels of crude oil [2].

The extraction of bitumen from the Canadian tar sands has thus far generated approximately 840 billion liters of oil sands process affected water (OSPW), currently being stored in tailing ponds that cover around 170 km^2; an area larger than the city of Vancouver [3]. OSPW has been found to be acutely toxic to various organisms, due to the presence of polycyclic aromatic hydrocarbons (PAHs), naphthenic acids (NAs), naturally occurring radioactive minerals (NORMS), and other pollutants [4]. Additionally, these ponds release various volatile contaminants into the environment [5]. Methane, a strong greenhouse gas, can be released during the degradation of hydrocarbon in OSPW [6]. The daily methane flux from tailing pond surfaces has been estimated to be approximately 17 L (at STP)/m^2 [7]. Under the assumption that a cow releases 200 L CH_4/day, and using 170 km^2 surface area, the ponds would represent 14.45 million heads of cattle, more cattle than is currently present in Canada. Methane causes 21 times as much warming as an equivalent amount of CO_2 [8]. The tailing ponds thus pose a serious environmental challenge with the continued risk of leaching or spilling into ground water and nearby waterways.

1.1.1. Oil Sands Overview

The tar sands, predominantly located in the province of Alberta, Canada, are spread across approximately 142 thousand square kilometers. Major deposits are found in the regions of: Athabasca, Cold Lake, and Peace River. The deposits vary in depth, with approximately 20 % being close enough to the surface for open-pit mining operations. The remaining 80 %, being too deep for mining, are exploited using *in-situ* techniques [3]. Current bitumen production is dominated by open pit mining, which accounts for 65 % of the total, with the remainder being produced from in-situ operations 35 % [9]. Open pit mining boasts a 87-90+ % recovery rate for bitumen from sand [9]. The tar sands are a mixture of bitumen and water embedded within sand and clay. By mass, the tar sand are primarily composed of: 74 – 76% quartz and silt sand [10]; 0 – 19% bitumen (12% on average) [10], [11]; 10% inter-bedded clay layers [10]; 3 – 6% entrapped water [10]; and an average naphthenic acid content 200 mg/kg [12].

It is the clay layers that contribute to the release of fines in the subsequent bitumen separation process [11]. These fines are a major constituent of fluid fine tailings (FFT) and mature fine tailings (MFT) which pose a serious environmental challenge due to their slow dewatering rate, taking approximately 125-150 years. The hydrophilic nature of the sand grains found in Canada facilitates the separation of bitumen through the application of water-based separation techniques [2].

1.1.2. Open Pit Mining Overview

Open pit mining is used for the oil sand deposits that are less than 75 m from the surface. The material above the deposit is referred to as overburden. The overburden must first be removed before mining of the oil sands can begin. It is either used in adjacent reclamation projects or to build tailing retention structures. In total approximately 4,746 km^2 of land is suitable for mining operations, to date 602 km^2 of land, or 12 % of the total, has been affected by mining activities [3].

Open pit mining operations, as opposed to in-situ operations, utilize a hot water-based separation technique referred to as the Clark caustic hot water extraction method. The process results in the use and subsequent generation of large volumes of contaminated water [13]. This water is referred to as oil sands process-affected water (OSPW). It is highly toxic to biological organisms

and poses a serious environmental and economic challenge for the continued development of this resource. Currently mine operators must abide to a zero discharge policy, meaning that all tailing water must be stored in accordance to specific regulations in large tailing ponds [14].

For every 1 bbl of bitumen produced approximately 12 – 14 bbls of water are required. From this water, approximately 3 – 4 bbls become unavailable due to losses inherent in the extraction process (e.g. evaporation) [15], or become fluid fine tailings (FFT) which cannot be re-used in the process [3]. The process thus needs to account for the lost water requiring the difference to be obtained from fresh sources, mainly the Athabasca River and its tributaries [3], [15]. Water reuse is limited by the deteriorating water quality in the tailing ponds due to continued recycling. Thus fresh water is required in order to dilute contaminants that can begin to negatively affect the bitumen extraction operation with respect to process chemistry, increase fouling, corrosion, etc [15].

During the Clark hot water extraction process, caustic soda (NaOH) promotes the release of natural surfactants found within the bitumen that include NAs. These help separate the bitumen from clay and sand, promoting the formation of a water-bitumen emulsion [11]. Due to the similar specific gravity of bitumen (1.01) and that of water, it is difficult to fully separate the bitumen from the process water. This leads to its presence as a contaminant in process tailing waste [10]. In addition, either a naphtha-based or paraffinic solvents are used to destabilize the water-bitumen emulsion in order to promote bitumen separation. This also leads to their presence in tailing waters even though solvent recovery and recycling methods are employed [10]. While the tailing streams have yet to be fully characterized [10], there are concerns regarding: naphthenic acids, solvents, pyrite, metals, NORMS that are present in tailing water.

1.1.3. In-situ Operations

In-situ operations differ from open-pit mining in that they are used to extract bitumen from ore deposits at depths below 75 m, through bored wells. The wells are used to pump a heat carrier (i.e. steam or solvents) into the ground to melt the bitumen for subsequent pumping to the surface. In-situ operations can recover and reuse about 90% of the water used, with the remainder lost in the ground [3]. Three types of in-situ methods are commonly used: Cycle Steam Stimulation (CSS), Steam Assisted Gravity Drainage (SAGD), Vapor Extraction Process (VAPEX).

In CSS, a single well is used in alternation between production (extraction) and steam injection. This method provides relatively poor bitumen recovery, in the range of 20-25% [9]. Cycle times are typically 6-8 months [3]. SAGD employs horizontal drilling techniques developed for petroleum production. Bitumen recovery ranges from 40-70% range [9]. SAGD is more economical than CSS and provides higher recovery rates. Companies are currently experimenting with combinations of both methods in order to boost recovery rates [3]. Another method that uses a heat carrier is the VAPEX, which is similar to SAGD though instead of using steam this method employs vaporized solvents to liquefy the bitumen for subsequent extraction [16].

1.2 Problem Statement

The scale and sheer volume of OSPW being stored in tailing ponds have generated serious public concerns. Reclamation efforts have two major challenges: the first is to successfully separate suspended particles (e.g. MFT), the second is to eliminate aquatic toxicity such that discharging and reintegration of OSPW into the natural hydrological cycle will be possible. Many emerging technologies have been investigated as treatment options for OSPW reclamation. These include: chemical modifications to membranes for pollutant removal and reduced fouling; hybridization of adsorbent, membrane, and bioreactor technologies to enhance the biological treatment of tailing water; photocatalytic oxidation; implementation of large-scale treatment wetlands [15].

Recent studies using petroleum coke, a relatively inexpensive and abundant feedstock, as an adsorbent after activation, has brought renewed attention to the use of adsorption processes for OSPW reclamation [17]–[22]. Adsorption is widely used for municipal and industrial water purification. It is a mature engineering technology and has a high potential to be easily deployed at the scale needed to treat the volumes of OSPW being generated. Treatment technologies aiming to reduce OSPW toxicity have targeted NA removal as these compounds have been attributed to be the main contributor to OSPW toxicity [12], [23]–[27]. The selective removal and future recovery of NAs are of interest since they are currently commercially extracted during petroleum refining, to mitigate corrosion [12], and subsequently utilized for various commercial applications [28]. The selective removal through adsorption of NAs from OSPW could potentially provide a new production stream for NAs. OSPWs have been found to have NAs concentrations ranging from 40-80 mg/L with maximum values reaching as high as 130 mg/L in fresh tailing water [6].

1.3 Research Objective

To determine the feasibility of using commercial granular activated carbon (GAC) to adsorb several NAs from a model solution in a batch adsorption process. The effect of process pH on both competitive and single solute adsorption was studied under steady state (i.e. isotherms) and transient conditions (i.e. kinetic).

Chapter 2: Literature Review

2.1 OSPW Naphthenic Acids

Naphthenic acids (NAs) have been considered by many to be a major contaminant contributing to oil sand process affected water (OSPW) toxicity [12], [23]–[27]. NAs present within oil sands bitumen are released during the bitumen extraction process as dissolved naphthenates, the acid in its deprotonated form (i.e. salt). Naphthenates are soluble in neutral or basic water solutions and are thus readily dissolved in the alkaline OSPW (pH ~8). The primary toxic components of NAs within OSPW have not yet been identified due to the complexity of the organic acid mixture [4]. Little information regarding the exact structure of OSPW NAs is known [6]. Additionally, NAs have varying levels of corrosivity and toxicity based on their size and structure [29]. NAs present in oil sand ore can differ in composition and concentration depending on the deposit [6]. The average concentration of NAs in oil sand ore was reported to be 200 mg/Kg [12]. Based on Syncrude production figures from 2000, Clement et al. (2005) estimated a potential release of 100 tonnes of NAs per day [12].

2.1.1. Commercial Application of Naphthenic Acids

Naphthenic acids are commercially extracted from petroleum and have a variety of applications such as: improve water resistance and adhesion of concrete; increase high pressure resistance of drilling oils; prevent foaming in jet fuel; prevent fungus growth in wood; preserve and act as flame retardant in fabric; increase insecticide solubility by acting as an emulsifier; catalyze rubber vulcanization; stabilize vinyl resins; catalyze production of alkyl and polyester resins; and wood preservative [12], [28].

2.1.2. Chemical Structures of NA

The term NAs is typically used by the petroleum industry to describe all the carboxylic acids found in crude oil [28]. NAs comprise of a mixture of alkyl-substituted and cycloaliphatic carboxylic acids [12]. They are non-volatile, chemically stable, and act as surfactants due to their hydrophobic (non-polar aliphatic) and their hydrophilic end (carboxyl group). They are naturally occurring in crude oil through biodegradation [12]. The International Union of Pure and Applied

Chemistry defines NAs as "acids, chiefly monocarboxylic, derived from cycloalkanes (naphthenes)". NAs have been described using the general formula:
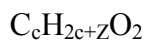
$$C_cH_{2c+Z}O_2$$

Where:

c = carbon number

Z = specifies the homologous series, is an even negative integer corresponding to proton deficiencies

Advancements in analytical techniques have allowed for the discovery of various other acid structures in OSPW [4], [27], [30]–[35]. The acid extracts once thought to be NAs adhering to the above formula, more recently referred to as the classical formula [20], [25], [27], [30], [33], [34], appear to have increased oxygen content, possibly due to multiple hydroxyl, carbonyl or carboxyl groups. Additionally other heteroatoms have been identified including sulphur and nitrogen. Varying levels of unsaturation (aromaticity) have also been observed. A revised version of the classical NAs formula for oxygenated naphthenic acids along with numerous other formulas for non-oxygen heteroatoms are provided below [35]. They can be classified as non-classical NAs:
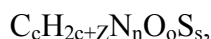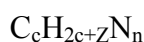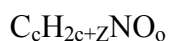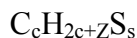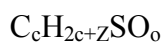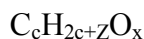
$$C_cH_{2c+Z}O_x$$
$$C_cH_{2c+Z}SO_o$$
$$C_cH_{2c+Z}S_s$$
$$C_cH_{2c+Z}NO_o$$
$$C_cH_{2c+Z}N_n$$
$$C_cH_{2c+Z}N_nO_oS_s,$$

Where:

c = carbon number

Z = specifies the homologous series, is an even negative integer corresponding to proton deficiencies

o = oxygen number, with values ranging from 2-7

n and s = nitrogen and sulfur number respectively

The previous homologous formulas identify groups of compounds that can exist as multiple isomers. For example, from the resulting classical formula, $C_{10}H_{18}O_2$, one can obtain 37 different carboxylic acid isomers [12].

As has been demonstrated, the term NA is loosely used to describe a wide variety of acids present in both crude oil and OSPW [36], [37]. The NAs isolated from petroleum sources and sold commercially (e.g. The Eastman Kodak Company) have been used by multiple groups to study different aspects of OSPW NAs [2], [13], [14]. Due to the loose definition of NAs, many have assumed that the acids found in petroleum are the same as those in OSPW. Studies indicate that the composition of NAs in OSPW is different than that of petroleum [32].

Some more recent studies have begun to classify these non-classical NAs as naphthenic acid fraction compounds (NAFC) [4], [31]. The specific nomenclature used to describe the broader definition of NAs present in OSPW has yet to be standardized. Other terms used include, acid extractable oil sand tailing organics (AEOSTO) [19], and oil sands tailings water acid-extractable organics (OSTWAEO) [35].

It is believed that microbial activity may alter the structure of NAs represented by the classical equations [35]. Corrosive and toxic effects of NAs are often structure-specific [35]. Additionally, NA structure may differ significantly between petroleum and oil sand deposits [32]. These observations further make the need for accurate chemical nomenclature critical, in order to ensure consistency and continuity of research. In this work the term NAs will be used to discuss compounds that fall within the full range of homologous organic acids presented above.

2.2. OSPW Chemical Composition

Some of the chemical constituents in OSPW have been determined and are tabulated below in Table 2-1. Other dissolved contaminants that may be present within OSPW but are not tabulated are asphaltenes, benzene, creosols, cyanide, humic acid, fulvic acids, phenols, phthalates, polycyclic aromatic hydrocarbons (PAH), toluene, methane and naturally occurring radioactive minerals (NORMS) [23], [10].

Table 2 - 1: Measured chemical composition of tailing ponds.

Variable	average [19]	[23]	[15]	[7]
pH	8.65	8.2		8.1 - 8.5
Conductivity (mS)	3.4			
TDS (mg/L)		2221	1900-2200	12.5 - 47.7 (g/100g)
Alkalinity (mg CaCO$_3$/L)	578.1			
Bicarbonate (mg/L)		775		960 – 1240
DOC (mg/L)	46.55	58 - 67		
BOD (mg/L)		25-70		
COD (mg/L)		86-350		
Naphthenic acids (mg/L)	60.35		50-70	61 – 88
Bitumen (mg/L)			25-7500	0.62 – 3.1
Oil & Grease (mg/L)		9-92		
Na$^+$ (mg/L)	680.35	659		438 - 895
Ca (mg/L)		17		3.4 – 7.3
Cl$^-$ (mg/L)	535.7	540	80-720	127 – 634
SO$_4^{2-}$(mg/L)	219.35	218	230-290	2 – 173
NH$_4^+$(mg/L)	6.6			6.7 – 10
NH$_3$ (mg/L)		14	3-14	
Al (µg/L)	36			
Ni (µg/L)	9			
Mo (µg/L)	276.65			
Mn (µg/L)	25.55			
Mg (mg/L)	8			2.6 – 9.7
Cu (µg/L)	171.5			
Pb (µg/L)	8.1			
V (µg/L)	11.1			
K (mg/L)				9.1 – 18.5

2.3. Model compounds

The exact composition of OSPW is currently unknown and thus the selection of appropriate compounds that can be used to accurately model OSPW is difficult if not impossible. A general approximation was made by selecting naphthenic acids that have been used as surrogates to mimic OSPW composition in recent publications. These compounds were used for calibration of analytical equipment or for environmental and toxicological studies. The acids identified have been tabulated in Table 2 - **2** below.

Table 2 - 2: List of model compounds identified during the literature survey
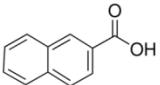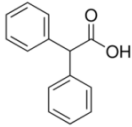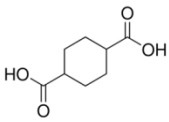
	Name:	Formula	MW
1	Ethanoic, Acetic Acid	$C_2H_4O_2$	60
2	Butanedioic, Succinic acid [25], [40]	$C_4H_6O_4$	118
3	Cyclopentane carboxylic acid	$C_6H_{10}O_2$	114
4	Hexanoic acid [25], [40]	$C_6H_{12}O_2$	116
5	Benzoic acid [41]	$C_7H_6O_2$	122
6	cyclohexanecarboxylic acid [25],[40], [30], [42], [41],	$C_7H_{12}O_2$	128
7	1,4-Cyclohexanedicarboxylic acid [25], [40]	$C_8H_{12}O_4$	128
8	3-methyl-1-cyclohexanecarboxylic acid [30]	$C_8H_{14}O_2$	142
9	trans-4-methyl-1-cyclohexane carboxylic acid [30]	$C_8H_{14}O_2$	142
10	4-methyl-1-cyclohexane carboxylic acid [30]	$C_8H_{14}O_2$	142
11	Adipic acid [25], [40]	$C_6H_6O_4$	142
12	3-Cyclohexanepropionic acid [12], [41], [43]	$C_9H_{16}O_2$	156
13	4-Methycyclohexaneacetic acid (4MACH, Sigma-Aldrich) [48]	$C_9H_{18}O_2$	158
14	cyclohexane butyric acid (4-cyclohexylbutanoic acid) [43], [44]	$C_{10}H_{18}O_2$	170
15	4-propylcyclohexanecarboxylic acid [42]	$C_{10}H_{18}O_2$	170

16	Citronellic acid [45]	$C_{10}H_{18}O_2$	170
17	Decanoic acid [25], [40], [46]	$C_{10}H_{20}O_2$	172
18	2-Naphthoic acid [12], [31], [41]	$C_{11}H_8O_2$	172
19	1-Methyl-1-cyclohexanecarboxylic acid [30], [42], [12],	$C_8H_{14}O_2$	172
20	1,2,3,4-tetrahydro-2-naphthoic acid [42]	$C_{11}H_{12}O_2$	176
21	1-adamantane carboxylic acid [42], [43], [45], [47]	$C_{11}H_{16}O_2$	180
22	Cyclohexanepentanoic acid [25], [40], [42], [43], [46]	$C_{11}H_{20}O_2$	184
23	trans-4-tert-butylcyclohexanecarboxylic acid [42]	$C_{11}H_{20}O_2$	184
24	1-adamantaneacetic acid [42]	$C_{12}H_{18}O_2$	194
25	trans-4-pentylcyclohexane carboxylic acid [41], [42]	$C_{12}H_{22}O_2$	198
26	Cyclohexylsuccinic acid [25], [40]	$C_{10}H_{16}O_4$	200
27	Lauric Acid; dodecanoic acid [44]	$C_{12}H_{24}O_2$	200
28	12-hydroxydodecanoic acid [42]	$C_{12}H_{24}O_3$	216
29	(4-cyclohexylphenyl)acetic acid	$C_{14}H_{18}O_2$	218
30	4-Heptyl benzoic acid [41]	$C_{14}H_{20}O_2$	220
31	3,5-Dimethyladamantane-1-acetic acid	$C_{14}H_{22}O_2$	222
32	Dicyclohexylacetic acid [42]	$C_{14}H_{24}O_2$	224
33	Diphenylacetic acid	$C_{14}H_{12}O_2$	212
34	4-Pentylbicyclo[2.2.2]octane-1-carboxylic acid	$C_{14}H_{24}O_2$	224
35	12-Methyltridecanoic acid	$C_{14}H_{28}O_2$	228
36	Myristic acid	$C_{14}H_{28}O_2$	228
37	(±)-6-Hydroxy-2,5,7,8-tetramethylchromane-2-carboxylic acid	$C_{14}H_{18}O_4$	250
38	(3aR)-(+)-Sclareolide	$C_{16}H_{26}O_2$	250

39	Palmitoleic acid [30]	$C_{16}H_{30}O_2$	254
40	hexadecanoic, Palmitic acid [44]	$C_{16}H_{32}O_2$	256
41	2-Hexyldecanoic acid [42]	$C_{16}H_{32}O_2$	256
42	Linolenic acid [30]	$C_{18}H_{30}O_2$	278
43	Linoleic acid [30]	$C_{18}H_{32}O_2$	280
44	Stearic acid [44]	$C_{18}H_{36}O_2$	284
45	1-pyrenebutyric acid [42]	$C_{20}H_{16}O_2$	288
46	12-hydroxysteric acid [42]	$C_{18}H_{36}O_3$	300
47	Abietic acid [42]	$C_{20}H_{30}O_2$	302
48	Arachidonic acid [30]	$C_{20}H_{32}O_2$	304
49	Phytanic acid [45]	$C_{20}H_{40}O_2$	312
50	cis-4,7,10,13,16,19-Docosahexaenoic acid [30]	$C_{22}H_{32}O_2$	328
51	5-beta-cholanic acid [42], [44]	$C_{24}H_{40}O_2$	360
52	Nervonic acid [30]	$C_{24}H_{46}O_2$	366
53	12-oxochenodeoxycholic acid [42]	$C_{24}H_{38}O_5$	406

Three model compounds were selected from Table 2-2 for this study. They are presented in Table 2 - **3** below. 1,4-Cyclohexaneacetic acid was selected due to its two carboxylic moieties which are thought to be the product of bio-degradation in OSPW. 2-Naphthoic acid was selected because of its chemical structure and similarity to the acidic compounds most often encountered in crude oils [41]. Diphenylacetic acid was selected because of its aromaticity and to be used as a comparison between its affinity to GAC and that of 2-naphthoic acid. Both diphenylacetic acid and 2-naphthoic acid are bicyclic acids, which are abundant in both oil sands and petroleum derived NA mixtures [45].

Table 2 - 3 : **Model NAs selected**

Name:	Formula:	MW:	pKa:	Structure:
1 2-Naphthoic acid Purchased from: VWR CAS Registry No: 93-09-04	$C_{11}H_8O_2$	172	4.161^3 4.20^4	
2 Diphenylacetic acid Purchased from: Sigma-Aldrich CAS Registry No: 117-34-0	$C_{14}H_{12}O_2$	212	4.72^4	
3 1,4-Cyclohexanedicarboxylic acid Purchased from: VWR CAS Registry No: 1076-97-7	$C_8H_{12}O_4$	172	1) $3.54 (0)^3$ 2) $4.46 (-1)^3$ 4.38^4	

3. Value obtained from Lang's Handbook [49].
4. Value obtained from SciFinder chemical database.

2.4. Detection Methods for Naphthenic Acids

Much progress has been achieved to characterise naphthenic acids found in crude oils, bitumen, and subsequently OSPW. Numerous analytical techniques have been attempted to characterise NA mixtures including: supercritical fluid extraction coupled with fast ion bombardment mass-spectrometry [36]; electrospray ionization and atmospheric pressure chemical ionization [34]; atmospheric pressure photo-ionization [34]; gas chromatography mass spectrometry [12]; liquid chromatography mass spectrometry [18]; liquid secondary ion mass spectrometry; high performance liquid chromatography (HPLC) used to analyse NAs as a group [44]; fourier transform ion cyclotron resonance mass spectrometers with nanospray ionization [29], [34]; thin layer chromatography [12]; negative-ion electrospray ionization orbitrap mass spectrometry [31]; flow injection analysis [30]; fourier transform infrared red spectroscopy [50]; UV-VIS spectroscopy [51]; negative ion electrospray ionization-mass spectrometry [12], [18], [13].

Reviews of detection methods have been completed by several groups, including [4], [12], [36]. Due to the relative simplicity of the above model solution, as compared to OSPW, the use of complex analytical techniques was not required. An HPLC system with an appropriately selected column was deemed sufficient as an analytical tool for the present study.

2.5. NAs Toxicological Studies

It is difficult to compare toxicological and environmental studies regarding NAs due to the complex nature of NAs and resultant ambiguity. Research typically differs in either the model compounds used, or the source of commercial NAs or OSPW used.

The toxicity of OSPW on rainbow trout was reported as early as 1975 [23]. Many toxicological studies outlining acute and chronic toxicity of OSPW have been carried out over the years [23], [24], [26], [52]–[55]. The toxicological effects of NAs on various organisms have been studied including: aspen, fish, zooplanton, rats, and bacteria. Though stated that NAs have been identified as the primary contributors to toxicity, isolation of NAs has proven to be difficult. Contributions of other unknown compounds within OSPW on toxicity have not been quantified [45]. OSPW may thus have a higher or lower overall toxicity than its individual components depending on their chemical interactions on organisms.

Increased toxicity of NAs has been linked to the hydrophobicity of carboxylic acids which increases with molecular weight (MW) [25]. The mode of toxicity is thought to be due to narcosis, in which the hydrophobic portion of a molecule penetrates the lipid bilayer of a cell. This disrupts cell function and leads to cell death [25], [45]. These findings are contradictory to the studies where it was found that biodegraded or aged OSPW exhibited reduced toxicity due to the digestion/degradation of low MW NAs [12]. Studies have found that commercial NA mixtures tend to be composed of carboxylic acids with low molecular weight which biodegrade much faster than larger MW NAs [39]. The biodegradation of tailing water may lead to the formation of large NAs with multiple carboxylic functional groups which would decrease hydrophobicity and thus their toxicity [25]. This may elucidate the previous contradiction of reported decreases in OSPW toxicity with ageing. Additionally, NA and OSPW have been found to be exhibit environmental estrogenic and androgenic activity [53], [56].

2.6. Treatment Methods

Many technologies have been investigated as treatment methods for OSPW. Detailed reviews of the current state of practice in the oil sands industry and technologies being considered by the private sector, have been compiled in reports and academic publications [10], [11], [15], [16], [57]. The general types of treatments being considered are those to dewater MFT and FFT, and those to remove chemical toxicity from OSPW. Decontamination technologies focusing on toxicity include: chemical modifications to adsorbents and membranes for pollutant removal and reduced fouling; hybridization of adsorbent, membrane, and bioreactor technologies to enhance the biological treatment; photocatalytic oxidation; implementation of large-scale treatment wetlands.

Several technologies being utilized by oil sands operators are [10]: composite tailings (CT) and non-segregating tailings (NST) (Syncrude & Suncor); thickened tailings (Shell - Albian Sands); in-line thickening with thin lift dewatering; in-line thickening with accelerated dewatering; centrifuge MFT; coke capping; wetland reclamation; water capped MFT. The technologies that have been implemented by industrial operators focus on dewatering of both MFT and fluid fine tailing (FFT). They do not address chemical contamination of the bulk OSPW. This focus is due to a regulation announced by the Alberta Energy Resources Conservation Board (ERCB) in 2009. directive 074 states that operators must capture or extract fine particles from water and provides disposal guidelines [14]. The directive also provides operators with reduction targets and deadlines. In 2009, nine tailing management plans were submitted to the government of Alberta to demonstrate compliance with directive 074. Only two of the plans submitted met the mandated requirements [58].

Much progress has thus been achieved with regard to reducing suspended solids in OSPW as provincial regulations have forced industry to ameliorate past practices. Progress remains to be made with regard to OSPW reclamation. Toxicity must be eliminated, such that process water can be re-introduced into the natural hydrological cycle. Allen, E. (2008) has compiled a list of recommended removal rates for OSPW contaminants, recommending 90-99% removal in order to obtain local background concentration in watersheds of 1-5 mg/L [23].

Recent studies using petroleum coke, a relatively inexpensive and abundant feedstock, as an adsorbent, before and after activation, have brought renewed attention to the use of adsorption processes for OSPW reclamation [17]–[22]. Adsorption is widely used today for municipal and industrial water purification. It is a mature engineering technology that has a high potential to be easily applied at the scale needed to treat the volumes of OSPW being generated today. There is thus a need to better quantify adsorbent performance with regard to NA removal from OSPW. This work will help address this need.

2.7. Adsorption Studies

Several studies have investigated the adsorptive properties of various soil types and clays in order to estimate environmental concerns regarding NA migration into hydrological systems (e.g. aquifers) [48], [59], [60]. Azad et al. (2013) studied the adsorption of commercial NAs on multiple adsorbents and found that both activated carbon and Ni-based alumina had the best performance removing 50 and 40 percent of total organic carbon (TOC), respectively. The study also confirmed that total dissolved solids (TDS) would negatively impact the adsorption of NAs [6]. The capacity of $Ni-Al_2-O_4$ with 10.7% Ni loading, was found to be 20 mg TOC/g adsorbent. Small et al. (2012) have reported a range of activation parameters for producing activated carbon from both delayed and fluid coke. The adsorption properties of activated coke for NA were inferior to that of commercial activated carbons [19]. The adsorption capacities of non-activated petroleum coke were found to be: 0.214-0.223 mg/g [19], or 0.39-0.86 mg/g [17]. These values greatly improved for activated petroleum coke: 515.2-588.8 mg/g. They also compared their results to a GAC which exhibited a capacity of 870.4 mg/g [19]. Leaching of heavy metals from coke into treated water was also observed [19], [17]. Interestingly, long contact times such as several months allowed some of the leached heavy metal compounds to be re-adsorbed [17]. Another study found that the treatment of OSPW with 22 % by weight of hot petroleum coke resulted in water that was non-toxic to V. Fischeri [22].

Table 2 - 4: Adsorption capacity of NAs on various adsorbents

Adsorbent	NA Adsorbent Capacity (mg/g)
GAC	870.4
Petroleum Coke	0.214-0.86
Activated Petroleum Coke	515.2-588.8

Adsorption rates for activated carbon have been successfully increased by chemical surface modifications [61], [62], and through the growth of bio-films [63]. Activated carbon, as other adsorbents, suffer from surface fouling due to oil and metal hydroxides, bacteria, and natural occurring organic matter (NOM) which reduce their adsorption capacity and kinetic performance [64]. Solution pH has also been found to affect adsorption properties [62]. Studies have found that acidification of OSPW was required to effectively adsorb NA [15].

The point of zero charge (pzc) is an important parameter in adsorption studies, as it affects adsorbent capacity [65]–[71]. An activated carbon of either acidic or basic character will permanently modify the pH of a solution if ion-exchange takes place [68]. The surface charge of an activated carbon is a function of the pH of the solution. At a specific pH the surface will exhibit a neutral charge, known as pH_{pzc}. The point of zero charge represents the point where the carbon surface is changed from either a net positive charge to a net negative charge. The surface charge will dictate whether anions or cations will preferentially adsorb on a given surface. There are several methods to determine the pzc of a surface, though the simplest is the pH drift method [65], [66], [70], [71]. The description of this method will be further elaborated in the materials and methods portion of this work.

Chapter 3: Adsorption Theory and Models

3.1. What is adsorption?

Adsorption is a surface phenomena that involves the interactions between a solid surface and fluids (gases and liquids), or dissolved solids. Gilles et al. (1974) have classified these three systems into vapor or gas phase adsorption (VPA), composite liquid adsorption (CLA) and solid solute adsorption (SSA) [72]. Interactions with the surface result in either weak or strong binding (adsorption) to the surface. Weak interactions are typically dominated by van der Waals forces and are referred to as physical adsorption or physisorption, while strong interactions are characterized by chemical bonding and are referred to as chemical adsorption or chemisorptions.

Typically adsorption is used as a separation technology with a multitude of applications. Adsorbates in these applications include organic compounds, inorganic material, proteins, and polymeric compounds. The use of adsorption is prehistoric, with records dating back two millennia found in Sanskrit manuscripts describing the use of charcoal to remove odour and taste from water [73]. The First World War brought about the development of granular activated carbon (GAC) used in the defence of chemical warfare [73]. Some modern applications in which adsorption is utilized for liquid-phase adsorption include: removing dissolved organics from drinking water; purifying drinking water supplies removing odour, taste, and color; decolourizing crude sugar syrup; decolourizing vegetable oil; purifying industrial/municipal waste. Gas-phase adsorption is also widely used and has many modern applications including: recovering organic solvent vapours; dehydrating gases; removing odour or toxic agent from air; air separation (oxygen/nitrogen separation); removal of carbon dioxide and sulphur compounds from natural gas.

3.1.1. Solid Solute Adsorption

The present work will discuss SSA where species (naphthenic acids) are dissolved in a solvent (water). The bulk of the solution, acting as a solvent, is assumed to behave in a constant manner and can thus be ignored. Adsorption, like many phenomena undergo two stages. The first is a transient, dynamic state, where the system concentrations are changing with time. This state is typically referred to as adsorption kinetics. The second is the steady state stage, in which the system reaches equilibrium and the concentrations remain constant over time. When equilibrium is reached, the maximum amount of solute that can be adsorbed for given conditions is obtained. These conditions include: initial concentration, temperature and carbon load. The amount adsorbed from a liquid system is a function of the composition of the adsorbent (e.g. silica, charcoal), solvent and the chemical characteristics of the adsorbate species (i.e. hydrophobic, polar, etc).

For SSA systems the adsorption equilibrium data is typically expressed as:

$$q = f(C, T)$$

      Where:

            q = amount adsorbed per unit mass of adsorbent (mol/g or mg/g)

            T = temperature (^{o}C)

            C = bulk concentration of the adsorbate within the liquid system

               (mg/L)

For the work presented herein, the temperature was held constant, and thus the expression above becomes that for an adsorption isotherm:

$$q = f(C) \; ; \; T = constant$$

If the adsorbate is ionizable (i.e. acid or base), the pH of the solution may greatly influence the extent of adsorption. In the case of organic acids, as discussed in this work, the total adsorption will include both the ionized and non-ionized species. The pH can also affect the electrostatic

field between the solution and the charged adsorbent surface, which can influence the extent of adsorption.

Typically the concentration of the compound initially retained by the adsorbent can be assumed to be zero. The concentration of the adsorbate on the adsorbent at equilibrium can be determined by:

$$\mathbf{q} = \frac{\mathbf{V}}{\mathbf{m}}(\mathbf{C_o} - \mathbf{C_e}) + \mathbf{q_o} \qquad (1)$$

Where:

V	=	volume of solution (L)
m	=	adsorbent mass (g)
C_o	=	initial solute concentration (mg/L)
C_e	=	final equilibrium solute concentration (mg/L)
q_o	=	amount of compound initially retained by solid (mg/g)
q	=	amount of adsorbate per unit mass of adsorbent (mg/g)

3.1.2. Isotherm Classification System

Giles et al. (1960) presented a system of classification for adsorption isotherms. Four main classes were identified in accordance to their initial slope. Sub-groups for each class were then also presented [74]. The four main isotherm classes identified by Giles were the: S, L, H and C-class. The Figure 3 - 1 illustrates this classification system.
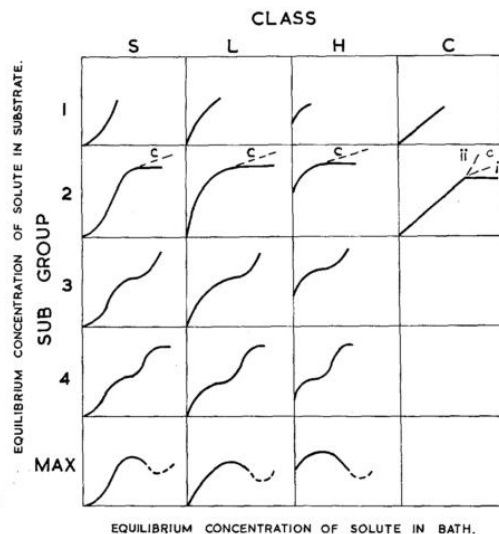
FIG. 1. System of isotherm classification. The 2c subgroup indicates microporosity in the substrate, and in the C-class, the second branch of the curve in the subgroup 2 may be horizontal, or have a less steep (ci) or a steeper (cii) slope than the main portion, according to the nature of the system. These slight variations from the earlier diagram (23) are made in the light of later results. Though only subgroups progressing from 1 through 4 are shown these obviously can be extended to 5 or beyond if further rises and steps occur.

Figure 3 - 1: Isotherm classification system described by Giles et al. (1960) [74]

S-class adsorption isotherm curve:

The S-class isotherm curve is representative of cooperative adsorption, where solute-solute forces are similar to solute-substrate forces. Lateral interactions between solute, or adsorbate molecules, on the substrate (adsorbent) help to increase the stability of the adsorbed species [72]. In this manner the energy of activation for desorption is increased with lateral interaction. Due to these intermolecular interactions, as the concentration of adsorbate on the adsorbent increases, the adsorption process is facilitated.

L-class or Langmuir type adsorption isotherm curve:

The L-class isotherm curve is commonly seen in dilute solution adsorption studies and is one of the most known forms of adsorption [74]. As the adsorbent active sites are filled, adsorption becomes increasingly more difficult. This is due to the decreased likelihood of solute molecules coming into contact with vacant adsorption sites.

H-class or high affinity adsorption isotherm curve:

The H-class adsorption isotherm curve is similar to the L-class but is distinguished by a marked vertical portion were the equilibrium concentration is zero. The H-class isotherm tends to have a larger adsorption affinity at low equilibrium concentrations, to such an extent that the affinity of the solute for the adsorbent is so large that the initial slope of the adsorption isotherm approaches infinity [74].

C-class or constant partition isotherm curve:

Typically, systems that exhibit a C-class isotherm curve are those where the adsorbent had a microporous structure. Another general characteristics of these systems is that the solute tends to have a higher affinity for the adsorbent than for the solvent [72]. The linear adsorption isotherm is one where the specific amount of adsorbate increases linearly with equilibrium concentration.

3.2. Adsorption Isotherms

For the SSA systems investigated, *single-component adsorption* will refer to the adsorption of a single dissolved species, or *adsorbate*, from solution. Similarly, *multi-component adsorption* will refer to the competitive adsorption of a mixture of compounds from solution.

3.2.1. Isotherm Models

Isotherms are typically used in the engineering of adsorption systems for the following: to determine the feasibility of adsorption for a particular application; to determine the equilibrium capacity and thus obtain a rough estimate of carbon usage needed for a preliminary design; to determine the difficulty or ease of removing particular contaminants; to identify changes in equilibrium capacity in the presence of other contaminants, changes in pH, changes in contaminant concentration, etc; to compare the efficiency of various carbons in order to identify the best candidates for dynamic testing (kinetic studies).

Due to the complexity of liquid-phase adsorption, it is best not to attach a high degree of significance to the isotherm models [75]. These should be interpreted as expressions that represent experimental data within limited concentration ranges [73].

3.2.2. The Langmuir Isotherm

Langmuir (1918) was one of the first to propose a theory of adsorption onto a flat surface based on kinetic principles. His model assumed that in order for the surface not to accumulate any adsorbate at equilibrium, desorption and adsorption rates must be equal. The underlying assumptions used to develop the Langmuir model are: the surface of the adsorbent is uniform (i.e. homogeneous) and ideal (i.e. adsorption energy is constant over all sites). Adsorbed molecules do not interact with adjacent molecules (i.e. adsorption is localised). Each adsorption site can hold one adsorbate molecule. In this way at maximum adsorption only a monolayer is formed. Finally, all adsorption occurs through the same mechanism.

$$q_e = Q^o \frac{K_L C_e}{1 + K_L C_e} \qquad (2)$$

Where:

C_e = equilibrium concentration (mg/L)

q_e = mass of adsorbate per unit mass of adsorbent (mg/g)

Q^o = mass of adsorbate per unit mass of adsorbent at complete surface coverage (mg/g)

K_L = Langmuir constant or affinity constant (L/mg)

The Langmuir constant provides a measure of how strongly an adsorbate molecule is attracted to a surface. It provides insight into the initial slope (i.e. at $C_e = 0$) of the adsorption isotherm plot. In this manner the separation factor (R_L), originally described by Webber and Chakkravorti, can be understood [76], [67]:

$$R_L = \frac{1}{1 + K_L C_o} \qquad (3)$$

R_L indicates how favourably the solute is adsorbed from the solution.

$R_L > 1$ unfavourable adsorption

$R_L = 1$ linear adsorption

$0 < R_L < 1$ favourable adsorption

$0 = R_L$ irreversible adsorption

Taking the limit of equation (2) as $C_e \rightarrow \infty$ yields the adsorbent capacity Q^o.

$$\lim_{C_e \to \infty} \left(Q^o \frac{bC_e}{1 + bC_e} \right) = Q^o$$

Linear Langmuir Isotherm

Depending on the algebraic manipulation used to linearize the Langmuir model, several different linear forms of the equation have been obtained, see Table 3 - 1. Using the Lineweaver-Burk equation, the experimental equilibrium adsorption data can be plotted as $\frac{1}{q_e}$ vs $\frac{1}{C_e}$. In this manner, the slope of the graph and the y-intercept allow for determination of the parameters Q^o and b. A similar approach can be used for the determination of the parameters for the other four equations. The results for the parameters will vary depending on the equation used. Further discussion on variations between linear expressions is presented in Chapter 5.

Table 3 - 1: Various linear forms of the Langmuir isotherm

	Linear Regression	Name:
1	$\dfrac{1}{q_e} = \dfrac{1}{q_m K_L}\dfrac{1}{C_e} + \dfrac{1}{q_m}$	Lineweaver-Burk [77]
2	$\dfrac{C_e}{q_e} = \dfrac{1}{q_m K_L} + \dfrac{C_e}{q_m}$	Hanes-Wolf [77]
3	$q_e = q_m - \dfrac{q_e}{K C_e}$	Eadie-Hofstee [77]
4	$\dfrac{q_e}{C_e} = -K_L q_e + K_L q_m$	[67]
5	$\dfrac{1}{C_e} = -\dfrac{K_L q_m}{q_e} + K_L$	[67]

3.2.3. Freundlich Isotherm

Real world adsorbents have complex surface and pore structures whose adsorptive properties are lost during the simplifications and assumptions used to develop fundamental models. It is for this reason that semi-empirical equations have been found to be quite useful in modeling the adsorptive process.

The Freundlich isotherm was first proposed as an empirical model though it has been since derived from first principles and can thus be considered semi-empirical. The assumptions used in its derivation are that, the surface is heterogeneous and patchwise, so sites having the same adsorption energy are grouped together in one patch. Patches are independent, with no interactions between patches. On each patch it is assumed that the adsorbate can only adsorb onto one adsorption site, thus following the Langmuir model for a specific patch. It is assumed that all patches have an energy distribution that follows an exponential decay function.

$$q_e = K_f C_e^{\frac{1}{n}} \quad (4)$$

Where:

K_f = empirical Freundlich constant

$1/n$ = index of the variability of free energy of a heterogeneous surface

To determine the saturation capacity of the adsorbent the equilibrium concentration can be made equal to the initial system concentration. At this point no more up-take would be occurring as the system is saturated:

$$q_m = K_f C_o^{\frac{1}{n}} \quad (5)$$

The constants 'K_f' and 'n' are usually temperature dependent. The constant 'n' is an indicator of non-linearity of the adsorption process. When 'n' is unity, the Freundlich equation becomes that of a straight line. As the value of n increases the resulting plot appears increasingly rectangular. The Freundlich equation has the problem that no upper limit to adsorption is set by the equation,

thus it is typically only used over narrow concentration ranges. It also encounters problems at either high or low concentrations.

The linear form of the Freundlich isotherm can be expressed as:

$$\log(q_e) = \log(K_f) + \frac{1}{n}\log(C_e) \qquad (6)$$

3.2.4. The Langmuir-Freundlich Isotherm

In order to set an upper limit to the Freundlich isotherm, Sips (1948), proposed an equation similar to that of Langmuir but with the addition of a parameter 'n'. When 'n' is unity the Sips equation becomes the Langmuir equation. The parameter 'n' is typically regarded as the degree of system heterogeneity. Thus as 'n' increases in magnitude the system is considered to be more heterogeneous. The Sips equation loses accuracy with low concentration ranges.

$$q_e = q_m \frac{(b\,C_e)^{1/n}}{1+(b\,C_e)^{1/n}} \qquad (7)$$

Where:

b = adsorption affinity coefficient (L/mg)

q_m = maximum adsorption capacity (mg/g)

n = nonlinear index [dimensionless]

C_e = equilibrium concentration (mg/L)

q_e = equilibrium adsorption capacity (mg/g)

The linear form of the Langmuir-Freundlich equation can expressed as:

$$\ln\frac{q_e}{q_m - q_e} = \frac{1}{n}\ln(C_e) + \ln\left(b\frac{1}{n}\right) \qquad (8)$$

3.2.5. Fowler-Guggenheim Isotherm

The Fowler-Guggenheim equation is one of the simplest equations allowing for lateral interactions between adsorbed molecules. The exponential term $e^{-c\theta}$ represents the adsorbate-adsorbate interactions. When c < 0, there is repulsion between the adsorbate molecules and the amount adsorbed is linearly proportional to the concentration of the solution. When c > 0, co-operative adsorption begins to take place, thus there is strong attraction between adsorbed molecules. Under these conditions the isotherm curve begins to take a sigmoidal shape. If c > 4 then a discontinuity occurs and the isotherm curve undergoes a vertical step, a complete mathematical description of this process is provided by [78].

$$bC_e = \frac{\theta}{1-\theta}\exp(-c\theta) \qquad (9)$$

$$b = b_\infty\exp\left(\frac{Q}{R_g T}\right) \qquad (10)$$

$$c = \frac{zw}{R_g T} \qquad (11)$$

The Fowler-Guggenheim equation can be expressed as a linear function in the form:

$$\ln\left[\frac{C_e(1-\theta)}{\theta}\right] = -c\theta - \ln(b) \qquad (12)$$

3.3. Adsorption Kinetics

Adsorption kinetics is important in adsorption system design as it provides insights into the rate of solute uptake. Thus residence or contact times for adsorption systems can be estimated, which are essential for fixed-bed or any flow-through system design. Two distinct general approaches have been devised to describe adsorption kinetics: adsorption reaction models and adsorption diffusion models.

The latter approach to modeling assumes that adsorption must first undergo several distinct steps: (i) solute transport through the bulk of solution (ii) diffusion across the liquid film around the adsorbent; (iii) pore diffusion or intra-particle diffusion; (iv) adsorption and desorption of adsorbate on active sites [79]. Adsorption reaction models assume that the adsorption and desorption on active sites are the limiting steps to the adsorption process [79]. In this work two of the most widely used adsorption reaction models were used to model the experimental results. Application of diffusion models was beyond the scope of this work.

3.3.1. Pseudo-First Order Model
This empirical model for liquid-solid adsorption systems was first described by Lagergren in 1898, and is still one of the most widely used kinetic models [80]. The model has since then been derived using first principles [81]. Lagergren's first order equation is:

$$\frac{dq_t}{dt} = k_1(q_e - q_t) \qquad (13)$$

Where:

k_1 = pseudo-first order rate constant (min^{-1})

q_e = mass of adsorbate per unit mass of adsorbent at equilibrium (mg/g)

q_t = mass of adsorbate per unit mass of adsorbent at time t (mg/g)

t = time (min)

Integrating equation (13) using a known integral with boundary conditions, $t = 0$ to $t = t$ and $q = 0$ to $q = q_e$:

$$\int \frac{1}{ax + b} dx = \frac{1}{a} \ln |ax + b|$$

$$\ln(q_e - q_t) = \ln(q_e) - k_1 t$$

Manipulating the above expression provides:

$$q(t) = q_e(1 - e^{-kt}) \qquad (14)$$

S. Azizian, derived the Lagergren equation using the classical Langmuirian model to form a generalized approached for describing pseudo-first and pseudo-second order kinetic models [81]. To obtain the Lagergren model, Azizian, found that when the initial solute concentration was large, the general Langmuirian model could be simplified to the Lagergren equation. This indicates that a pseudo-first order (PFO) system may result due to large initial solute concentration. In this derivation, it was found that the PFO rate constant, k_1, is in fact a combination of the adsorption (k_a) and desorption (k_d) constants. This finding implies that the PFO rate constant is not the intrinsic adsorption rate constant – which had been reported [81]. The derivation also found that the PFO rate constant is a linear function of the initial concentration of solute:

$$k_1 = k_a C_o + k_d \qquad (15)$$

By this logic one would be able to determine k_a and k_d by determining k_1 for various initial C_o.

At steady state the assumptions used to derive pseudo-first and second order kinetic models by Azizian becomes the well-known Langmuir isotherm equation. Thus the foundations of both first and second order kinetic models are based on the assumptions used in the Langmuir isotherm (e.g. homogenous surface, one site occupancy, etc).

3.3.2. Pseudo-second Order Model

The pseudo-second order (PSO) model was proposed by Blanchard et al. to describe the adsorption kinetics of heavy metal ion removal by zeolites [82]. The empirical equation he proposed can be written as:

$$\frac{dq_t}{dt} = k_2(q_e - q_t)^2 \quad (16)$$

Where:

$k_2 =$ pseudo-second-order rate constant of sorption $\left(\frac{g}{mg \cdot min}\right)$

$q_e =$ mass of adsorbate per unit mass of adsorbent at equilibrium (mg/g)

$q_t =$ mass of adsorbate per unit mass of adsorbent at time t (mg/g)

$t =$ time (min)

By integrating the above equation with the boundary conditions, $t = 0$ to $t = t$ and $q = 0$ to $q = q_e$ the following equations can be obtained:

$$\frac{1}{q_e - q} = \frac{1}{q_e} + k_2 t \quad (17)$$

The linear form is:

$$\frac{t}{q} = \frac{1}{q_e}t + \frac{1}{k_2 q_e^2} \quad (18)$$

Plotting t/q vs t, the slope of the line yields the value for q_e while the y-axis intercept provides the second order sorption rate constant k_2. The general form for q(t) is provided below:

$$q(t) = q_{eq}\frac{q_{eq}k_2 t}{q_{eq}k_2 t + 1} \quad (19)$$

Azizian found that k_2 is a complex function of the initial concentration of solution C_o. The derivation demonstrated that when the initial concentrations of solute were not too elevated, the term assumed to be negligible for the pseudo-first order model could not be omitted. The resulting system follows the pseudo-second order kinetic adsorption.

3.4. Multi-component adsorption

Experimental data for multi component systems is difficult and tedious to obtain. It is for this reason that many models developed rely on single compound adsorption results to approximate multi-component adsorption behaviour [83]. Commonly used models include the Extended-Langmuir model and the Extended Langmuir-Freundlich model.

3.4.1. The Extended-Langmuir Model

The Extended-Langmuir model maintains the assumptions used to develop the original Langmuir model. A limitation of the Extended-Langmuir model is that it requires the single solute adsorption to follow the Langmuir regime. The single solute adsorption constants are then used in the multi-component Extended-Langmuir model [83].

$$q_i = \frac{a_i c_i}{1 + \sum_{j=1}^{N} b_j c_j} \qquad (20)$$

Where:

c_i = concentration of the i_{th} adsorbate in the solution (mg/L)

a_i and b_i = single-component liquid-phase adsorption isotherm

parameters of the i_{th} adsorbate (L/g)

3.4.2. The Extended Langmuir-Freundlich Model

Similarly to the extended Langmuir model the single compound Langmuir-Freundlich equation has been extended to multi-component systems as follows:

$$q_i = \frac{a_i c_i^{1/n_i}}{1 + \sum_{j=1}^{N} b_j c_i^{1/n_j}} \qquad (21)$$

Where:

c_i = concentration of the i_{th} adsorbate in the solution

$[(mg/L)^{1/n}]$

a_i and b_i = single-component liquid-phase adsorption isotherm

parameters of the i_{th} adsorbate $[\frac{L^{1/n} \, mg^n}{g}]$

Chapter 4: Materials & Methods

The equilibrium and kinetic adsorption experiments for each model naphthenic acid (NA) were first conducted. Subsequently, the multi-component adsorption of the mixture of the model NAs was performed to determine the equilibrium and kinetics of adsorption. The following section describes the methodology employed in this study.

4.1. Preparation of Activated Carbon

The granular activated carbon (GAC) used for the adsorption experiments was Norit ROW 0.8 SUPRA (CAS Number: 7440-44-0), purchased from Sigma-Aldrich Canada Co. (Oakville, Ontario, Canada). Prior to use the GAC was first washed in order to remove fines and subsequently dried. The washing was performed by using a 1 L Erlenmeyer flask and adding approximately 2 g of GAC with 400 mL of MilliQ water. The flask was agitated for 15 min using a MaxQ 4000 Bench-top Orbital Shaker (Thermo Scientific) set to 170 rpm, after which the water was decanted along with any GAC that did not sink to the bottom of the flask. Two more rinses of 45 min were performed, using 400 mL of MilliQ water. Once completed, the water was decanted and the flask was placed in a heated oven at 110 ºC for 3 hrs. After 3 hrs the hot GAC was transferred to a glass jar, capped and placed in a desiccator. The moisture of the dried carbon was assumed to be negligible and thus any carbon measured for the experiments was on a dry basis.

4.2. Characterization of the Activated Carbon

A scanning electron microscope (SEM) image taken of the GAC is shown in Figure 4-1. The particle size distribution was obtained for the washed GAC and the results are shown in Table 4 - 1. The general characteristics of the GAC used are provided in Table 4 - 2. The values tabulated are those provided by the manufacturer (Cabot Norit Activated Carbon).

Table 4 - 1: Particle size distribution results for washed granular activated carbon

Particle Size Distribution	
X_{10}	551.63 ± 0.45 μm
X_{50}	694.32 ± 0.33 μm
X_{90}	836.39 ± 0.11 μm

Table 4 - 2: General characteristics of GAC used for adsorption study

General Characteristics		
Iodine number	1175	-
Methylene blue adsorption	24	g /100 g
Total surface area (BET)	1300	m^2 / g
Apparent density	400	kg / m^3
Particle Size < 0.60mm	0.1	Mass - %
Ash content	7	Mass - %
pH	Alkaline	
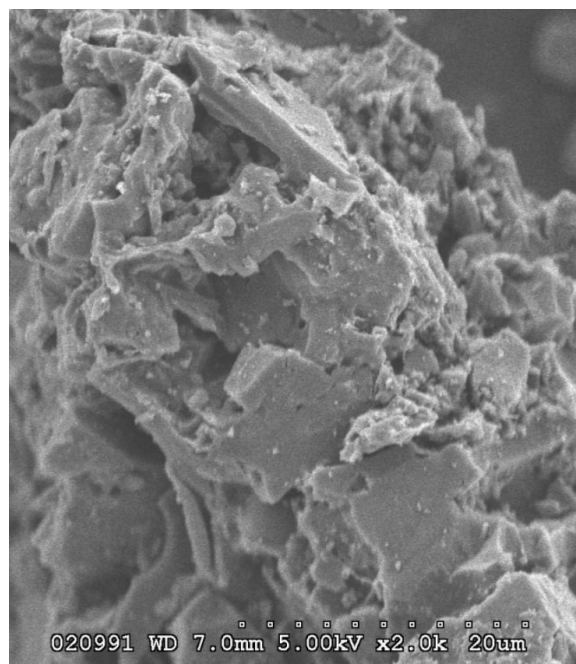
Figure 4 - 1: SEM of commercial GAC used
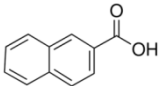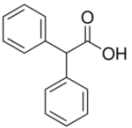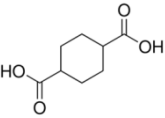
4.2.1. Point of Zero Charge

The point of zero charge of the GAC was determined using the pH drift method [65], [66], [70], [71]. 50 mL of 0.1 M NaCl solution was adjusted to pH values between 3 and 11, by adding either HCl or NaOH. Then 0.15 g GAC was added to vials with NaCl solution. The vials were then flushed with nitrogen gas, capped, and placed in an orbital shaker at 170 rpm for 32 hrs at room temperature (23 °C). The vials were opened and the pH values recorded, with final pH plotted against the initial pH. The point which $pH_{initial} = pH_{final}$ was taken to be the point of zero charge.

4.3. Preparation of Naphthenic Acid Solution

The acids selected as model compounds for this investigation were 2-naphthoic acid, diphenylacetic acid, and 1,4-cyclohexanedicarboxylic acid. Relevant chemical information is presented in Table 4 - 3.

Table 4 - 3: Model compounds used for both single and multi-component experiments

	Name:	Formula:	MW:	pKa:	Structure:
1	2-Naphthoic acid Purchased from: VWR CAS Registry No: 93-09-04	$C_{11}H_8O_2$	172	4.16^3 4.20^4	
2	Diphenylacetic acid Purchased from: Sigma-Aldrich CAS Registry No: 117-34-0	$C_{14}H_{12}O_2$	212	4.72^4	
3	1,4-Cyclohexanedicarboxylic acid Purchased from: VWR CAS Registry No: 1076-97-7	$C_8H_{12}O_4$	172	1) $3.54 (0)^3$ 2) $4.46 (-1)^3$	

3. Value obtained from Lange's Handbook of Chemistry [49].

4. Value obtained from SciFinder online chemical data base.

4.3.1. NA Solution Preparation

The model acids purchased were all in crystal form. No studies citing the solubility of the three model NAs used were found. Solubility values were obtained from Sci-finder, which uses a predictive algorithm to estimate compound solubility based on molecular structure. The predicted solubility for each model compound is provided in Table 4 - 4.

Table 4 - 4: Model compound solubility as reported by Sci-finder

Model Compound	Predicted Solubility (g/L)
1,4-Cyclohexanedicarboxylic acid	28
2-Naphthoic acid	0.26
Diphenylacetic acid	0.28

The predicted solubility values conflicted with the experimental trials for 2-naphthoic acid. It was found that solutions with concentrations greater than 50 mg/L resulted in solute re-crystallization upon cooling during preparation. Diphenylacetic acid and 1,4-cyclohexanedicarboxylic acid had no observable re-crystallization with solutions of up-to 100 mg/L. Selecting the least soluble compound as the reference, the initial concentration used for the single compound solutions investigated was 40 mg/L. To make the acid solutions, the appropriate amount of acid was first weighed with a Metrohm Toledo AB304-S/FACT, and subsequently transferred to a volumetric flask. The flask was partially filled with MilliQ water and the solution was left over 48 hrs to stir on a hot plate at 70 °C. Thereafter, the solution was allowed to stir for another 24 hrs after which MilliQ water was added to make the desired concentration.

4.3.2. Multi-Component Solution Preparation

For the multi-component solutions, made from the three NAs, the concentration of each NA was 40 mg/L. In this manner the total NA concentration of the solution was 120 mg/L. The same protocol to make the solutions was used for the multi-component mixture as that described for single component solutions.

4.4. Batch Adsorption Experiments

Batch adsorption experiments were carried out using a MaxQ 4000 Bench-top Orbital Shaker (Thermo Scientific). The unit was operated at room temperature (23 ^{0}C) and 170 rpm. The experiments were carried out using 500 mL Erlenmeyer flasks, filled with 175 mL of solution. The volume of the solutions used for the adsorption studies were held fixed in order to ensure that no variation in agitation, or carbon loading to solution ratio occurred. All adsorption studies were carried out in duplicates, whose values were averaged and subsequently analyzed.

The rpm was selected by measuring the adsorption rate during the transient stage of adsorption. If the adsorption was limited by poor mixing then it was expected to increase with rpm. However, the inverse was observed, with adsorption rates decreasing at elevated values of rpm. This may be the result of vortexing, with most of the GAC being concentrated in the center of the vortex, while the bulk of the fluid was at the outer rim of the flask. Based on these preliminary tests an rpm of 170 was selected. Preliminary adsorption experiments concluded that equilibrium was reached within 48 hrs. This duration was used for all subsequent adsorption experiments. For the kinetics adsorption experiments, ten samples of 1 mL were taken at 5 min, 15 min, 30 min, 1 hr, 2 hr, 4 hr, 6 hr, 8 hr, 24 hr, and 48 hr. With a 175 mL sample this represented a reduction in volume of less than 6 % and was deemed acceptable. Samples for both kinetic and isotherm experiments were taken by first pipetting 1 mL from the Erlenmeyer flasks and then filtering them using a 0.45 μm nylon syringe filter.

4.5. NAs Analysis

A UV-VIS-NIR spectrophotometer, Shimadzu UV-3600, was used to scan over the UV-VIS range to determine the spectral absorption profile for the NA. Two Starna Far UV Quartz Cells (Mandel Scientific Company Inc.) of 3.5 mL were used. The UV spectral profile of 2-naphthoic acid and diphenylacetic acid showed a peak for the carboxyl moiety and a triple peak for the benzene rings. The profile obtained is similar to that found by [84], for 2-naphthoic acid. The maximum peak for the benzene moiety was found to occur at 280 nm, while that for the carboxyl moiety occurred at 188 nm. The maximum UV absorbance values for each moiety (benzene and

carboxyl) were used to set-up the UV-VIS detector of the high-performance liquid chromatography (HPLC) system.

4.6. HPLC System

A Dionex ICS-3000 was used in an isocratic HPLC configuration to detect the model acids selected for the experiment using an Acclaim Fast LC Column 120 C18, 3 x 75 mm. The mobile phase used was an acetonitrile (ACN) water mixture. For 2-naphthoic acid and diphenylacetic acids the mobile phase was 60% ACN and 40% H_2O (MilliQ). For 1,4-cyclohexane dicarboxylic acid the mobile phase used was 47% ACN and 53% H_2O (MilliQ).

The mobile phase was prepared in a 2 L volumetric flask, and was acidified with sulphuric acid to pH 2.15, which was above the minimum recommended pH for the C18 column. Acidification of the mobile phase was performed in order to ensure that the acids were in molecular form during analysis. For the acidification, the mobile phase was stirred in a 2 L beaker and sulphuric acid was slowly added until the pH was 2.15. The pH was measured using an Orion Star A111 pH bench-top meter ± 0.01 pH. The mobile phase was then filtered using a vacuum filtration apparatus with a 0.20 μm, 47 mm polytetrafluoroethylene (PTFE) disk filter. Filtration was performed to remove any insoluble contaminants that may be present within the sulfuric acid.

Prior to any analysis the HPLC system was initialized and allowed to equilibrate for 60 min or until the baseline was stable. Upon completion of an analysis the column was rinsed with 20% ACN water solution in order to wash out the acidic mobile phase which could deteriorate the column over long exposure.

Chapter 5: Results and Discussion

The first half of this chapter presents the single compound isotherm results, section 5.1., followed by the single component kinetics, section 5.2. The second half presents multi-component adsorption isotherms and kinetics, in sections 5.3 and 5.4, respectively. Two sets of experiments conducted in triplicates were first performed to determine the maximum error. The experiments were performed for 2-naphthoic acid at pH 7 and 8 for which the maximum error was found to be less than 5 %. All the adsorption results presented in this chapter are average values obtained from experiments carried out in duplicates with errors less than 5%.

5.1. Single Compound Adsorption

The typical concentration vs time plots for the adsorption of model naphthenic acids at pH 4 are shown in Figure 5 - 1. The percentage removal increased with carbon dosage as shown in Table 5 - 1. The maximum percentage removal occurred within the first 8 hrs (480 min) and steadily declined until quasi-equilibrium was reached at 48 hrs (2880 min). Based on the percentage removal for 57 mg/L carbon loading, the relative affinity of the model compounds to the GAC was: 1,4-cylohexanedicarboxylic acid (70 %) > 2-naphthoic acid (50 %) > diphenlyacetic acid (25 %). The carbon loading for each compound varied within the range of 50 mg/L - 600 mg/L.

Table 5 - 1: Typical removal rates for model compounds at pH 4

2-Naphthoic Acid	
% Removal:	Carbon Load:
50	57 mg/L
Diphenylacetic Acid	
% Removal:	Carbon Load:
25	57 mg/L
1,4-Cyclohexanedicarboxylic Acid	
% Removal:	Carbon Load:
70	57 mg/L

The adsorption isotherm data for the single solute adsorption experiments was fitted using nonlinear regression methods in MatLab. More specifically the curve fitting toolbox was used, accessed through the command line by entering: *cftool*. The model parameters for 2-naphthoic acid were initially determined using the linearized equations for the adsorption models described in Chapter 3. The model parameters obtained in this manner did not fit the experimental data better than those obtained by using MatLab. Linear regression was thus not used for further isotherm model fitting.

It must be noted that the need to linearized equations was once very important before the advent of computers. With today's powerful computational programs (i.e. MatLab, Excel, SigmaPlot, etc) there is no need to use linearized models as nonlinear regression algorithms can easily be employed [85]. Multiple linear forms of a single adsorption model can be obtained through algebraic manipulation [67], [77]. Linearized adsorption models have been found to distort error and lead to differing results during the determination of the unknown model parameters [67], [77], [86]. Since distortions can vary depending on the form of the linear equation being used, it would appear that linearized models should no longer be employed for adsorption studies, though this is not the case today.

In order to determine the closeness to which an adsorption model represented the experimental data, appropriate error functions were used. These functions are presented in Table 5 - 2 below. Multiple error functions have been used to analyze adsorption data, though no standardized error analysis has been developed [75]–[77], [85].

a)

b)

c)
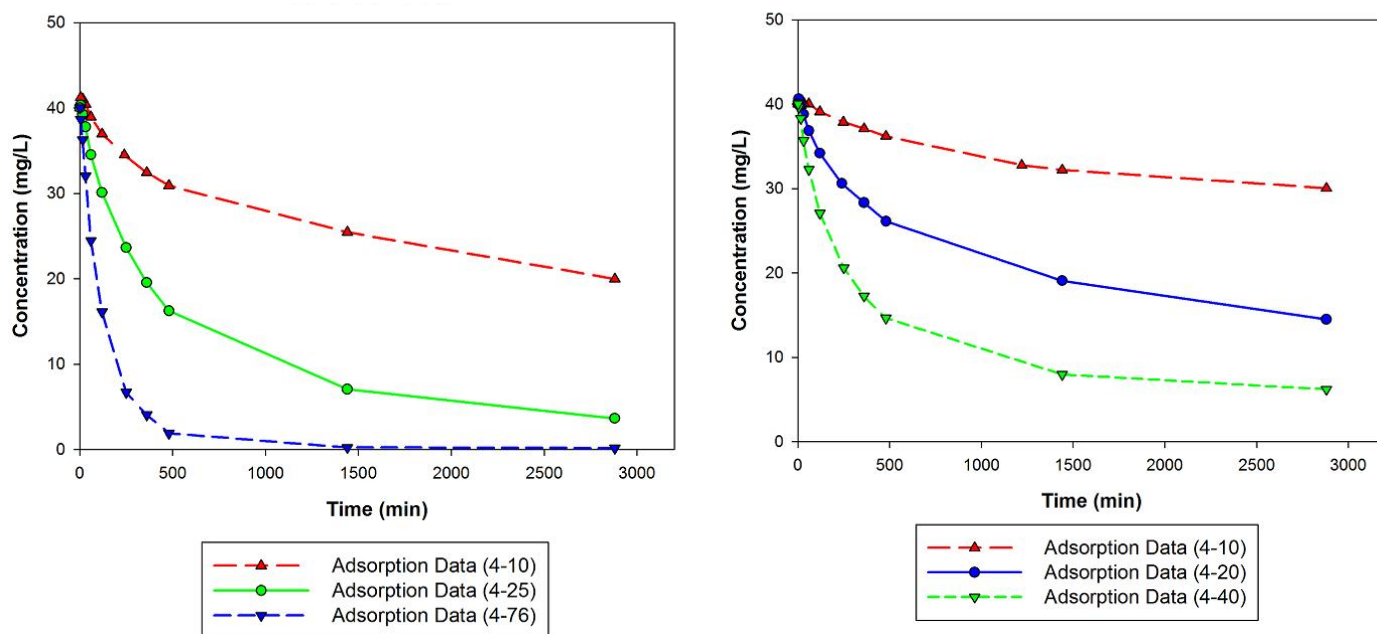
Figure 5 - 1: Typical concentration vs. time plots for: a) 2-naphthoic acid; b) diphenylacetic acid; c) 1,4-cyclohexanedicarboxylic acid

Figure legend entries within parenthesis, (#1-#2), indicate experimental conditions with #1 referring to the pH and #2 to the weight of carbon added to the 175 mL samples prepared. Thus, (4-10) indicates initial pH of 4 and 10 mg of GAC/175mL solution, resulting in a carbon loading of 57 mg/L.

Table 5 - 2: Error functions used to compare experimental data to theoretical adsorption models

Error Function:	Abbreviation:	Expression:
Coefficient of determination	R^2	$$1 - \frac{SSE}{SS_{yy}} = 1 - \frac{\sum_i^n (y_{measured,i} - y_{fit,i})^2}{\sum_i^i (y_{measured,i} - \bar{y})^2}$$
Sum of the squared errors	SSE	$$\sum_{i=1}^{n} (q_{e,calc} - q_{e,meas})_i^2$$
Nonlinear chi-square test	χ^2	$$\sum_{i=1}^{n} \left(\frac{(q_{e,calc} - q_{e,meas})^2}{q_{e,meas}} \right)_i$$

The simplest used measure of the goodness of fit is the sum of the square error (SSE), which determines the square of the error between a given data point and its corresponding theoretical value. Another error function commonly used is the nonlinear Chi-square test. For both the SSE and Chi-squared error functions, a best fit is one that results in zero, or a value that approaches zero. If SSE and Chi-squared values resulted in conflicting best fitting models, then the SSE was selected as the indicative error function.

The values for the coefficient of determination (R^2) have been calculated as this is the most commonly used coefficient for determination of the goodness of fit. The coefficient of determination may be biased when applied to nonlinear functions. SS_{yy} represents the total variation in y and thus the squared error from the mean of the data set. The term SSE/SS_{yy} can be understood as the percentage that the model fails to describe the said data set. Since the mean of can be biased towards an extreme of the data, the errors resulting from the difference can fail to accurately represent the fit of the model to the data. Values for the coefficient of determination vary from 0 to 1, with 1 being an exact fit between the model and the data set. The model parameters and the resulting error functions obtained for single compound isotherm experiments are presented in Table 5 - 3 to Table 5 - 5.

Table 5 - 3: 2-Naphthoic acid Langmuir, Freundlich and Langmuir-Freundlich adsorption model parameters

2-Naphthoic Acid
	Langmuir					**Freundlich**					**Langmuir-Freundlich**					
pH	K_L	q_m	R^2	SSE	χ^2	K_F	n	R^2	SSE	χ^2	K_s	n	q_m	R^2	SSE	χ^2
4	1.53	322.9	0.9084	8131	56.71	163.30	4.42	0.9663	2330	10.15	4.26E-1	2.65	567.6	0.9735	1825	8.34
7	4.37	181.7	0.8190	3009	23.69	115.70	6.35	0.9724	431	2.32	3.99E-1	4.51	410.8	0.9705	619	3.11
8	3.29	156.7	0.6418	3792	31.77	95.76	5.80	0.9202	841	7.60	3.19E-1	1.80	259.8	0.9065	4996	55.77
9	3.52	148.1	0.6179	2449	19.52	87.44	5.09	*0.9486*	336	3.42	2.49E-1	1.92	297.1	*0.9404*	2027	26.24

Table 5 - 4: Diphenylacetic acid Langmuir, Freundlich and Langmuir-Freundlich adsorption model parameters

Diphenylacetic Acid
	Langmuir					**Freundlich**					**Langmuir-Freundlich**					
pH	K_L	q_m	R^2	SSE	χ^2	K_F	n	R^2	SSE	χ^2	K_s	n	q_m	R^2	SSE	χ^2
4	0.13	392.3	0.9142	2190	9.33	99.30	2.97	0.8533	3733	16.16	3.98E-2	0.56	328.2	0.9362	1617	6.52
7	0.95	148.7	0.6546	585	4.06	100.10	9.38	0.8475	348	2.19	2.30E-3	7.23	40910	0.8531	248	1.71
8	1.99	131.9	0.4738	1206	10.74	87.75	7.22	0.7887	483	4.45	4.88E-3	8.48	19910	0.7826	734	6.98
9	1.04	144.0	0.6247	1182	9.71	85.07	5.96	0.8694	406	3.34	3.34E-3	6.75	26850	0.8656	440	3.48

Table 5 - 5: 1,4-Cyclohexanedicarboxylic acid Langmuir, Freundlich and Langmuir-Freundlich adsorption model parameters

1,4-Cyclohexanedicarboxylic Acid
	Langmuir					**Freundlich**					**Langmuir-Freundlich**					
pH	K_L	q_m	R^2	SSE	χ^2	K_F	n	R^2	SSE	χ^2	K_s	n	q_m	R^2	SSE	χ^2
4	5.18E-2	787.2	0.5458	31984	95.48	77.32	1.85	0.4954	35130	104.37	1.34E-7	0.14	452.6	0.8793	8411	23.82
7	*	*	*	*	*	*	*	*	*	*	*	*	*	*	*	*
8	*	*	*	*	*	*	*	*	*	*	*	*	*	*	*	*
9	*	*	*	*	*	*	*	*	*	*	*	*	*	*	*	*

* Models investigated were unable to converge or provide meaningful fitting for the experimental data obtained due to insufficient data points.

Table 5 - 6: Models that provided the best fit for isotherm adsorption experiments

	2-Naphthoic Acid	Diphenylacetic Acid	1,4-Cyclohexanedicarboxylic Acid
pH	Best fit model:	Best fit model:	Best fit model:
4	Langmuir-Freundlich	Langmuir-Freundlich	Langmuir-Freundlich
7	Freundlich	Langmuir-Freundlich	No fit
8	Freundlich	Freundlich	No fit
9	Freundlich	Freundlich	No fit

By analysing the values of the error functions obtained for the adsorption studies it was found that the Langmuir model failed to accurately fit the data. Only for the solution pH of 4 did the Langmuir model provide a reasonable fit. This was not surprising as the model assumes a homogenous surface. Since activated carbon has a heterogeneous surface it was expected that the results favour either the Freundlich or Langmuir-Freundlich isothermal models. None of the three models provided acceptable fits for 1,4-cyclohexanedicarboxylic acid for pH other than four. The models resulting in a best fit for 2-naphthoic acid and diphenylacetic acid at each pH are presented in Table 5 - 6.

The adsorbent saturation capacity, q_m (mg adsorbed/g adsorbent), was calculated and tabulated in Table 5 - 7 and Table 5 - 8 for 2-naphthoic acid and diphenylacetic acid, respectively. The values in bold correspond to the saturation capacity of the best fit model for the respective experiment. Though no values for the saturation capacity were obtained for pH's other than 4, for 1,4-cyclohexanedicarboxylic acid, it is interesting to note that the values of q_e measured were larger than the values of q_m obtained for both 2-naphthoic acid and diphenylacetic acid. Indicating that the saturation capacity of 1,4-cyclohexanedicarboxylic acid is most likely larger than those of the other two model compounds studied. With two carboxylic acid groups, 1,4-cycloheanedicarboxylic acid exhibited better affinity toward basic activated carbon surface.

For diphenylacetic acid, the values obtained for q_m for the Langmuir-Freundlich model were typically too large to be physically representative of the saturation capacity of the adsorbent.

This can indicate that the Langmuir-Freundlich model parameter q_m was not a physically representative value of the adsorbent capacity but simply an empirical constant used to fit data.

In Table 5 - 7 and Table 5 - 8 the values presented for the Langmuir-Freundlich model are the values of q_e at $C_e = C_o$ (40 mg/L). These values are tshus assumed to be the saturation capacity, q_m. Similarly the value of q_e for the Freundlich model was determined at $C_e = C_o$ to obtain q_m – refer to Chapter 3 Freundlich model.

The marked reduction in q_m as a function of increasing pH for both 2-naphthoic acid and diphenylacetic acid is shown in Figure 5 - 2. Both compounds approach an asymptotic minimum where their adsorption capacity drops by 50 % from its maximum at pH 4. 2-Naphthoic acid from a maximum of 357 mg/g to 180 mg/g, and diphenylacetic acid went from a high of 318 mg/g to 158 mg/g. Similar reductions in adsorbent capacities with increased pH have been found with other organic compounds [65], [66], [69], [71]. Additionally it has been reported that if acidification of OSPW was not performed the effective adsorption of naphthenic acids on activated carbon decreased [15]. 2-Naphthoic acid showed a higher adsorption capacity compared to diphenylacetic acid. It is interesting to note that the overall percentage drop with increasing pH was the same for both compounds. Both compounds with one carboxyl moiety and similar pK_A values, showed similar performance with pH variation.

The reduction in adsorptive capacity with increasing pH may be explained by the surface charge of the activated carbon. The carbon used was basic and had a point of zero charge of approximately 9.7 (as shown in Figure 5 - 3). At pH < pH_{pzc}, the net surface charge of activated carbon is positive while for pH > pH_{pzc} the surface charge is negative [87]. It is believed that the dissociated acids have a preferential attraction to the positively charged surface, and hence better adsorption capacity at low pH.
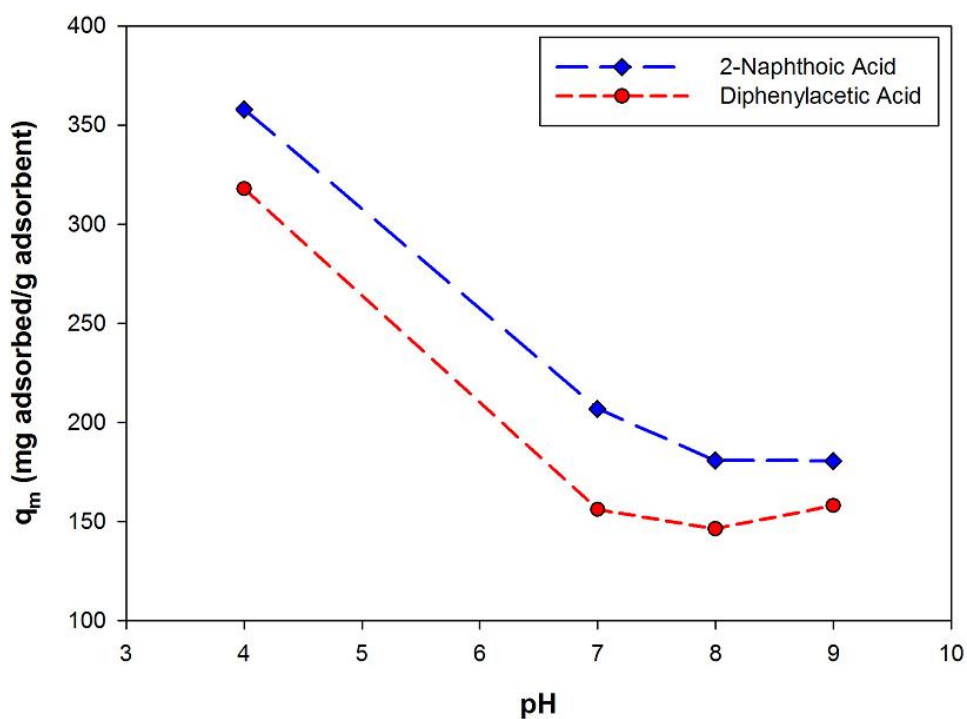
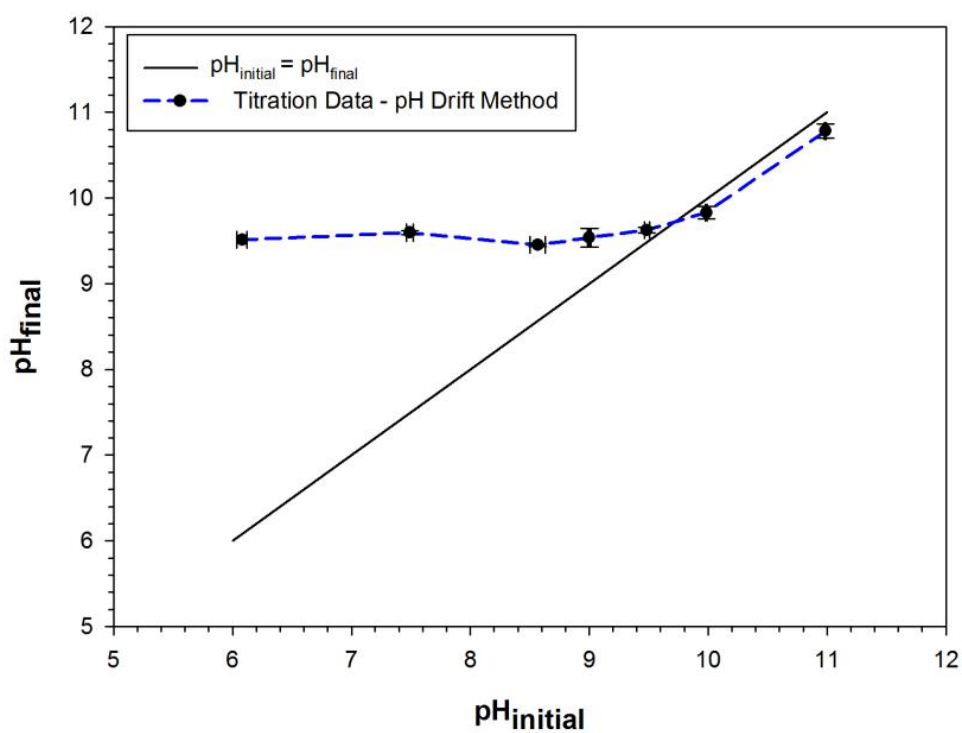**Figure 5 - 2: Reduction in adsorbent capacity vs. solution pH for 2-naphthoic acid and diphenylacetic acid**

Figure 5 - 3: Point of zero charge for Norit ROW 0.8 SUPRA by pH drift method

Table 5 - 7: Saturation capacity q$_m$ of 2-naphthoic acid

2-Naphthoic Acid			
	Langmuir	Freundlich	Langmuir-Freundlich
pH	q$_m$	q$_m$	q$_m$
4	323	376	*358*
7	182	*207*	195
8	157	*181*	185
9	138	*180*	*187*

Table 5 - 8: Saturation capacity q$_m$ of diphenylacetic acid

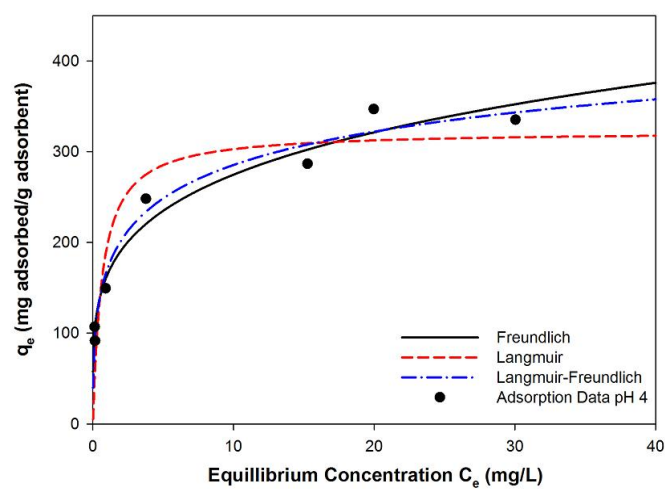| Diphenylacetic Acid			
	Langmuir	Freundlich	Langmuir-Freundlich
pH	q$_m$	q$_m$	q$_m$
4	392	344	*318*
7	149	148	*156*
8	132	*146*	149
9	144	*158*	154

From the isotherm plots of 2-naphthoic acid (Figure 5 - 4), we see that the initial slope is very high. The adsorption isotherms of this nature fall within the H isotherm category as defined by Giles et al [72], [74]. For diphenylacetic acid (Figure 5 - 5), it can be seen that at pH 4 the adsorption isotherm is similar to the L-class. As the pH is increased the isotherm becomes H-class. The isotherms for 1,4-cyclohexanedicarboxylic acid (Figure 5 - 6) appear to be S-class which can have significant vertical portions where adsorption capacity is increased with increasing surface coverage. Only at pH 4 and 8, the plots appear to begin to reach a steady value for q$_e$. The lack of data over a wide range of equilibrium concentrations makes it difficult to clearly analyze the results, though we can preliminarily predict that cooperative adsorption, typically denoted by a sudden increase in q$_e$, is taking place. It is similar to the Langmuir-Freundlich model that was fitted for the data at pH 4. The apparent vertical portion of the graphs suggest that the isotherms adheres best to the Fowler-Guggenheim model which exhibits a vertical discontinuity and includes lateral adsorbate interactions [78].

The importance of comparing isotherm profiles and their classifications is that they dictate the capacity of the adsorbent at varying equilibrium concentrations. If a process requires the removal of a contaminant to low levels then it is best that the adsorbent follow an H-class isotherm profile where it has a relatively high capacity at low concentrations. The S-class profile shown for 1,4-cylclohexanedicaboxylic acid though showing high values of equilibrium capacity at elevated equilibrium concentrations showed little removal for lower concentrations. This may be a problem if low concentration of the acid is needed for detoxification of process waters.

Since it was found that adsorption capacity was sensitive to pH, it must be noted that a limitation of this work was the experimental method used for batch adsorption which did not actively control the pH. The pH was only adjusted prior to the onset of adsorption, thus fluctuations due to acid adsorption, ion exchange with the activated carbon, and CO_2 diffusion into the system were not accounted for. The maximum and minimum values measured for pH at the completion of the isotherm experiments are presented in Table 5 - 9.

Table 5 - 9: Final equilibrium pH for the isotherm experiments, showing maximum and minimum pH values obtained
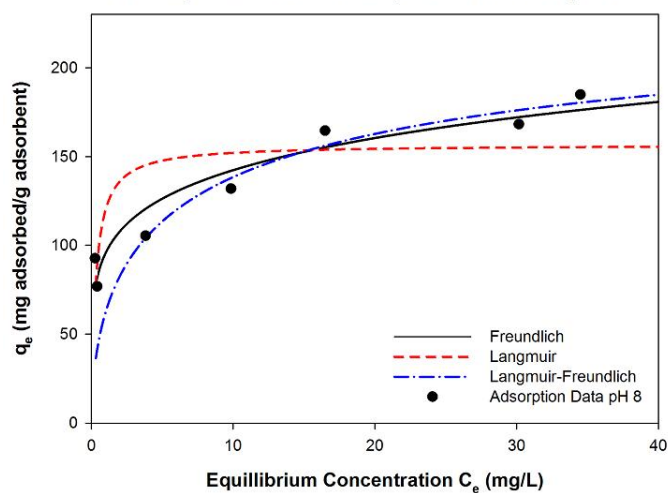
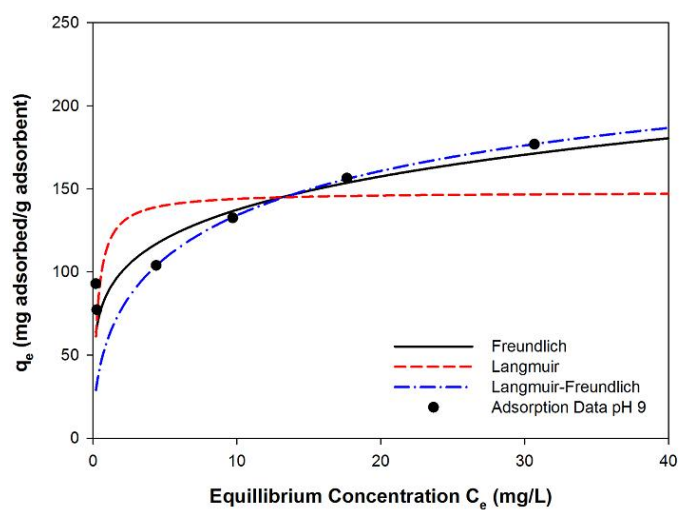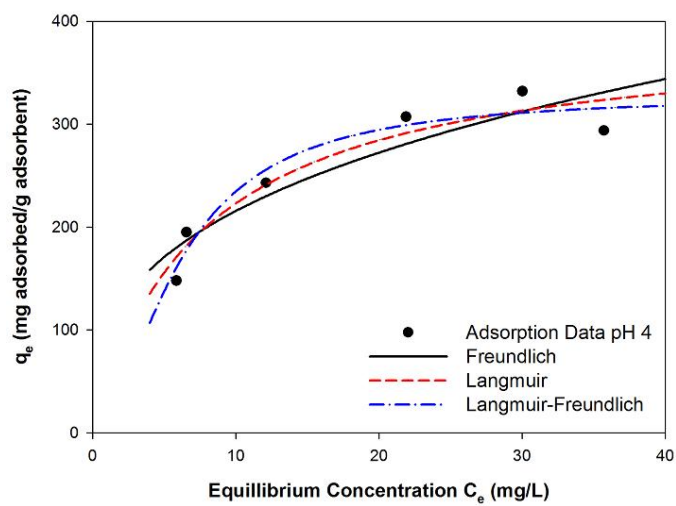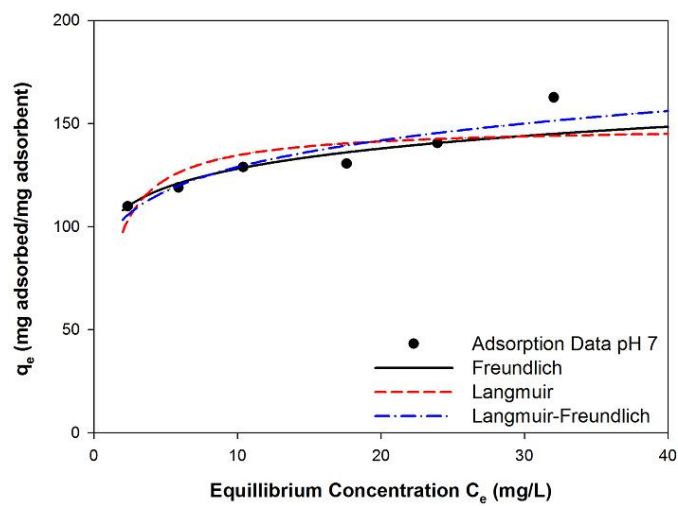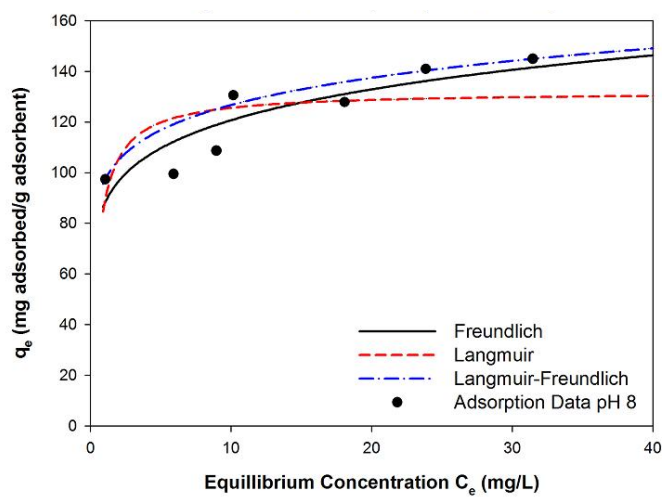| Initial pH:	2-Naphthoic Acid	Diphenylacetic Acid	1,4-Cyclohexanedicarboxylic Acid
4	4.19 – 6.81	4.12 – 6.39	4.11 – 4.48
7	7.32 – 8.15	7.01 – 7.64	7.12 – 7.75
8	7.52 – 9.07	7.30 – 7.97	7.38 – 7.95
9	7.68 – 9.21	7-39 – 8.25	7.26 – 7.87

a)
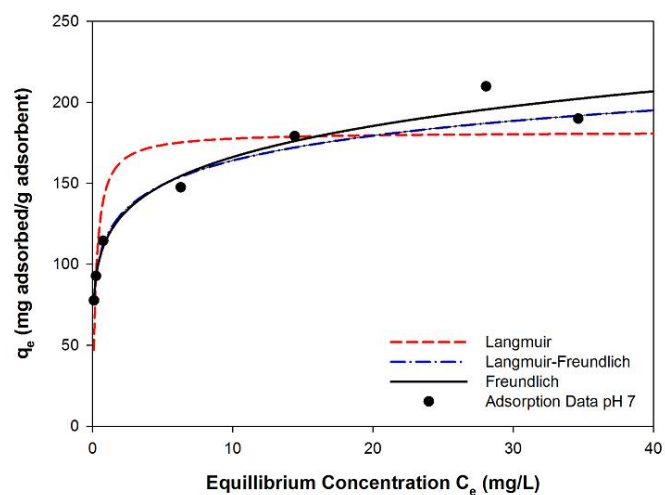
b)

c)

d)

Figure 5 - 4: 2-Naphthoic acid adsorption isotherm results: a) pH 4; b) pH 7; c) pH 8; d) pH 9
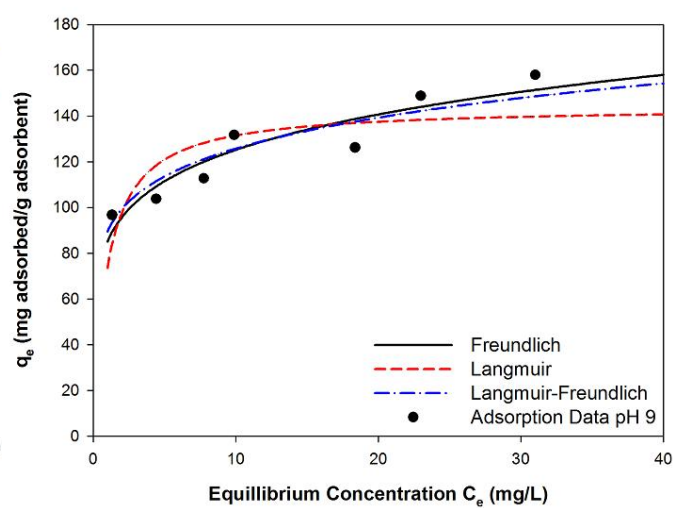
a)

b)

c)

d)

Figure 5 - 5: Diphenylacetic acid adsorption isotherm results: a) pH 4; b) pH 7; c) pH 8; d) pH 9
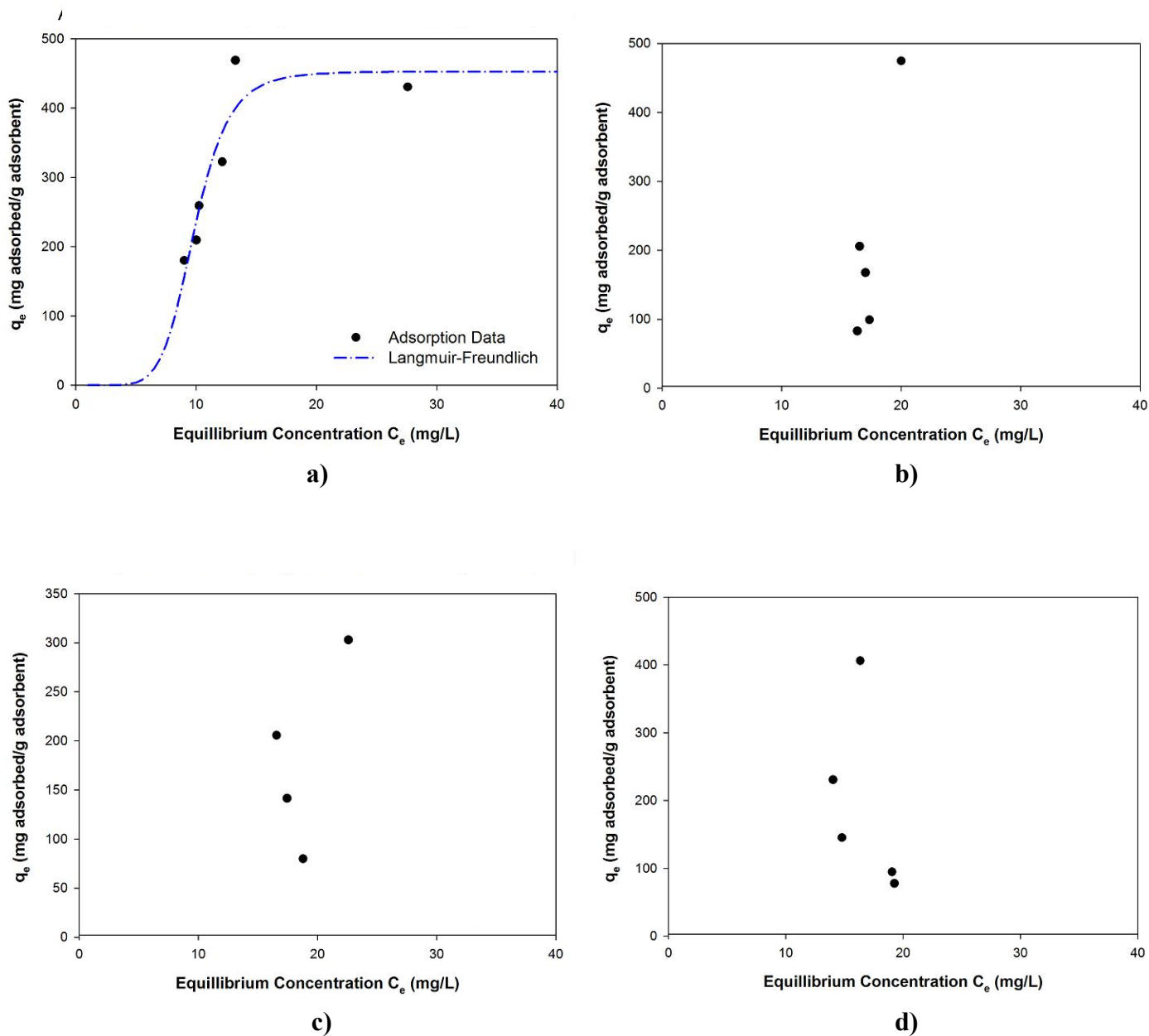
Figure 5 - 6: 1,4-Cyclohexanedicarboxylic acid adsorption isotherm results: a) pH 4; b) pH 7; c) pH 8; d) pH 9

5.2. Single Compound Kinetic Results

As shown in Table 5 - 10, Table 5 - 12 and Table 5 - 14, both PFO and PSO kinetic models provided good fits under different experimental conditions for the three NAs. For a description of both models refer to Chapter 3. The analysis of the data will be limited to a comparative study of the changes in the response time resulting from changes in experimental conditions and compounds. To appropriately quantify the system response, the time constant (τ), a measure of the time a first-order system takes to reach 63.2 % (q_t/q_e) of the final steady state response, was determined. The half-time (t_{50}), time for the system to reach 50 % of the steady state response, was also calculated as a comparative parameter to other adsorption studies. The time constant was preferred as it is widely used in numerous kinetic processes in chemical engineering to provide insight into the response time of first-order systems.

5.2.1. 2-Naphthoic Acid Kinetic Results

A compilation of the parameters of the PFO and PSO models along with the results of the three error functions, for 2-naphthoic acid, are presented in Table 5 - 10. From these results it is observed that both PFO and PSO models fit the data well under the different experimental conditions. The best fitting model for each experiment and its corresponding response time is presented in Table 5 - 11. Graphs of the experimental data and resulting PFO and PSO fitted curves are shown in Figure 5 - 7.

Table 5 - 10: Summary of the kinetic modeling using pseudo-first order and pseudo-second order models for 2-Naphthoic acid

2-Naphthoic Acid											
		Pseudo-First Order (PFO)					Pseudo-Second Order (PSO)				
pH	CL*	k_1	q_e	R^2	SSE	χ^2	k_2	q_e	R^2	SSE	χ^2
4	434	7.69E-3	90.34	0.9989	15.45	0.47	9.99E-5	100.40	0.9917	143.98	5.90
4	142	2.27E-3	251.79	0.9966	324.04	19.5	9.17E-6	290.30	0.9990	116.01	36.81
4	57	1.24E-3	290.30	0.9890	2019.38	10.05	2.00E-6	471.30	0.9929	991.45	7.46
7	428	4.22E-3	92.49	0.9979	52.61	2.36	5.15E-5	105.50	0.9956	72.00	1.73
7	142	1.65E-3	186.00	0.9954	221.25	4.79	7.82E-6	222.41	0.9921	351.00	3.03
7	57	1.32E-3	179.82	0.9776	1078.09	20.90	4.74E-6	234.70	0.9882	598.80	19.86
8	428	4.21E-3	92.13	0.9984	31.89	1.71	4.74E-5	106.80	0.9957	75.98	2.48
8	142	1.88E-3	161.00	0.9956	154.85	57.00	9.71E-6	195.80	0.9986	52.72	82.57
8	57	1.37E-3	187.00	0.9877	690.34	111.80	5.38E-6	228.70	0.9941	255.01	128.60
9	428	5.00E-3	91.48	0.9977	50.59	2.38	5.79E-5	104.30	0.9965	54.73	0.70
9	142	1.76E-3	157.2	0.9980	66.68	12.26	8.93E-6	191.08	0.9974	126.75	18.54
9	57	8.03E-4	207.2	0.9873	681.80	7.40	1.85E-6	295.40	0.9911	369.40	4.64

*CL = carbon load (mg/L)

**Table 5 - 11: 2-Naphthoic acid kinetic data and best fit used**

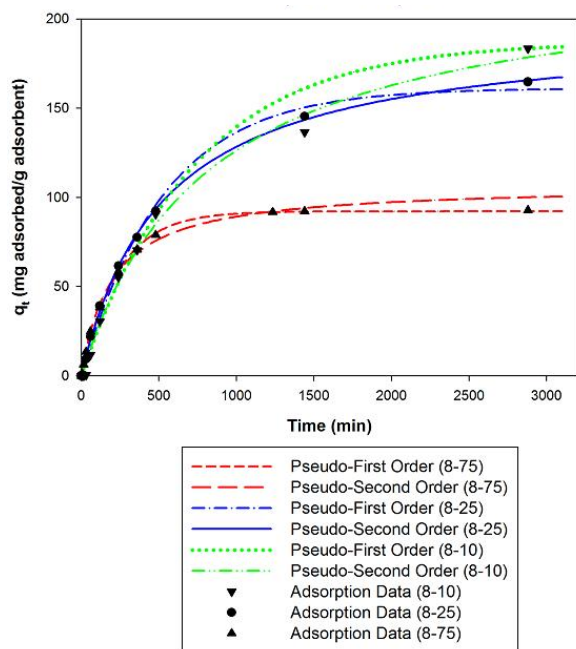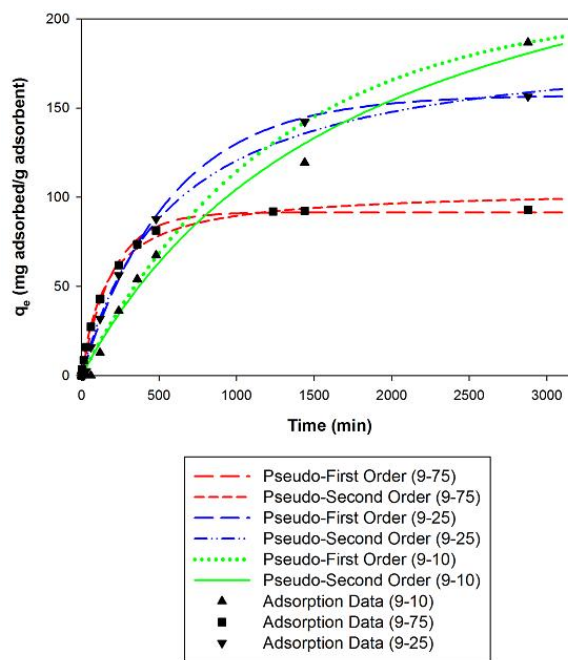| 2-Naphthoic Acid							
pH	CL*	t_{50}	τ	q_e	q_m	$\theta = \dfrac{q_e}{q_m}$	Best Fit:
4	434	90	129	90	357.9	0.25	PFO
4	142	300	481	258	357.9	0.72	PSO
4	57	610	905	344	357.9	0.96	PSO
7	428	165	235	92	206.8	0.44	PFO
7	142	415	596	184	206.8	0.89	PFO
7	57	560	875	180	206.8	0.87	PSO
8	428	165	236	92	180.8	0.51	PFO
8	142	385	600	165	180.8	0.91	PSO
8	57	520	810	178	180.8	0.98	PSO
9	428	140	198	91	180.5	0.50	PFO
9	142	390	562	156	180.5	0.86	PFO
9	57	800	1144	180	180.5	0.99	PSO

*CL = carbon load (mg/L)
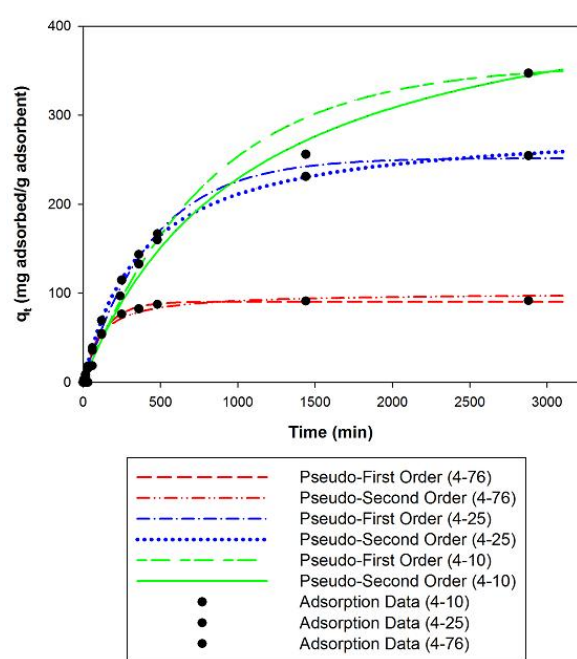
a)
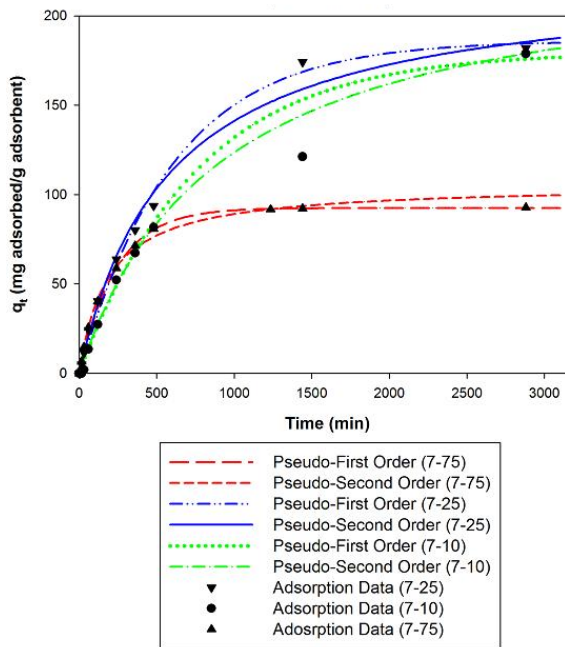
b)

c)

d)

Figure 5 - 7: 2-naphthoic acid kinetic adsorption results for various pH's; a) pH 4; b) pH 7; c) pH 8; d) pH 9

From Figure 5 - 8 it is apparent that the time constant of 2-naphthoic acid is relatively insensitive to changes in pH but is extremely sensitive to changes in carbon loading. This implies that initial rate of adsorption for 2-naphthoic acid is very similar at all pH, under fixed carbon loading. The increase in time constant at higher surface coverage is expected from kinetic theory since the rate of desorption is typically a function of surface coverage fraction (θ).

$$v_d = k_d\theta \qquad (22)$$

Where:

v_d = desorption rate

k_d = desorption rate constant

θ = surface coverage fraction

Since lower carbon dosages have less available surface area and thus less active adsorption sites, the effect of desorption becomes significant at an earlier stage of adsorption. The ratio of vacant sites to occupied sites is a measure of the driving force for adsorption; as the surface coverage fraction approaches 1 the adsorbent reaches saturation. Figure 5 - 9 illustrates that the time constant is a function of surface coverage and increases with surface coverage following an exponential function. Note that the values for q_m used to determine the value of θ were those obtained from the experimental isotherm studies, and the numerical values for the data plotted in Figure 5 - 9 are also presented in Table 5 - 11.
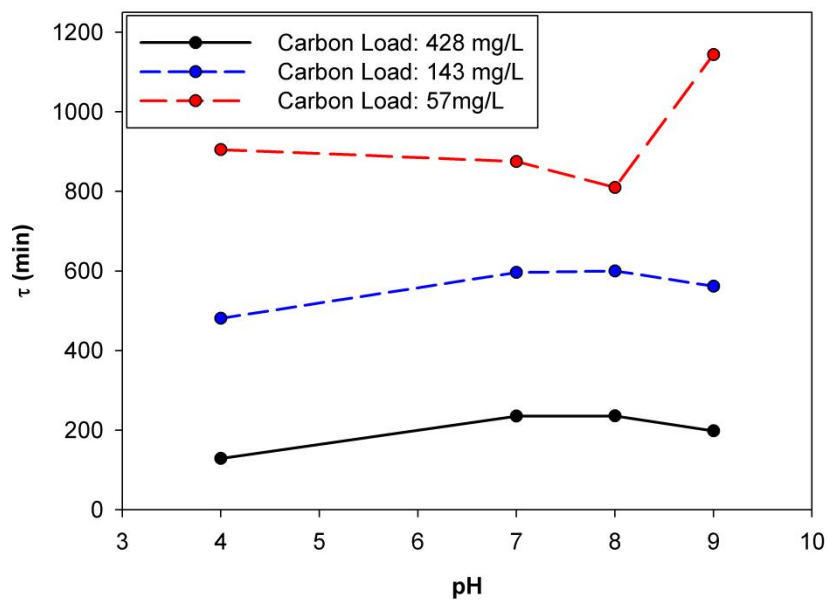
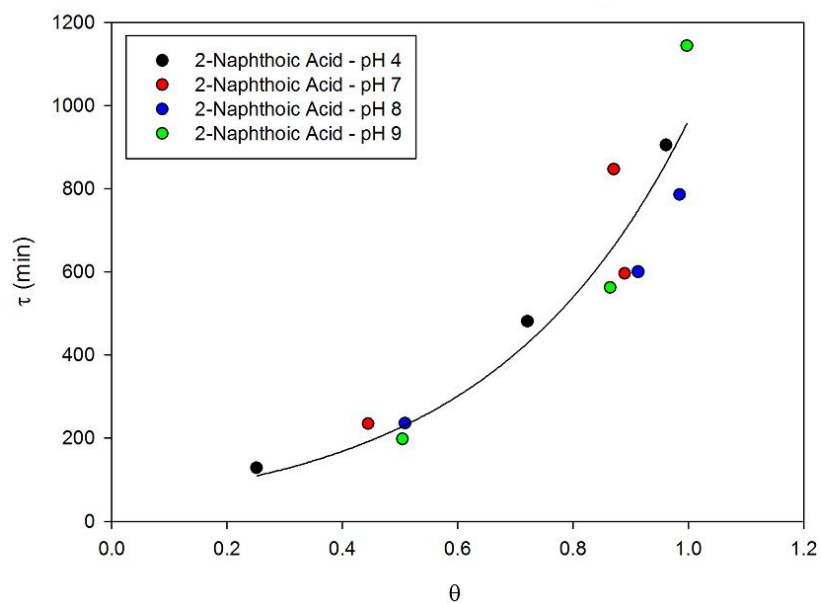**Figure 5 - 8: 2-Naphthoic acid time constant vs. pH**

Figure 5 - 9: 2-Naphthoic acid time constant vs. surface coverage fraction – four data sets fitted with single exponential function

5.2.2. Diphenylacetic Acid Kinetic Results

Similarly as with 2-napthoic acid both kinetic models investigated provided good fit for all conditions. Diphenylacetic acid is overall more accurately described by the PSO than PFO as is shown in Table 5 - 13. The graphical results for the kinetic experiments and two kinetic models is show in Figure 5 - 12.
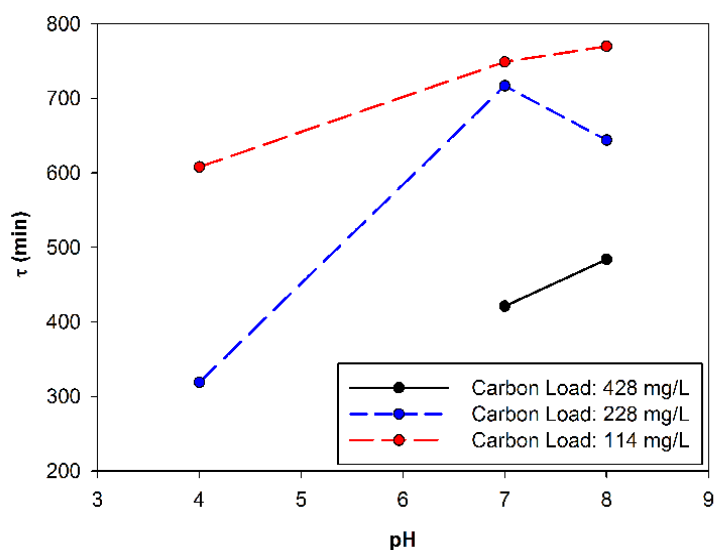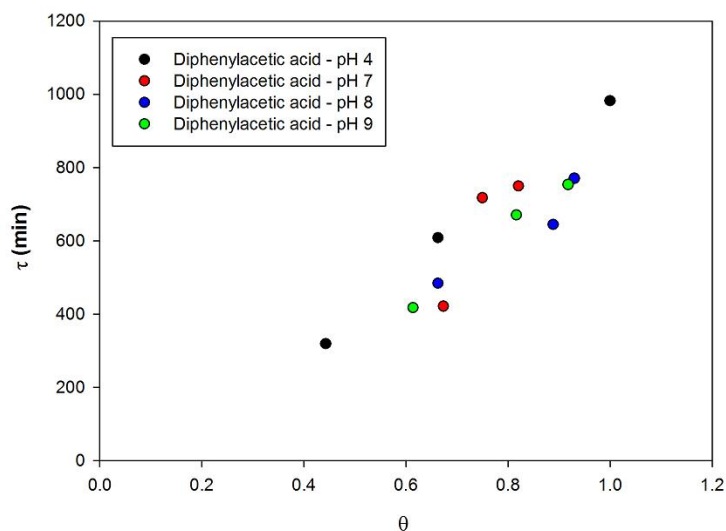

Figure 5 - 10: Diphenylacetic acid time constant vs. pH

Figure 5 - 11: Time constant vs surface coverage fraction

It is interesting to note the difference between Figure 5 - 10 and Figure 5 - 8. From these it is observed that the time constant of diphenylacetic acid is clearly sensitive to changes in system pH. This is contrary to what was observed for 2-naphthoic acid. It is noted that in Figure 5 - 10 the carbon loading for 428 mg/L carbon had only three data points. The missing point, the value at pH 4, was not obtained as the equilibrium concentration for such elevated loading was below detection levels. There is also an interesting change in how the time constant varies as a function of the surface coverage fraction. While for 2-naphthoic acid the relationship was clearly exponential, the one for diphenylacetic acid was more linear. The difference in how the time constant of diphenylacetic acid behaved as a function of the surface coverage fraction and pH, as compared to 2-naphthoic acid may indicate a significant difference in the adsorption mechanisms of these two compounds.

From Figure 5 - 12 plots b, c, and d, it is observed that the lower activated carbon loading experiments, 228 mg/L and 114 mg/L, showed a less distinguishable plateau at 48 hrs. This indicated that the experiment duration was insufficiently long as to allow the system to reach equilibrium for lower carbon loadings as the time constant increased. From these graphs we see that the PSO model is best able to approach these values where a plateau has yet to be clearly defined. The PFO model tends to underestimates the adsorption. A similar observation can be made for the kinetic results of 2-naphthoic acid (Figure 5 - 7) where the lower two carbon loadings (143 mg/L and 57 mg/L) did not reach explicit plateaus. In the case of 2-naphthoic acid the PFO model was able to effectively fit lower carbon loadings, which was not the case for diphenylacetic acid.

Note that the determination that 48 hrs was an appropriate duration for the experiments to reach steady state, was based on preliminary experiments with relatively high carbon loadings. As was observed, decreasing carbon loads, resulted in increased time constants. The determination of the run time needed to reach steady state should have been performed using the minimum carbon loading experimentally required.
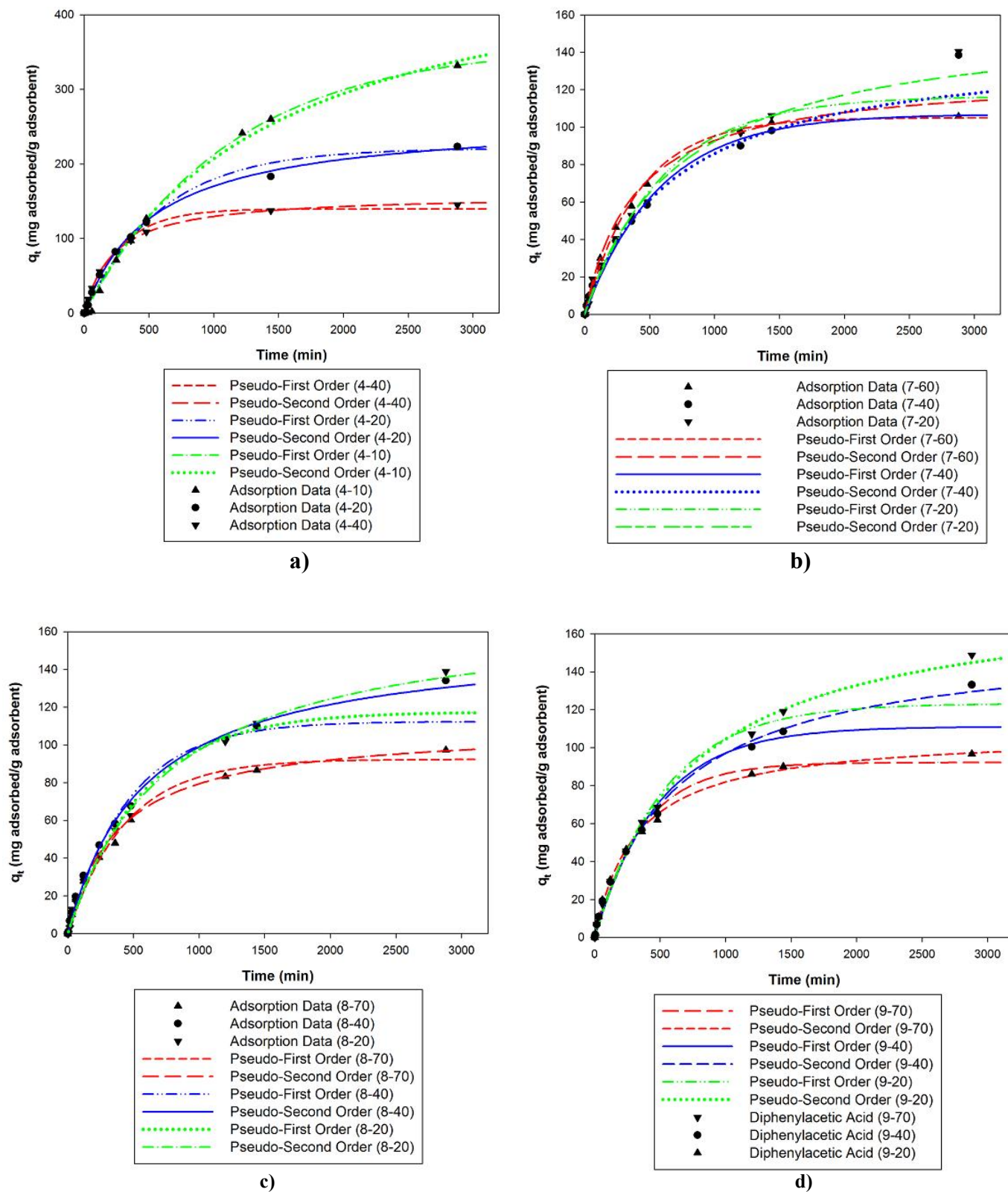
Figure 5 - 12: Diphenylacetic acid kinetic adsorption results for various pH's; a) pH 4; b) pH 7; c) pH 8; d) pH 9

Table 5 - 12: Diphenylacetic acid summary of the kinetic fitting results for pseudo-first order and pseudo-second order models

		Pseudo-First Order (PFO)					Pseudo-Second Order (PSO)				
							Diphenylacetic Acid				
pH	CL*	k_1	q_e	R^2	SSE	χ^2	k_2	q_e	R^2	SSE	χ^2
4	228	3.61E-3	139.60	0.9973	182.34	3.89	2.78E-5	158.90	0.9999	15.57	2.56
4	114	1.68E-3	220.72	0.9955	603.76	26.53	7.16E-6	261.35	0.9990	142.32	38.77
4	57	8.93E-4	359.40	0.9988	454.85	193.59	1.34E-6	509.69	0.9981	731.96	226.86
7	342	2.38E-3	105.00	0.9990	48.98	5.47	2.01E-5	128.63	0.9984	92.94	6.96
7	228	1.74E-3	106.90	0.9612	1134.52	27.89	9.94E-6	145.30	0.9839	505.61	26.04
7	114	1.67E-3	116.50	0.9750	742.92	9.10	8.54E-6	160.00	0.9916	244.00	4.46
8	400	2.29E-3	92.33	0.9959	149.74	6.62	2.40E-5	109.50	0.9983	50.40	1.96
8	228	2.16E-3	112.40	0.9898	608.12	9.96	1.09E-5	156.90	0.9958	98.59	4.69
8	114	1.78E-3	117.50	0.9902	625.10	10.12	7.49E-6	172.40	0.9980	117.74	5.64
9	400	2.74E-3	92.18	0.9962	148.17	6.67	2.93E-5	107.8	0.9991	31.89	1.74
9	228	2.08E-3	111.00	0.9892	635.50	10.53	1.02E-5	157.5	0.9982	108.35	5.22
9	114	1.89E-3	123.2	0.9891	801.89	12.75	7.36E-6	182.3	0.9984	114.29	7.86

*CL = carbon load (mg/L)

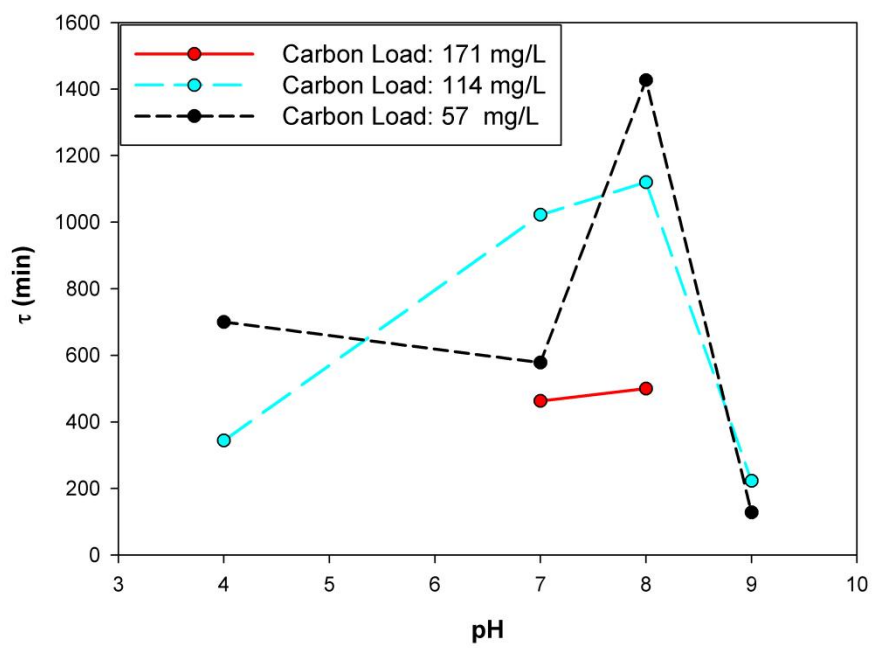**Table 5 - 13: Diphenylacetic acid kinetic adsorption data and best fit used along with fitting method.**

| pH	CL*	t_{50}	τ	q_e	q_m	$\theta = \dfrac{q_e}{q_m}$	Kinetic Model:
4	228	195	319	147	*332*	0.44	PSO
4	114	390	608	220	*332*	0.66	PSO
4	57	695	982	332	*332*	1	PFO
7	342	290	421	105	*156*	0.67	PFO
7	228	455	717	117	*156*	0.75	PSO
7	114	490	749	128	*156*	0.82	PSO
8	400	300	490	97	*146.3*	0.66	PSO
8	228	415	644	130	*146.3*	0.89	PSO
8	114	505	688	136	*146.3*	0.93	PSO
9	400	260	420	97	*158*	0.61	PSO
9	228	435	675	129	*158*	0.81	PSO
9	114	490	751	145	*158*	0.92	PSO

*CL = carbon load (mg/L)

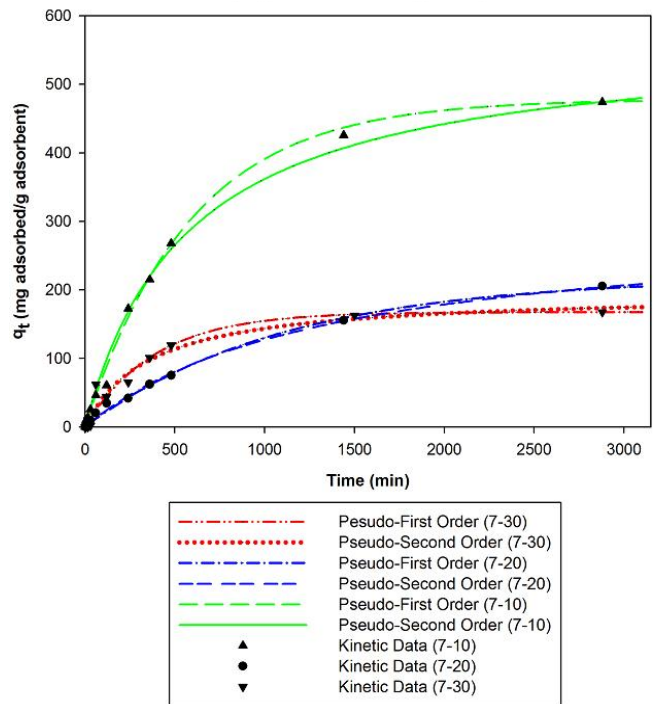### 5.2.3. 1,4-Cyclohexanedicarboxylic Acid Kinetic Results

Both kinetic models investigated provided good fits for all conditions as can be seen in Table 5 - 14. The graphical results for the kinetic experiments are show in Figure 5 - 14, along with the curve fits of PFO and PSO. Since insufficient data was collected for the isotherms of this compound a comparison of the change in time constant as a function of surface coverage fraction was impossible, as the values for the saturation capacity were unknown. Figure 5 - 13, illustrates the change in time constant with pH. It would appear that different carbon loads respond quite differently with changes in pH. This can be seen in the divergence in time constants for carbon loadings 57 mg/L and 114 mg/L. It would be expected that the time constant would either increase or not change with pH. Instead, the time constant for the carbon loading of 57 mg/L decreased, while for 114 mg/L it increased. This is in contrast to 2-naphthoic acid which showed that the time constant was relatively insensitive to changes in pH. Interestingly the time constants for carbon loads 57 mg/L and 114 mg/L converge towards a similar value at pH 9. Indicating that for elevated pH the system response appears to become insensitive to carbon loading. Additionally the values obtained for the time constant for pH 9 indicate a reduction in response time, which can also be seen from Figure 5 - 14, d). The spike in time constant for pH of 8 for carbon loading of 57 mg/L was in reality much larger than recorded. This is seen in Figure 5 - 14, c), were the values for (8-10) are not even beginning to flatten out and approach a constant. For the calculations the final measured value was recorded as the steady state q_e, which graphically appears to be underestimated which would thus indicate that the resulting time constant was much larger as well. A significant slowing down of adsorption was thus observed at pH 8.
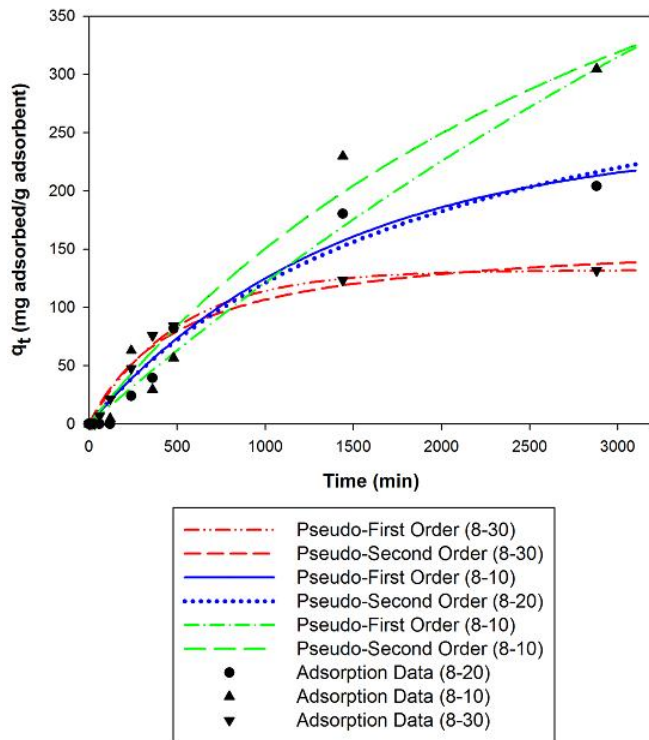
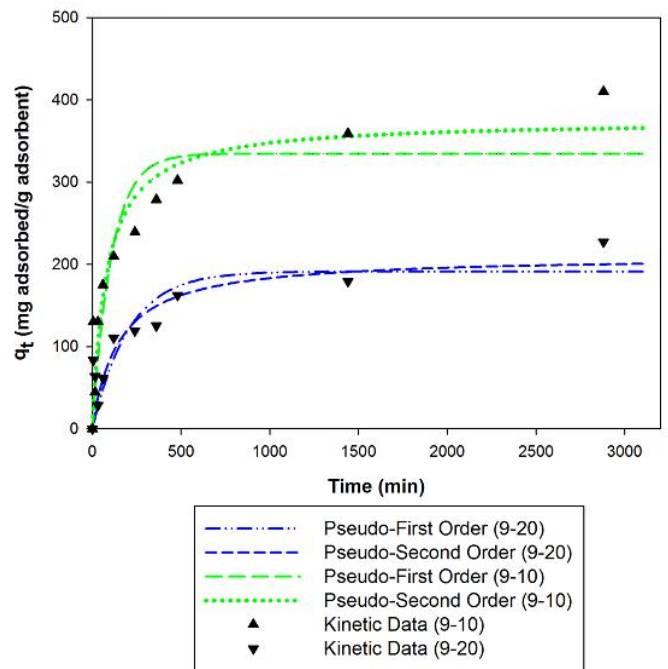**Figure 5 - 13: 1,4-Cyclohexanedicarboxylic acid time constant vs. pH**
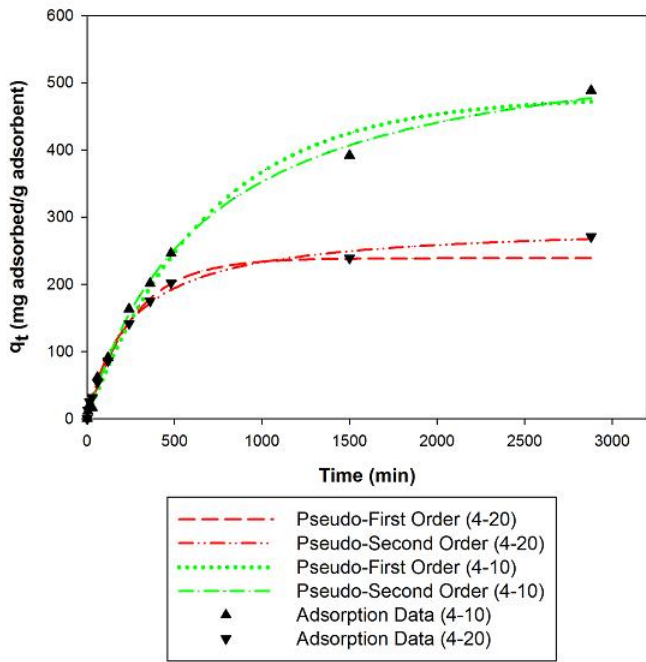
Figure 5 - 14: 1,4-Cyclohexanedicarboxylic acid kinetic adsorption results for various pH's; a) pH 4; b) pH 7; c) pH 8; d) pH 9

Table 5 - 14: 1,4-Cyclohexanedicarboxylic acid summary of the kinetic fitting results for pseudo-first order and pseudo-second order models

1,4-Cyclohexanedicarboxylic Acid									
		Pseudo-First Order				Pseudo-Second Order			
pH	CL*	K_1	q_e	R^2	SSE	K_2	q_e	R^2	SSE
4	114	3.83E-3	238.50	0.9895	1326	1.394E-5	290.00	0.9955	441
4	57	1.45E-3	478.88	0.9922	2767	2.561E-6	586.80	0.9973	783.37
7	171	2.57E-3	167.60	0.9576	1768	1.431E-5	195.10	0.9576	1754
7	114	9.07E-4	218.00	0.9957	347	2.461E-6	299.80	0.9961	271
7	57	1.71E-3	477.80	0.9966	1069	3.088E-6	568.20	0.9943	1991
8	171	2.20E-3	131.90	0.9929	274	1.198E-5	161.60	0.9860	482
8	114	7.17E-4	243.90	0.9753	1757	1.307E-6	370.80	0.9689	2089
8	57	1.53E-4	852.70	0.9601	5175	7.173E-8	13760	0.9710	3559
9	114	4.87E-3	191.10	0.8269	12363	3.226E-5	210.00	0.8476	9701
9	57	9.22E-3	334.30	0.8598	29384	3.338E-5	375.00	0.9069	18075

*CL = carbon load (mg/L)

Table 5 - 15: 1,4-Cyclohexanedicarboxylic acid kinetic adsorption data and best fit used along with fitting method

| pH	CL*	t_{50}	τ	q_e	q_m	$\theta = \dfrac{q_e}{q_m}$	Kinetic Model:
1,4-Cyclohexanedicarboxylic Acid
4	114	210	344	267	453	0.589	PSO
4	57	455	700	476	-	-	PSO
7	171	288	463	174	-	-	PSO
7	114	700	1022	204	-	-	PSO
7	57	402	578	474	-	-	PFO
8	171	345	500	132	-	-	PFO
8	114	800	1120	213	-	-	PFO
8	57	1048	1427	312	-	-	PSO
9	114	134	223	200	-	-	PSO
9	57	75	128	365	-	-	PSO

*CL = carbon load (mg/L)

5.3. Multi-component Isotherm Results

Typical concentrations vs. time plots for the adsorption of naphthenic acids from the multi-component solution are shown in Figure 5 - 15. Similar to the single compound adsorption plot the majority of removal occurred within the first 8 hrs. Additionally it is observed that the affinity to the activated carbon in increasing order was: 2-naphthoic acid > diphenylacetic acid > 1,4-cyclohexanedicarboxylic acid regardless of pH. The order follows well the increase in solubility of these compounds (Table 4 - 4), with the most soluble compound having the smallest affinity to the GAC.
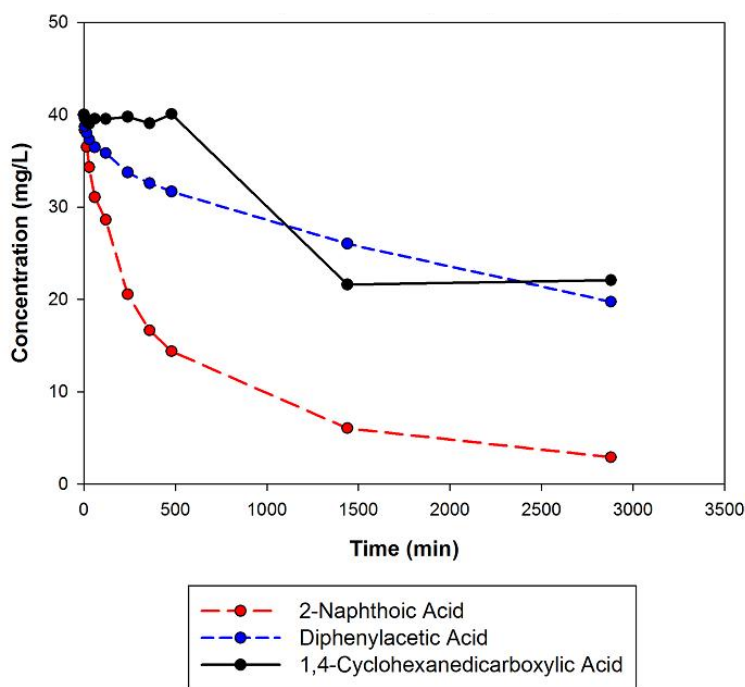
The multi-component adsorption isotherms for the three selected NAs in solution are presented in Figure 5 - 16 to Figure 5 - 18, and Figure 5 - 19. Each figure provides the isotherm results at a specified pH and compares the results of multi-component isotherm to those of single compound. The change in adsorbent saturation capacity (q_m) under multi-component and single component adsorption is summarised in Table 5 - 16 and illustrated by Figure 5 - 21, for 2-naphthoic acid and diphenylacetic acid.
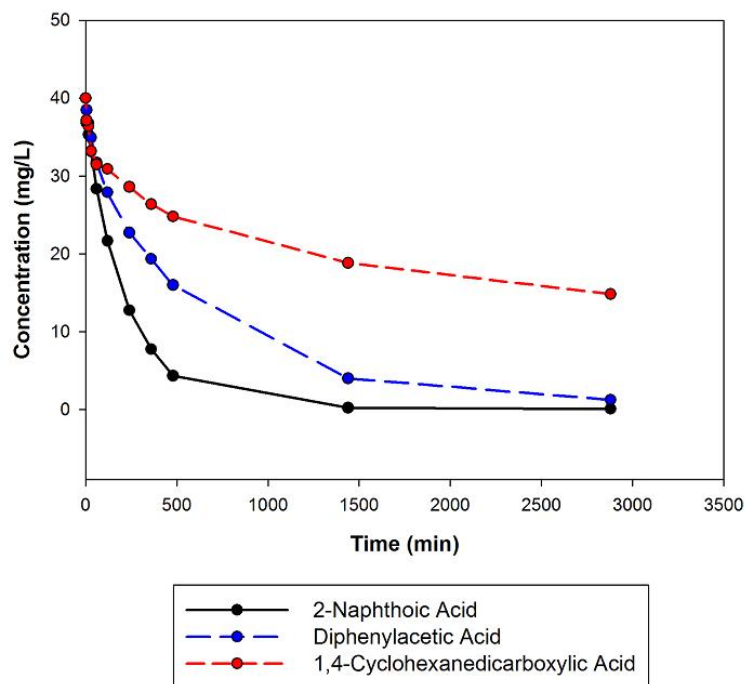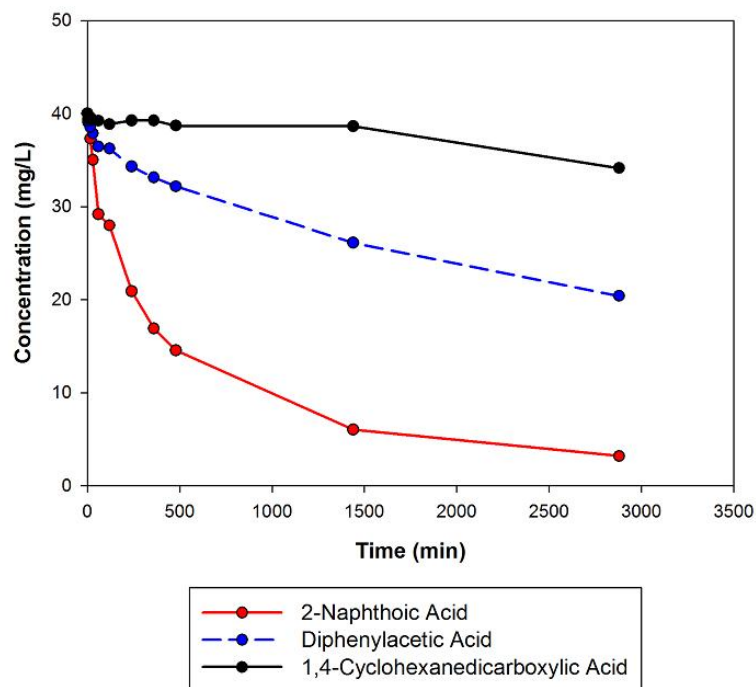
a)
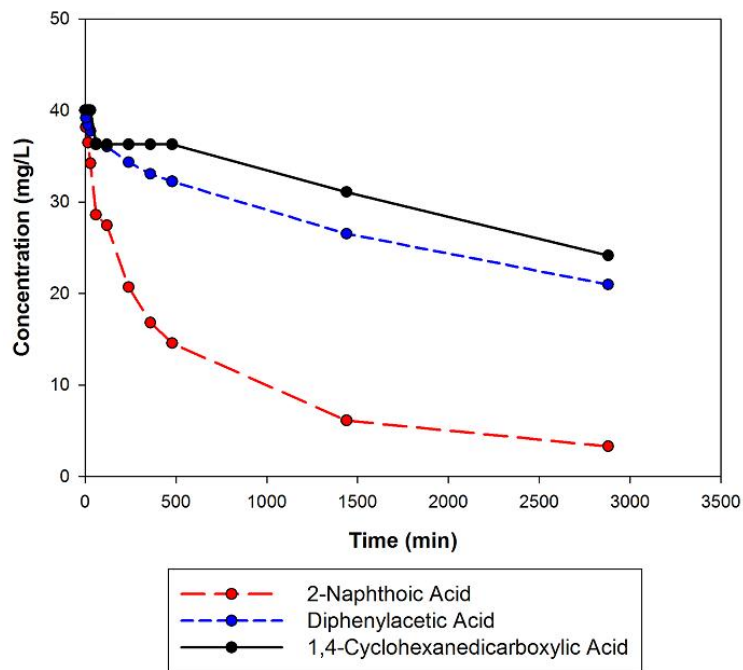
b)

c)

d)

Figure 5 - 15: Multi-component adsorption concentration vs time for 400 mg/L; a) pH 4; b) pH 7; c) pH 8; d) pH 9
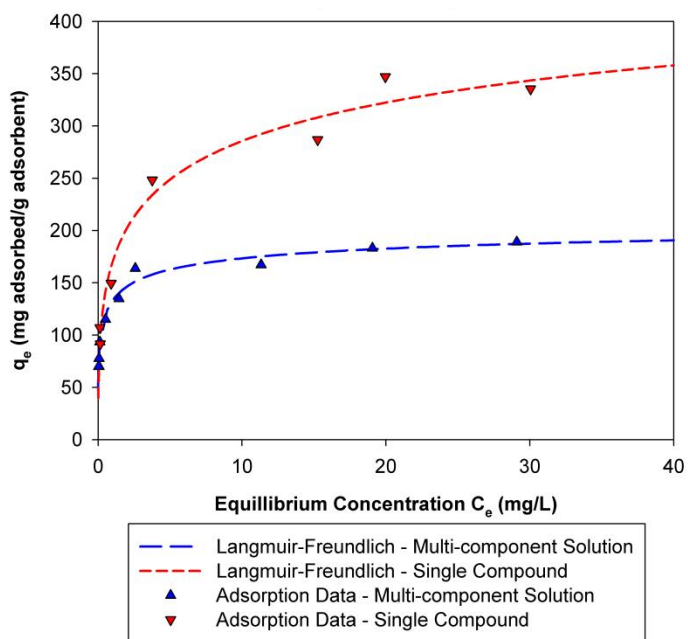
5.3.1. Multi-component Isotherm – pH 4

In Figure 5 - 16, 2-naphthoic acid and diphenylacetic acid exhibit an H-class adsorption isotherm which is similar to their single compound results. They both have a clear plateau, indicating the adsorbent saturation for these compounds has been reached. The isotherm for 1,4-cyclohexanedicarboxylic acid is dissimilar to the pure compound isotherm, in that it does not exhibit cooperative adsorption. As expected, saturation of the adsorbent occurred more readily as compared to single compound adsorption. The adsorption capacity of activated carbon for 2-naphthoic acid, diphenylacetic acid, and 1,4-cyclohexanedicarboxylic acid in mixture decreased as compared to the single compound values by 46.8%, 71.7%, and 91.4% respectively. Therefore, the reduction due to the mixture was more pronounced for 1,4-cyclohexanedicarboxylic acid, due to the absence of cooperative adsorption.

The isotherm of 1,4-cyclohexanedicarboxylic acid exhibits a maximum for q_e followed by a reduction in equilibrium capacity with increasing equilibrium concentration. For single solute isotherms it has been postulated that such maxima in q_e may occur when the solute-solute attractive forces are greater than the substrate-solute forces [74]. Though the single solute isotherms for 1,4-cyclohexanedicarboxylic acid did not exhibit this phenomenon, it may well be that 2-naphthoic acid and diphenylacetic acid occupying the active sites reduced the cooperative lateral interactions taking place on the surface of the adsorbent, thus reducing the affinity of the compound. However, a calorimetric study could further elucidate this discussion.
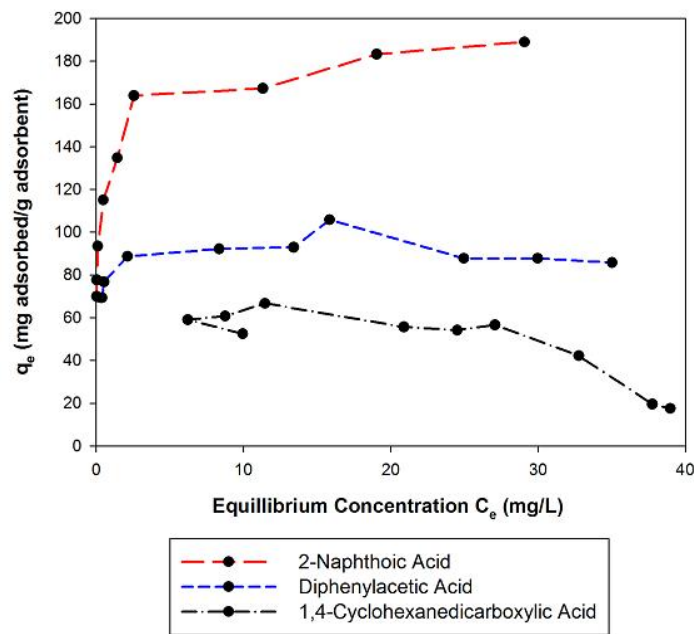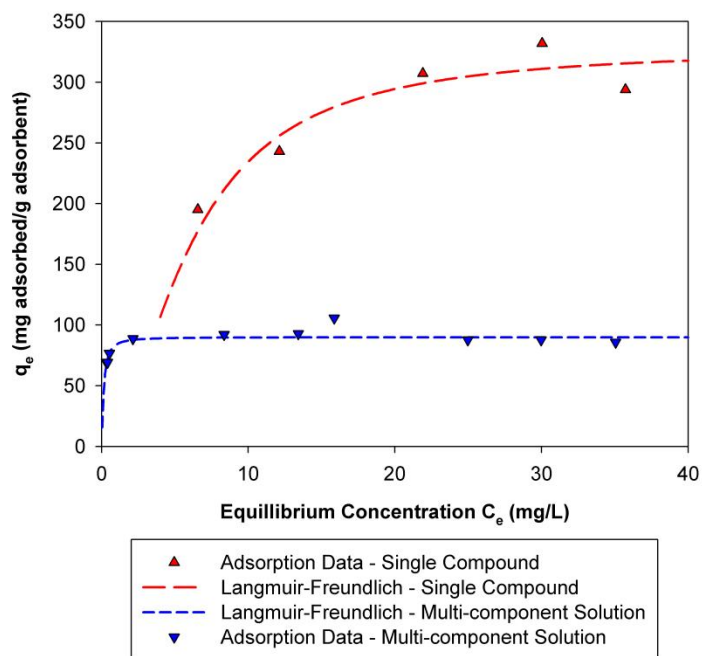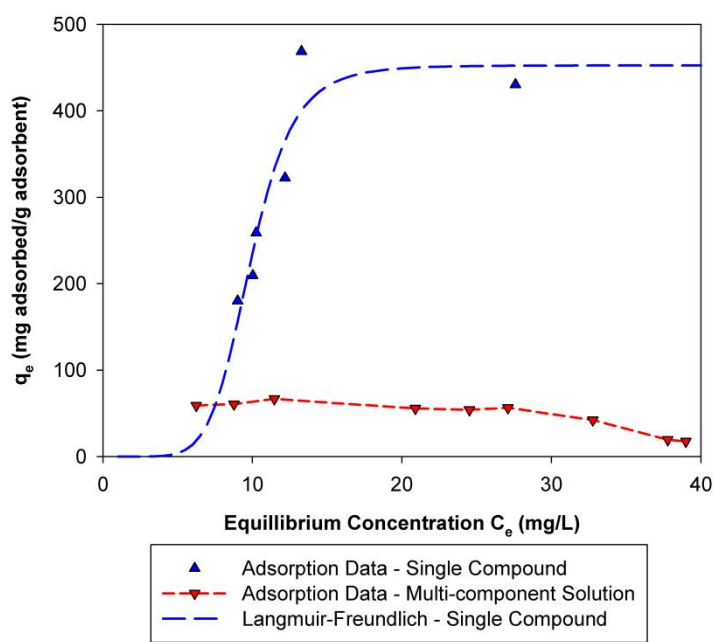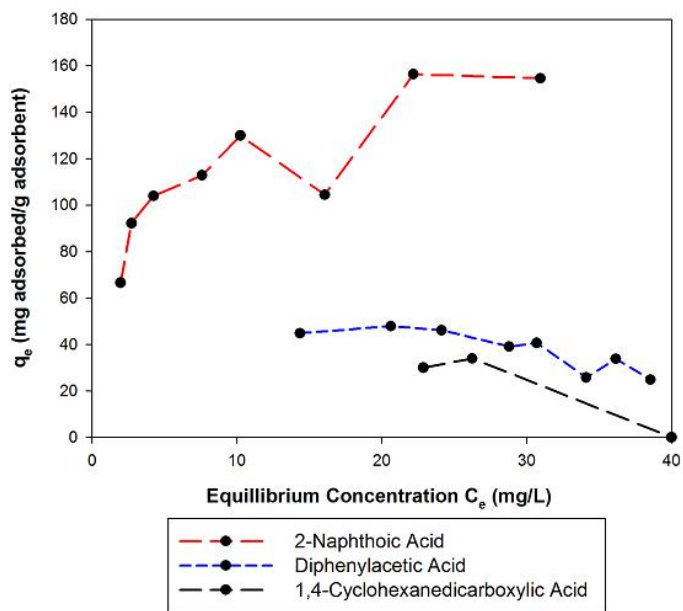
Figure 5 - 16: a) Adsorption isotherms for the mixture of NAs at pH 4; b) Isotherm of 2-naphthoic acid as single component and multi-component adsorption at pH 4; c) Isotherm of diphenylacetic acid as single component and multi-component adsorption at pH 4; d) Isotherm of 1,4-cyclohexanediacarboxylic acid as single component and multi-component adsorption at pH 4

5.3.2. Multi-component Isotherm – pH 7

In Figure 5 - 17, 2-naphthoic acid exhibited lower initial adsorption as compared to pH 4; which is due to both increasing pH as well as competition. It is unclear whether it conforms to the H or L-class in this case, since no data was obtained for low equilibrium concentrations. For diphenylacetic acid there was a marked change in the isotherm behaviour as compared to that obtained for pH 4. A similar plateau for q_m with a maxima exhibited by 1,4-cyclohexanedicarboxylic acid at pH 4 was observed for diphenylacetic acid. At pH 7, the drop in adsorption capacity for 2-naphthoic acid and diphenylacetic acid as compared to single compound values is 21.6% and 74%, respectively. 1,4-Cyclohexanedicarboxylic acid showed a marked decrease in adsorption with an increase in pH from 4 to 7. There was no adsorption of 1,4-cyclohexanedicarboxylic acid at lower carbon dosages until the dosage was increased to 343 mg/L.
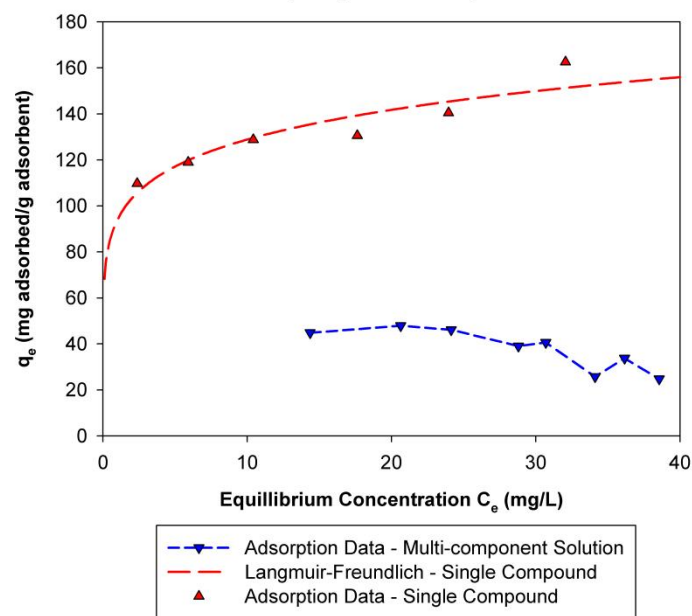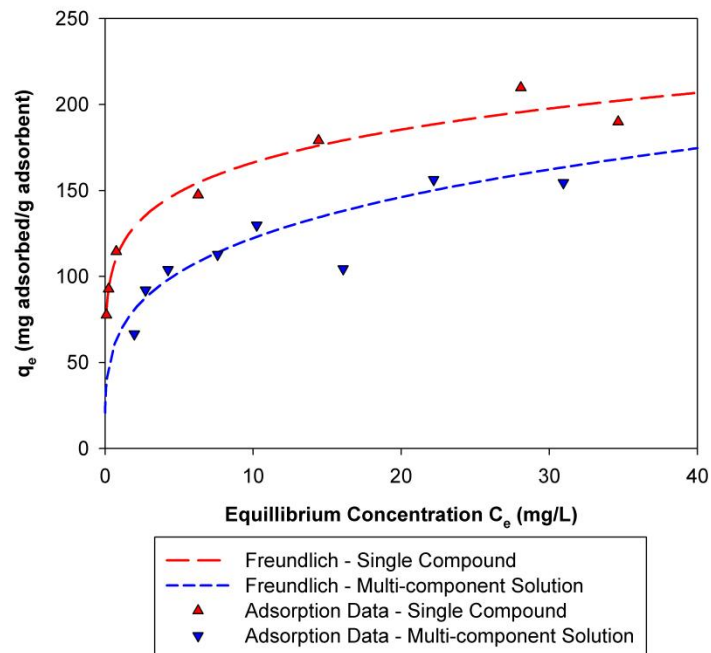
Figure 5 - 17: a) Adsorption isotherms for the mixture of NAs at pH 7; b) Isotherm of2-naphthoic acid as single component and multi-component adsorption at pH 7; c) Isotherm of diphenylacetic acid as single component and multi-component adsorption at pH 7; d) Isotherm of 1,4-cyclohexanediacarboxylic acid as single component and multi-component adsorption at pH 7
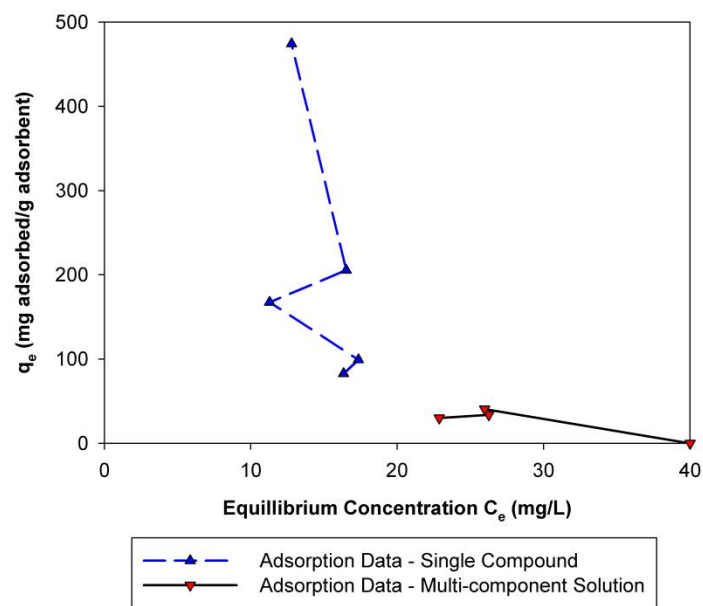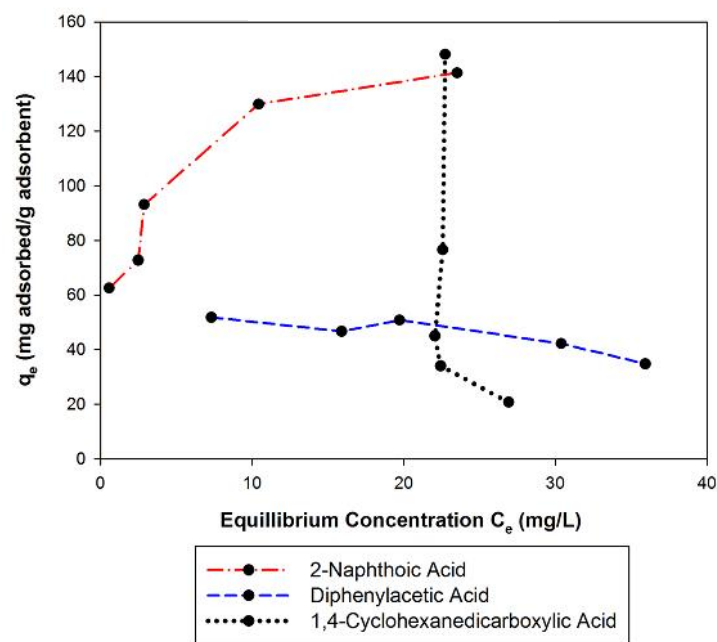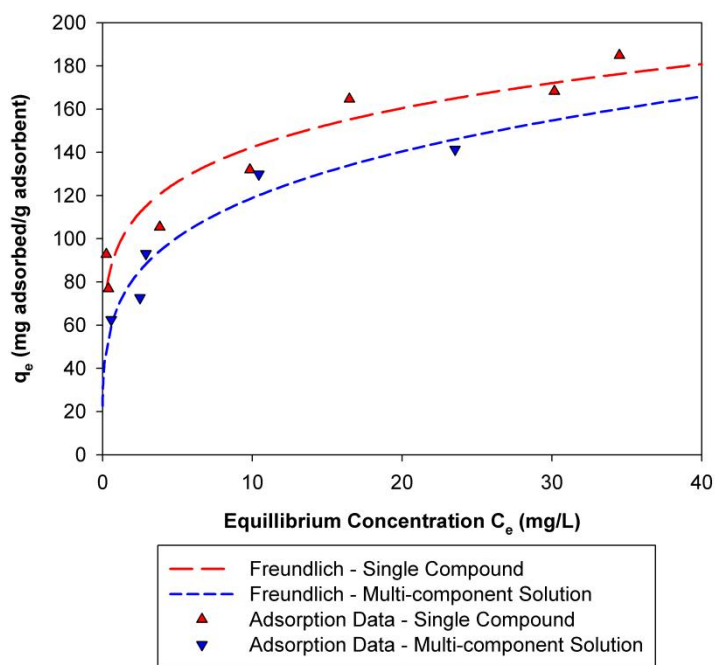
5.3.3. Multi-component Isotherm – pH 8

In Figure 5 - 18 it is observed that 2-naphthoic acid exhibits more clearly the H-class adsorption isotherm at pH 8 than for pH 7. Diphenylacetic acid showed a slight increase in its affinity to the adsorbent as compared to pH 7, though not significantly. For the multi-component system, the adsorption capacity of 2-naphthoic acid and diphenylacetic acid decreased in adsorbent capacity as compared to single compound adsorption values by: 8.3% and 64.6%, respectively.

The major difference between pH 7 and pH 8 was the dramatic change in adsorption behaviour of 1,4-cyclohexanedicarboxylic acid. The adsorption of 1,4-cyclohexanedicarboxylic acid dramatically increased and changed the adsorption profile to an S-class curve corresponding to cooperative adsorption. The change may be explained by the observed decrease in the adsorptive capacity of the other two species. As their values of q_e decreased, this may have allowed the surface concentration of 1,4-cyclohexanedicarboxylic acid to grow sufficiently dense in order to allow lateral interactions between adsorbed molecules. Thus allowing the cooperative adsorption mode to take effect as was seen in the single solute isotherms. This same explanation can be used to understand why 1,4-cyclohexanedicarboxylic acid did not demonstrate an S type adsorption profile for pH 4 and 7. As 2-naphthoic acid and diphenylacetic acid occupied sufficient sites as to prevent the reinforcing effect of lateral interactions needed for cooperative adsorption. The increase in solubility at elevated pH for 2-naphthoic acid and diphenylacetic acid may also contribute to the decrease in adsorbent affinity. Since these compounds go from sparingly soluble (e.g. < 0.28 g/L) to very soluble at pH 8 (e.g. < 354 g/L), they experience a larger change in relative solubility with increase in pH then does 1,4-cyclohexanedicarboxylic acid which was already very soluble at low pH.

a)

b)
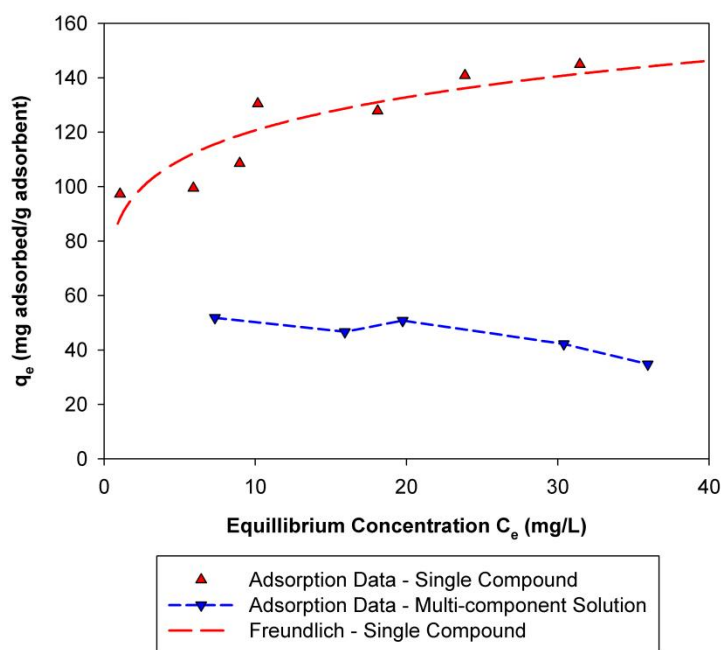
c)

d)

Figure 5 - 18: a) Adsorption isotherms for the mixture of NAs at pH 8; b) Isotherm of 2-naphthoic acid as single component and multi-component adsorption at pH 8; c) Isotherm of diphenylaceticacid assingle component and multi-component adsorption at pH 8; d) Isotherm of 1,4-cyclohexanediacarboxylic acid assingle component and multi-component adsorption at pH 8

5.3.4. Multi-component Isotherm – pH 9

In Figure 5 - 19, it can be seen that the isotherm of 2-naphthoic acid has changed to an L-class isotherm curve. This indicates that the compounds affinity to the adsorbent at low concentrations has been substantially reduced. Additionally, it is observed that q_e of 2-naphthoic acid has not reached a plateau in the test concentration range, and thus the adsorbent is not fully saturated. Interestingly, the adsorbent capacity for 2-naphthoic acid for the multi-component system appears to be larger than that for the single component at pH 9. This effect is similar to what was seen earlier at pH 8 for 1,4-cyclohexanedicarboxylic acid. For the multi-component system 2-naphthoic acid actually had an increase in adsorbent capacity of 20.2% as compared to the single solute isotherm where as diphenylacetic acid showed a drop of 69.3%. Once again 1,4-cyclohexanedicarboxylic acid appears to be presenting cooperative adsorption, resulting in an S-class isotherm.
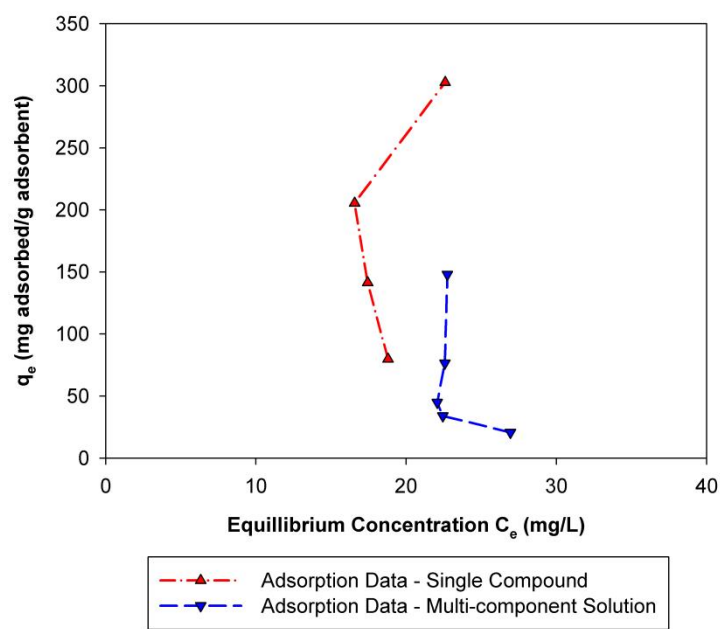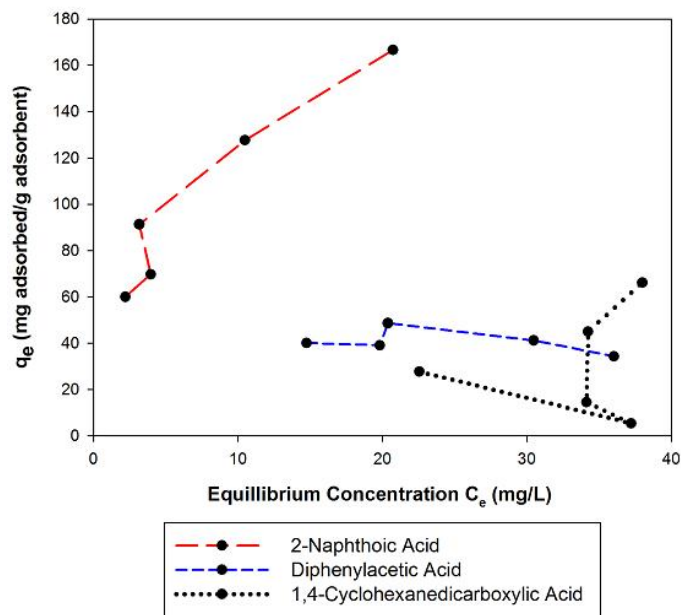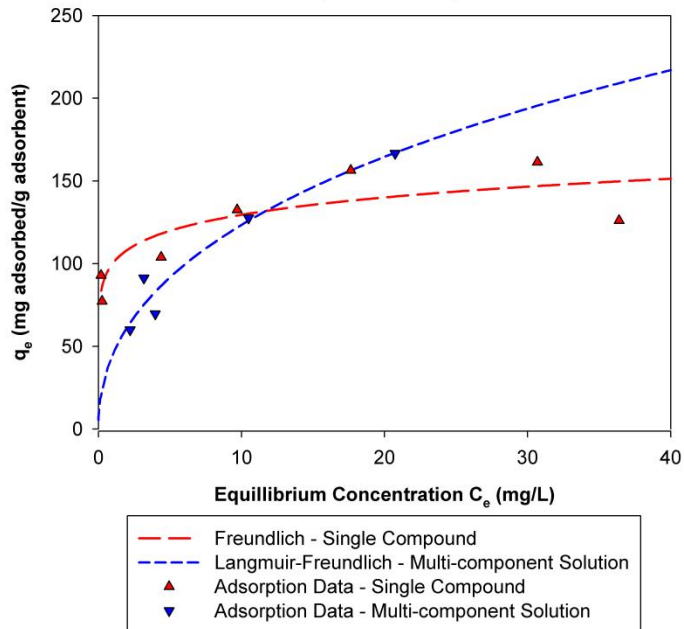
a)

c)

d)

e)

Figure 5 - 19: a) Adsorption isotherms for the mixture of NAs at pH 9; b) Isotherm of2-naphthoic acid as single component and multi-component adsorption at pH 9; c) Isotherm of diphenylaceticacid as single component and multi-component adsorption at pH 9; d) Isotherm of 1,4-cyclohexanediacarboxylic acid as single component and multi-component adsorption at pH 9
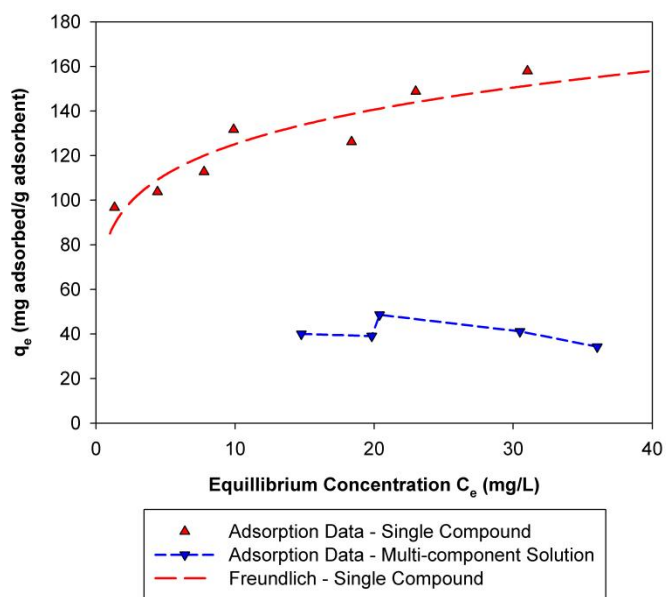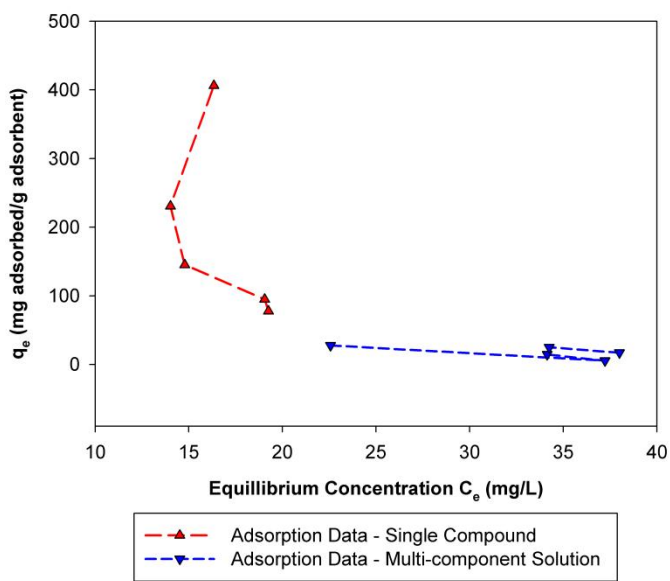
5.3.5. Overall Adsorption Isotherms:

In order to provide a better overview of the adsorption results the overall adsorption isotherms were plotted. Instead of calculating the adsorption equilibrium capacity (q_e) for each chemical, the total mass of the three model compounds removed was used to determine the overall equilibrium capacity. It is interesting to note the shift that occurs in Figure 5 - 20 as pH increased. The overall isotherm curve for pH 4 is a standard curve that would fit either the Langmuir-Freundlich or Freundlich models. As the pH increased to seven we see a similar profile as at pH 4 though with a marked decrease in overall capacity. For pH 8 and 9 we see a shift from standard L or H-class adsorption profiles to C-class (linear). The change in adsorption profile is accompanied with an increase in overall capacity. The slope of the line for pH 8 then decreases for pH 9 and results in a lower capacity. The pH in which we see a change from L type to C type corresponds to the pH in which 1,4-cyclohexanedicarboxylic acid demonstrates an S type adsorption. This indicates an interesting change in adsorption mechanism when the pH was above 8.
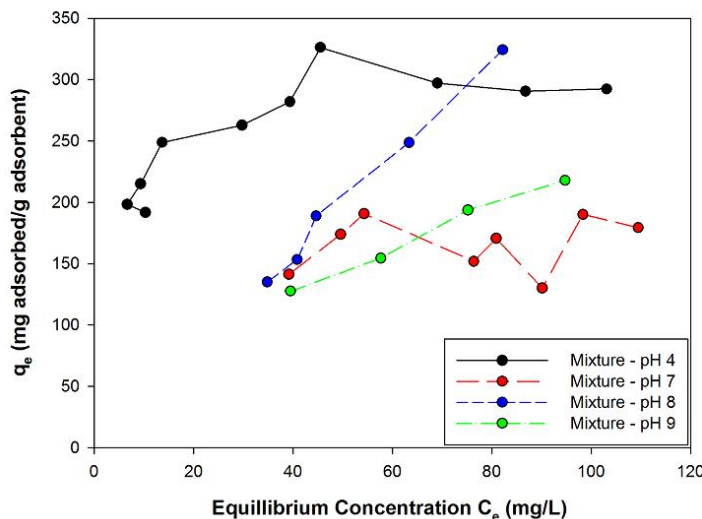
Figure 5 - 20: Overall adsorption isotherm results for multi-component adsorption

5.3.6. Summary of Isotherm Results

From the experiments it was observed that there is a marked decrease in adsorbent capacity with increasing pH. We observed that the adsorption capacity of individual components exhibited a relatively high degree of sensitivity to changes in pH (Figure 5 - 21). The adsorption capacity for the multi-component system did not demonstrate such sensitivity. A decrease in adsorbent capacity for multi-component adsorption was observed with increasing pH though the change was not nearly as significant as with the single compounds (Figure 5 - 21).

The adsorption results for 2-naphthoic acid were fairly standard with its multi-component adsorption isotherms being of H or L type. Diphenylacetic acid exhibited a maximum for adsorbent capacity for pH 7 to 9 that then decreased as the equilibrium concentration approached the initial concentration. For pH of 8 and 9 1,4-cyclohexanedicarboxylic acid showed a significant change in its isotherm curve. It went from an isotherm curve with a local maximum which decreased with increasing equilibrium concentration, to an S-class isotherm curve. It was observed that the overall adsorption isotherms, Figure 5 - 20, showed a change in profile at the same pH in which 1,4-cyclohexanedicarboxylic acid became S-class, pH 8 and 9. In Figure 5 - 20, it was observed that the overall isotherm went from an L or H-class to a C-class (linear) isotherm. Additionally the overall adsorbent capacity at pH 8 was higher than at pH 4. This finding is positive, as adsorption systems could be deployed to treat OSPW whose pH is approximately 8.

Small et al. (2012) found that the isotherm profile for acid-extractable oil sands tailing organics (AEOSTO) had a marked vertical portion [19]. The authors were unable to model the adsorption isotherm using traditional methods. They concluded that competitive adsorption along with the resulting complex interactions yielded the strange isotherm. In this work we found that co-operative adsorption, or S type isotherm profile, took place for 1,4-cyclohexanedicarboxylic acid. The vertical portion observed by Small et al. (2012) in the isotherm may be due to the S type adsorption, cooperative adsorption profile of oxygenated naphthenic acids present in OSPW. Additionally it was found that isotherm modeling of NA mixtures may be made difficult due to the occurrence of multiple modes of adsorption, for specific compounds in the mixture as was observed in this work.

a)

b)
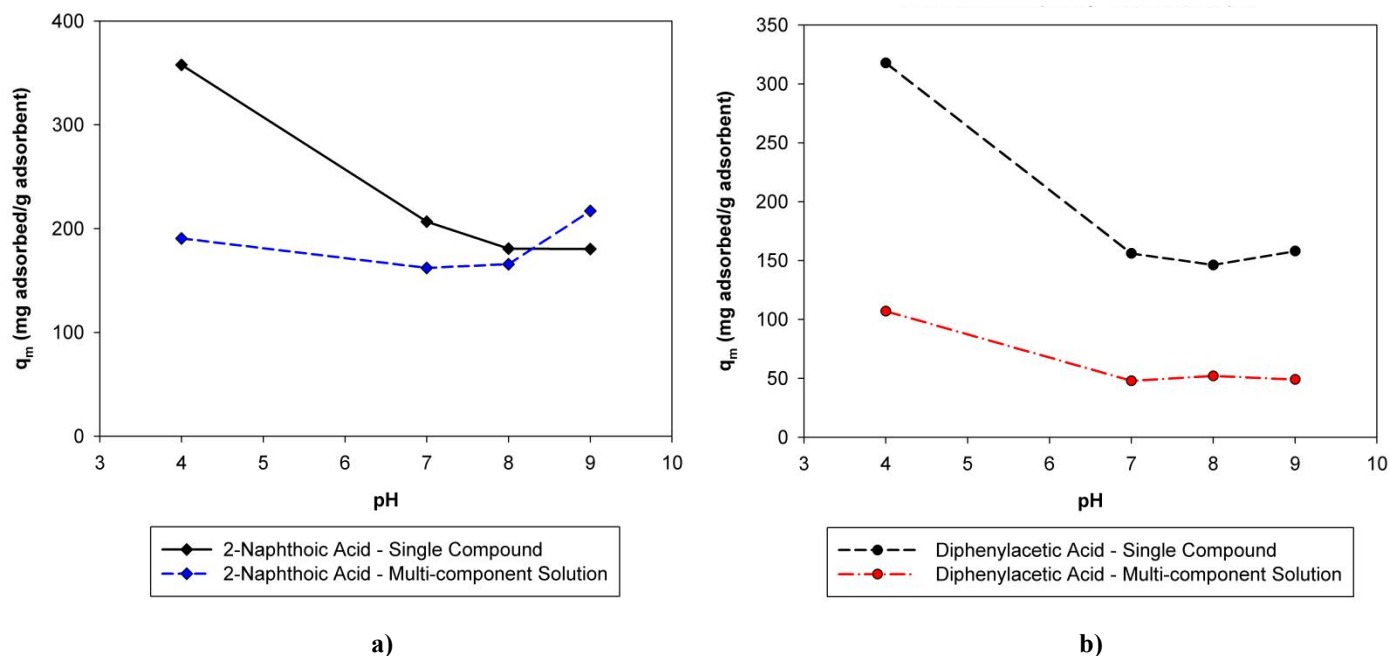
Figure 5 - 21: Comparison between the adsorbent capacity of single compound and multi-compound adsorption vs change in pH. a) 2-Naphthoic acid; b) Diphenylacetic acid

Table 5 - 16: Change in the adsorption removal capacity from single solute adsorption to multi-component solution; q_{m1} represent the single solute maximum capacity and q_{m2} the multi-component capacity

Fraction Change in Adsorption Capacity									
	2-Naphthoic Acid			Diphenylacetic Acid			1,4-Cyclohexanedicarboxylic acid		
pH	q_{m1}	q_{m2}	% *Change*	q_{m1}	q_{m2}	% *Change*	q_{m1}	q_{m2}	% *Change*
4	357.9	190.6	0.468	317.7	89.9	0.717	453	39.0	0.914
7	206.8	162.2	0.216	156.0	40.6	0.740	-	-	-
8	180.8	165.8	0.083	146.3	51.8	0.646	-	-	-
9	180.5	217.0	-0.202	158.0	48.6	0.693	-	-	-

5.4. Multi-component Kinetics

The multi-component adsorption kinetics for the three selected NAs in solution is presented in the appendix, in Figure A - 1 to Figure A - 4. The results are subdivided by specific compound and a summary of the resulting time constants as a function of both pH and surface coverage are presented in Figure 5 - 22 to 5-25.

5.4.1. 2-Naphthoic Acid Kinetics

It can be seen that barring a moderate increase in time constant for initial increase in pH, multi-component adsorption time constant of 2-naphthoic acid is relatively insensitive to changes in pH. A more significant observation is the one shown in Figure 5-23 where the time constant no longer changes with surface coverage as an exponential function. Additionally the maximum time constant values obtained for the multi-component solution (Figure 5 - 23 b) are smaller than those for the pure solution (Figure 5 - 23 a). Additionally larger scatter between data sets with different pH is observed as compared to pure solute adsorption. Maintaining low values for the adsorption time constant is important for continuous column adsorption systems, as throughput dictates the contact time which in turn affects the overall removal of contaminants.
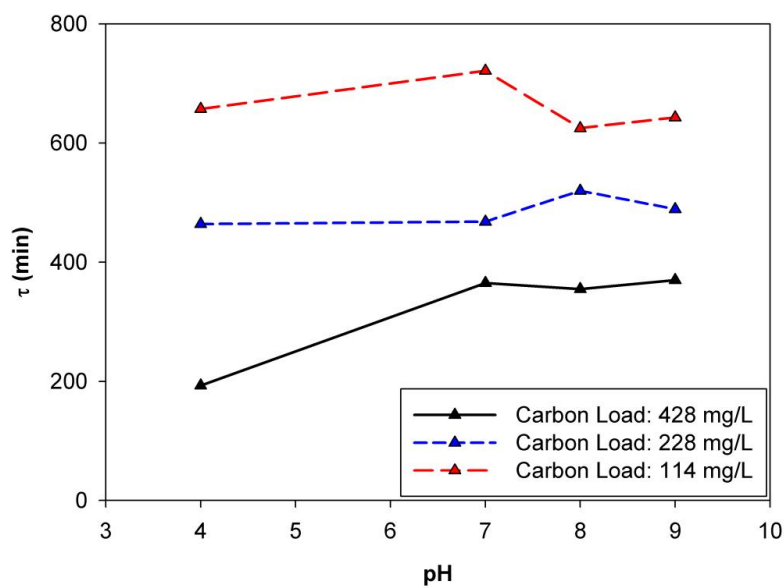
85

Figure 5 - 22: 2-Naphthoic acid multi-component time constant as a function of pH
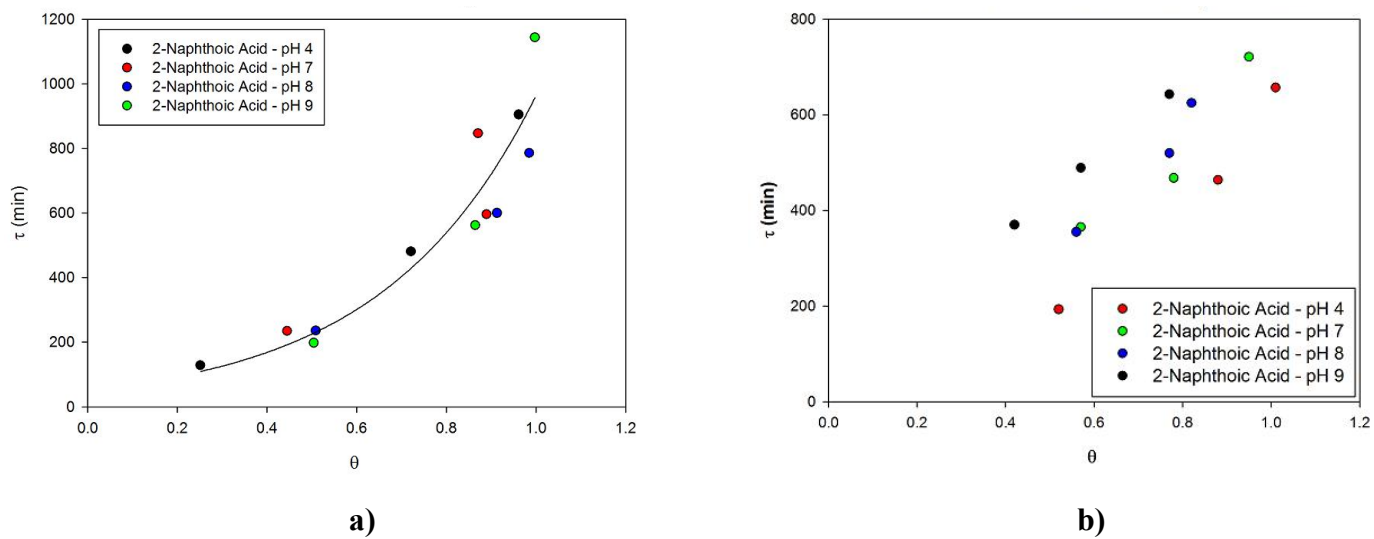

a)

b)

Figure 5 - 23: 2-Naphthoic acid time constant vs. Surface coverage; a) Single compound; b) Multi-component

Table 5 - 17: 2-Naphthoic acid multi-component adsorption kinetic results of the half life, time constant, best fitting model, and surface coverage

Multi-component Kinetics 2-Naphthoic Acid							
pH	CL*	t_{50}	τ_2	Model	q_e	q_m	$\theta = \dfrac{q_e}{q_m}$
4	400	134	193	PFO	98.2	190.6	0.52
4	228	288	464	PSO	167.6	190.6	0.88
4	114	420	657	PSO	191.8	190.6	1.01
7	400	224	365	PSO	91.7	162.2	0.57
7	228	291	468	PSO	126.2	162.2	0.78
7	114	465	721	PSO	154.6	162.2	0.95
8	400	217	355	PSO	92.6	165.8	0.56
8	228	326	520	PSO	127.2	165.8	0.77
8	114	398	625	PSO	136.7	165.8	0.82
9	400	227	370	PSO	91.8	217	0.42
9	228	305	489	PSO	124.2	217	0.57
9	114	410	643	PSO	166.7	217	0.77

*CL = carbon load (mg/L)

5.4.2. Diphenylacetic Acid Kinetics

The adsorption kinetics for diphenylacetic acid in mixture adheres best to the PSO model as shown in Table 5 - 18. From Figure 5 - 24, b, we see that the time constant increases with increasing surface coverage for pH 8 and 9, though this relationship appears not to hold for pH 4 and 7. Another major variation observed from the adsorption results can be seen in Figure 5 - 25, where we see that the time constant is sensitive to both pH and carbon loading. Interestingly the values of the time constant diverge for carbon loads 400 mg/L and 114 mg/L. These results are completely the opposite of what has been observed thus far. Typically larger carbon loadings resulted in reduced time constant values. This is not observed in Figure 5 - 25, as the lowest carbon loading for pH 9 has the smallest time constant.

a)   b)

Figure 5 - 24: Diphenylacetic acid multi-component results for time constant vs. Surface coverage; a) Single compound; b) Multi-component

Figure 5 - 25: Diphenylacetic acid multi-component time constant as a function of system pH
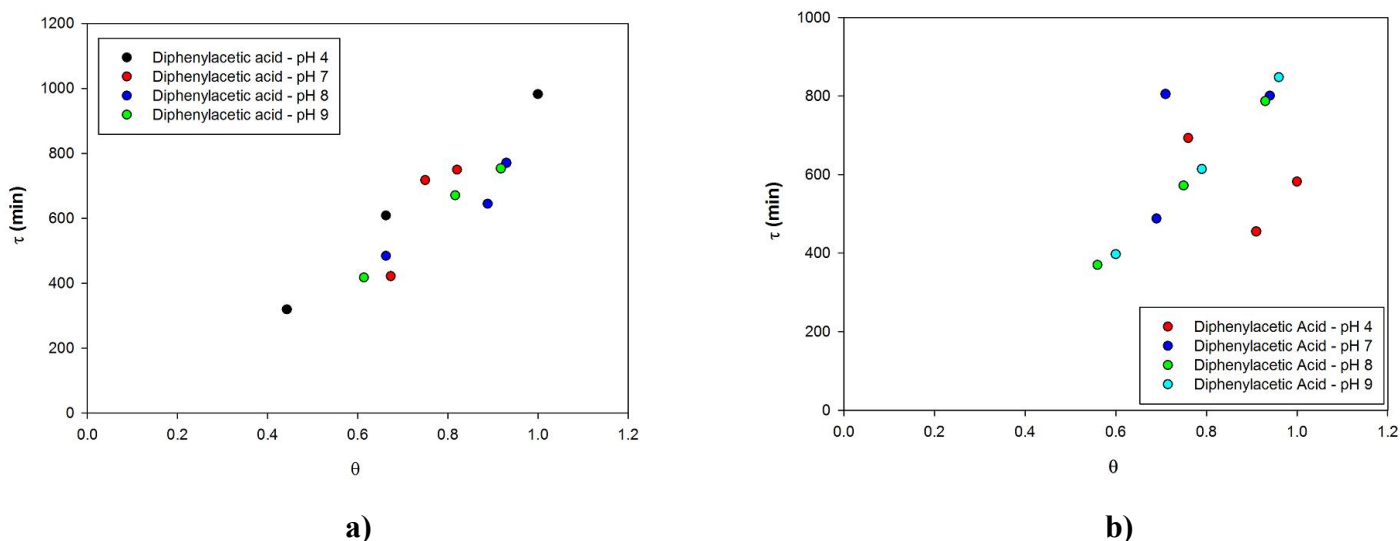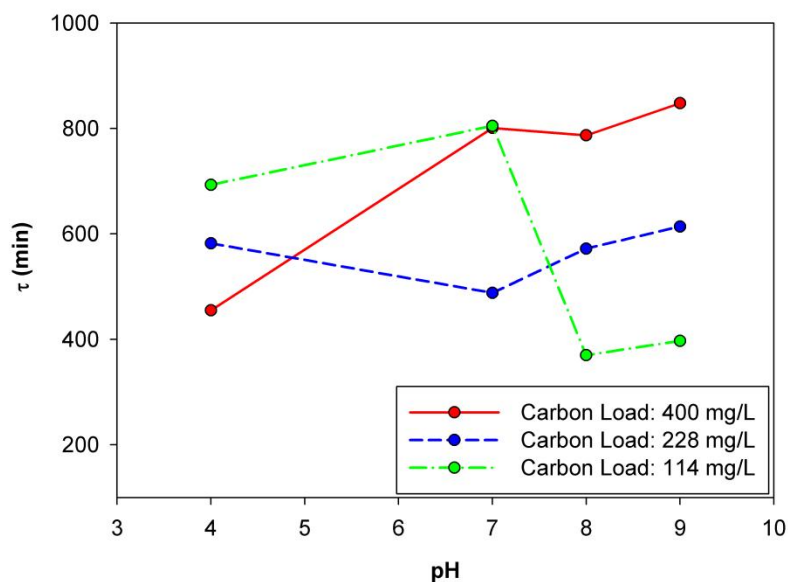
Table 5 - 18: Diphenylacetic acid multi-component adsorption kinetic results of the half life, time constant, best fitting model, and surface coverage

Multi-component Kinetics: Diphenylacetic Acid							
pH	CL*	t_{50}	τ_2	Model	q_e	q_m	$\theta = \dfrac{q_e}{q_m}$
4	400	282	455	PSO	97.2	107	0.91
4	228	368	582	PSO	106.7	107	1.00
4	114	445	693	PSO	81.4	107	0.76
7	400	523	801	PSO	45.3	48	0.94
7	228	304	488	PSO	33.2	48	0.69
7	114	526	805	PSO	34.3	48	0.71
8	400	513	787	PSO	48.3	52	0.93
8	228	361	572	PSO	38.8	52	0.75
8	114	227	370	PSO	29.3	52	0.56
9	400	557	848	PSO	47.1	49	0.96
9	228	390	614	PSO	38.6	49	0.79
9	114	275	397	PFO	29.4	49	0.60

*CL = carbon load (mg/L)

5.4.3. 1,4-Cyclohexanedicarboxylic Acid Kinetics

1,4-Cyclohexanedicarboxylic acid kinetic results for pH 7 to 9 could not be accurately fitted using PFO and PSO models. Only the kinetic runs at pH 4 could be accurately modeled by the PSO model as can be seen in Table 5 - 19. From these limited results we see that the time constant does not decrease with a decrease in the surface coverage fraction as has been the case for the other compounds.

Table 5 - 19: 1,4-Cyclohexanedicarboxylic acid multi-component adsorption kinetic results of the half life, time constant, best fitting model, and surface coverage

Multi-component Kinetics:					1,4-Cyclohexanedicarboxylic Acid		
pH	CL^1	t$_{50}$	τ_2	Model	q_e	q_m	$\theta = \dfrac{q_e}{q_m}$
4	400	176.0	290.5	PSO	56.5	67	0.84
4	228	85.5	144.1	PSO	64.8	67	0.97
4	114	19.6	33.5	PSO	61.8	67	0.92
7	400	*	*	*	*	*	*
7	228	*	*	*	*	*	*
7	114	*	*	*	*	*	*
8	400	*	*	*	*	*	*
8	228	*	*	*	*	*	*
8	114	*	*	*	*	*	*
9	400	*	*	*	*	*	*
9	228	*	*	*	*	*	*
9	114	*	*	*	*	*	*

1. CL = carbon load (mg/L)

* PFO or PSO kinetic model did not converge to a solution.

5.4.4. Summary of Multi-component Kinetics

For the multi-component kinetics it was found that the sensitivity of the time constant to pH for 2-naphthoic acid was minor, which was a similar finding with the pure compound adsorption. For diphenylacetic acid there was a marked change in sensitivity with pH and a reverse trend could be seen (i.e. lower carbon loading yielding larger time constants). Overall the time constants remained lower than those obtained for pure solution kinetics.

Chapter 6: Conclusions & Future Work

6.1. Conclusions

Activated carbon was a suitable adsorbent for the removal of naphthenic acids from water. Comparing the affinity of each model compound, under single solute adsorption conditions, the compounds were ranked from highest to lowest affinity as follows: 1,4-cyclohexanedicarboxylic acid > 2-naphthoic acid > diphenylacetic acid. Various isotherm models such as Langmuir, Fruendlich, and Langmuir-Freundlich were used to describe the equilibrium adsorption. Non-linear regression methods were best suited for parameter determination for the adsorption models used. For single compound adsorption, both the Freundlich and Langmuir-Freundlich models fitted the experimental data in all conditions. Both of these models account for the heterogeneous nature of the activated carbon and were thus more appropriate than the Langmuir model. The model compound affinity to the GAC changed under multi-component adsorption. In decreasing order, the model compound affinity to GAC was found to be: 2-naphthoic acid > diphenylacetic acid > 1,4-cyclohexanedicarboxylic acid. The disruption of cooperative adsorption for 1,4-cyclohexanedicarboxylic acid during competitive adsorption was proposed as the mechanism for the observed drop in its affinity.

The single solute isotherm results for 2-naphthoic acid and diphenylacetic acid were found to exhibit common isotherm curves, classified as H and L type, while 1,4-cyclohexanedicarboxylic acid exhibited a S type isotherm curve, consistent with cooperative adsorption. It was suggested that the Fowler-Guggenheim equation may best describe S type adsorption as it can exhibit a discontinuous vertical jump in its adsorption isotherm. The model accounts for lateral surface interactions between adsorbate molecules which is the underlying explanation for cooperative adsorption. For single solute isotherms it was found that the saturation capacity (q_m) decreased significantly with increasing pH; decreasing as the pH value approached the pH_{pzc}. This finding indicated that the positive surface charge at $pH < pH_{pzc}$, promoted anion adsorption. As the pH increased the surface charge decreased, which decreased the affinity of acid anions to the surface. For the single compound results it was observed that the time constant (time to reach 63% of the equilibrium adsorption) increased with surface coverage.

An overall decrease in adsorbent capacity for all three compounds was observed during multi-component adsorption. Similar to single compound adsorption, the adsorption capacity for the three compounds decreased with increasing pH, over the range of 4 to 7. The isotherms of diphenylacetic acid and 1,4-cyclohexanedicarboxylic acid exhibited local maxima in adsorption capacity, due to competitive adsorption. 2-Naphthoic acid did not exhibit any major changes in its adsorption profile in multi-component adsorption, maintaining either an H or L profile. Interestingly, for pH 9, 2-naphthoic acid showed an approximate increase in adsorption of 20% as compared to the single compound value. Additionally 1,4-cyclohexanedicarboxylic acid showed a significant increase in affinity to the activated carbon at pH 8 and 9 due to a shift towards cooperative adsorption. The overall adsorption capacity was found to decrease from pH 4 to 7 and shift from either L or H adsorption profile to a C profile for pH 8 and 9. The shift to pH 8 resulted in the maximum overall adsorption capacity. This finding is beneficial for NA removal from OSPW due to its alkaline pH, which would indicate that elevated adsorption capacities can be obtained under real operating conditions. Additionally the values of the time constants for multi-component adsorption as compared to single component adsorption were slightly smaller; indicating that the kinetic performance was not negatively impacted for multi-component adsorption.

A significant finding in this work was the cooperative adsorption observed for 1,4-cylohexanedicarboxylic acid which may corroborate the anomalous behavior observed in OSPW acid fraction adsorption observed by Small et al. (2012). Oxygenated NAs resulting from biodegradation with multiple carboxyl groups may be the cause of this isotherm profile. Additional complexity in modeling OSPW NA adsorption may result from NAs adhering to different isotherm profiles as was observed in this work. The resulting isotherm profile of the OSPW NAs may be a combination of multiple superimposed models.

6.2. Future Work

Future adsorption studies should include calorimetric measurements, as these are essential for model validation. They provide significant insight into the thermodynamics of adsorption which is required for any in depth study in the field. A stoichiometric pH adjustment using an appropriate buffer in the place of NaOH should be used in order to control pH throughout the adsorption experiments. Additionally further study with regards to the identification of functional groups, their energy of adsorption, the effects of pore size distribution, or other physical adsorbent properties could be performed.

The finding of cooperative adsorption for 1,4-cyclohexanedicarboxylic acid can be further explored. Other oxygenated naphthenic acids can be studied individually to see their respective adsorption profiles. These findings can then be compared to OSPW NA fraction adsorption. If cooperative adsorption is observed, as may have been by Small et al. (2012) then the structure of NAs can be alluded to. Analytical advances regarding OSPW composition should be coupled with adsorption studies which can help to confirm composition based on adsorption profiles as discussed by Gilles et al. (1960).

For the application of adsorption systems for OSPW remediation, more insight into the effect of other OSPW constituents on adsorption need to be investigated (e.g. total dissolved solids, metal ions, etc). Adsorbent fouling due to oil and metal hydroxides, bacteria, and natural occurring organic matter (NOM) which reduce adsorption capacity and kinetic performance needs to be studied. In addition, regeneration studies of the adsorbent should be conducted in order to determine the viability of selective removal of NAs.
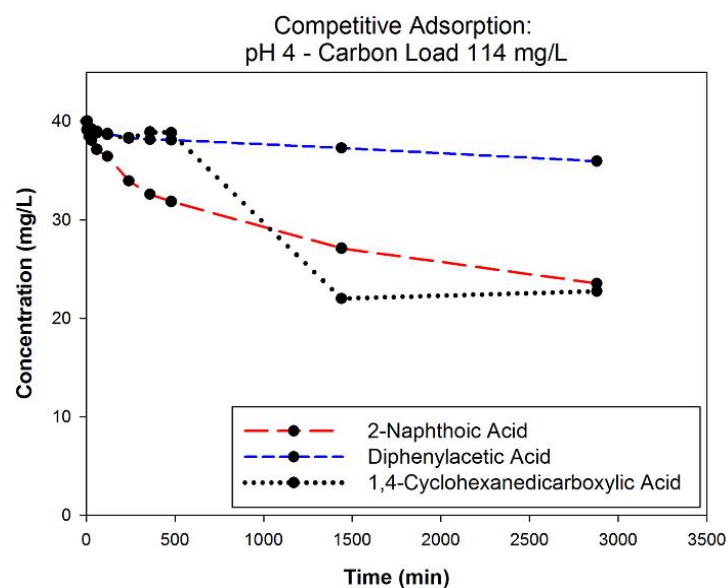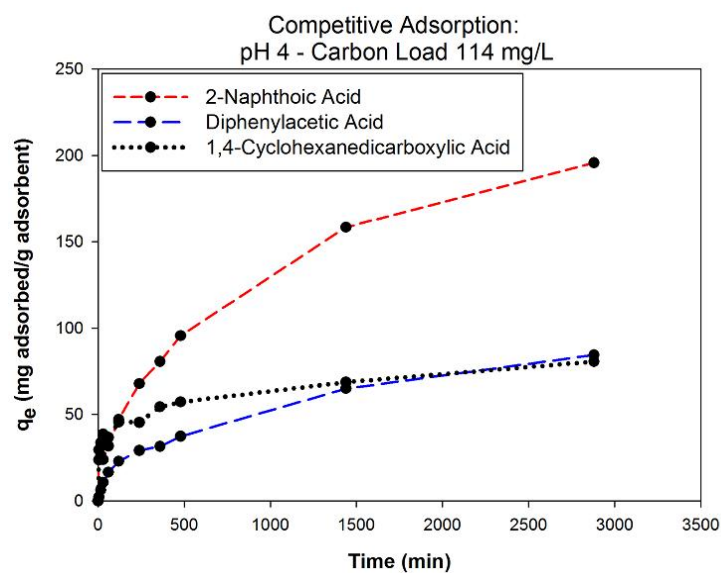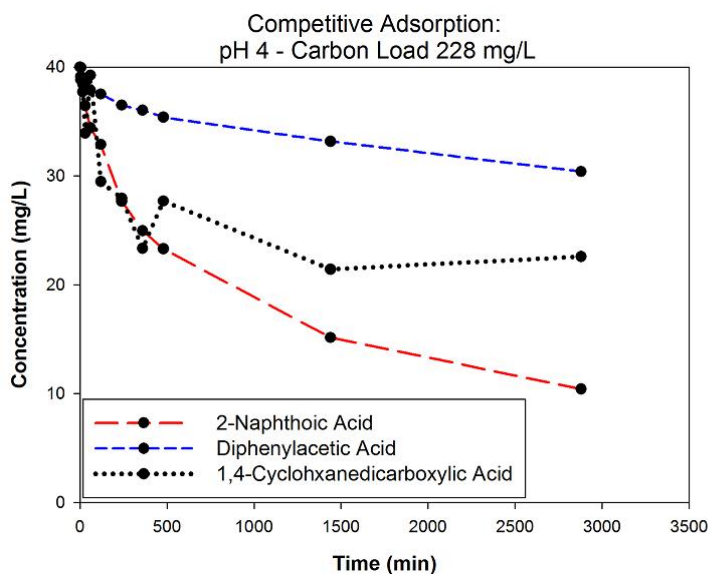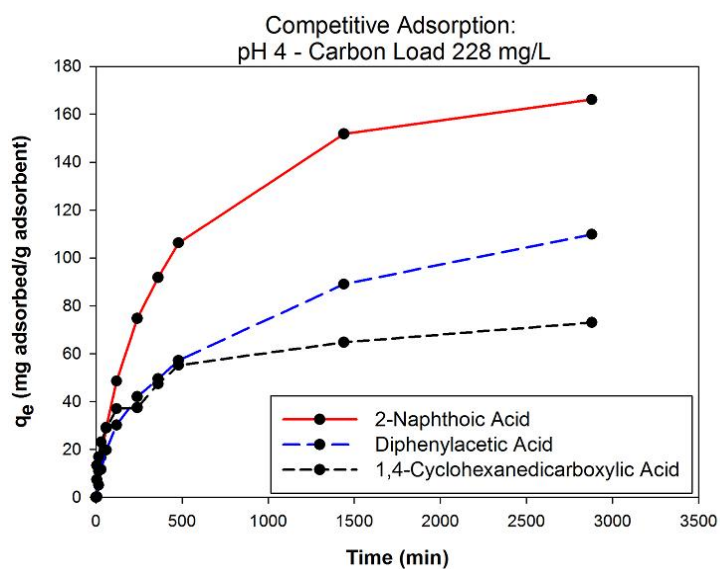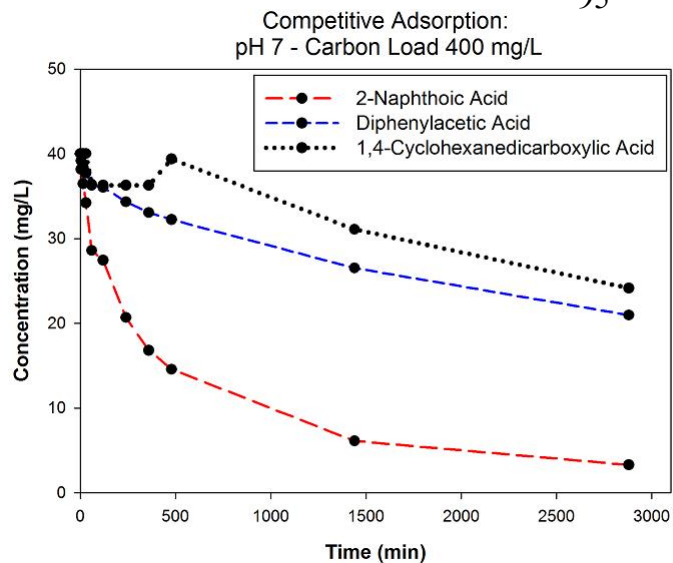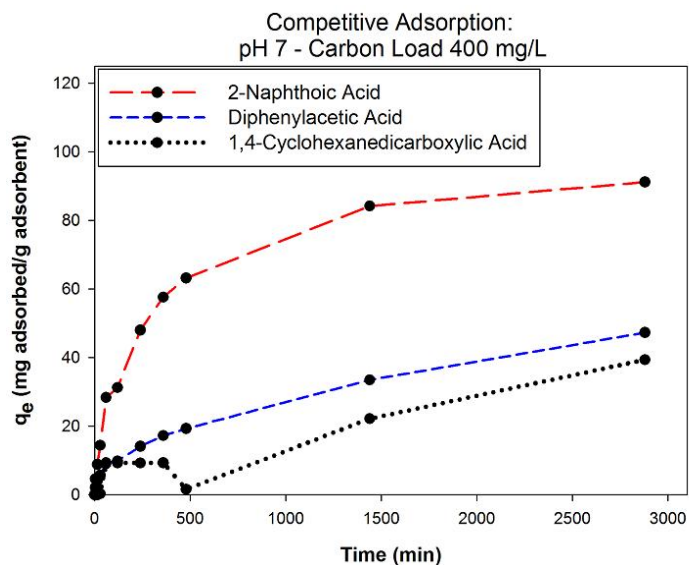
Appendix

Multi-component Kinetic Graphs

Figure A - 1: Multi-component adsorption pH 4

Figure A - 2: Multi-component adsorption pH 7

Figure A - 3: Multi-component adsorption pH 8

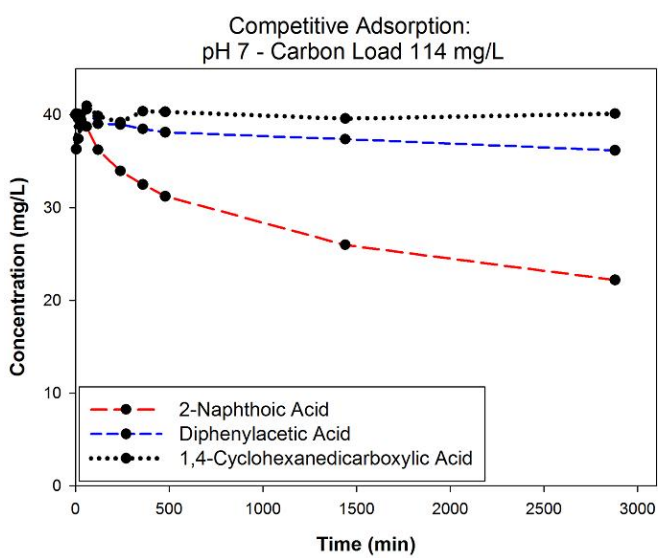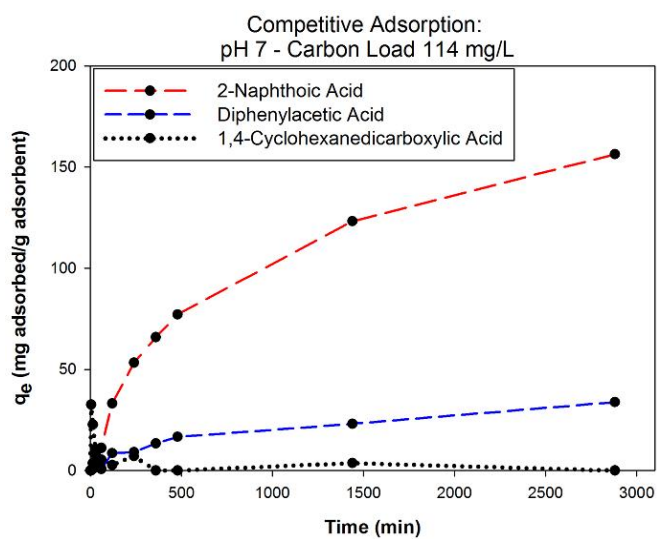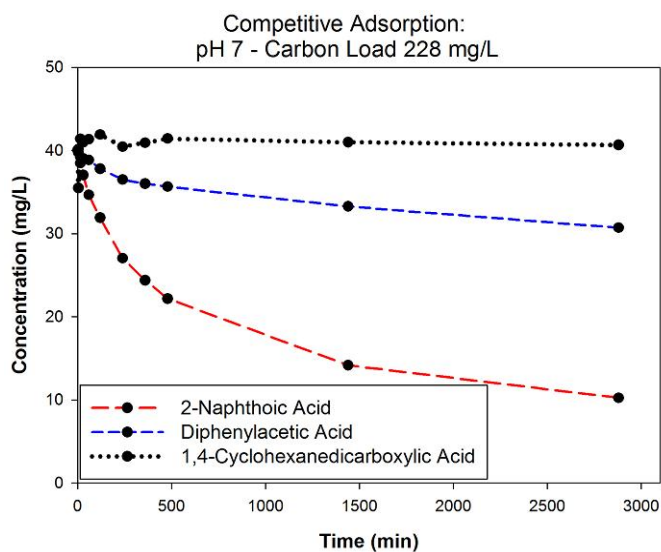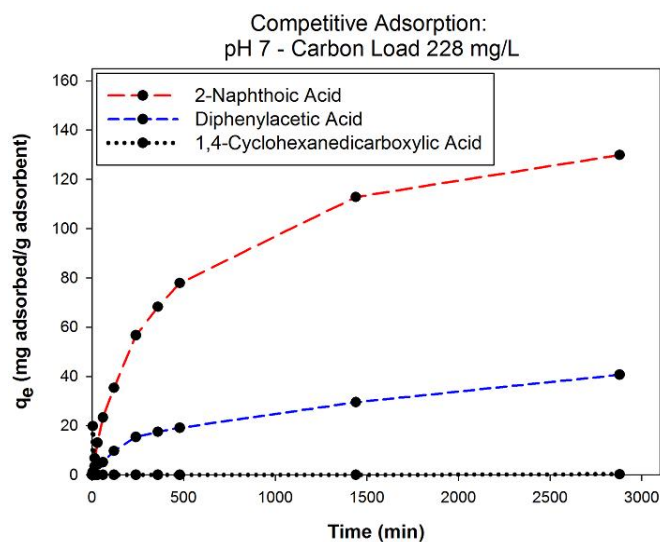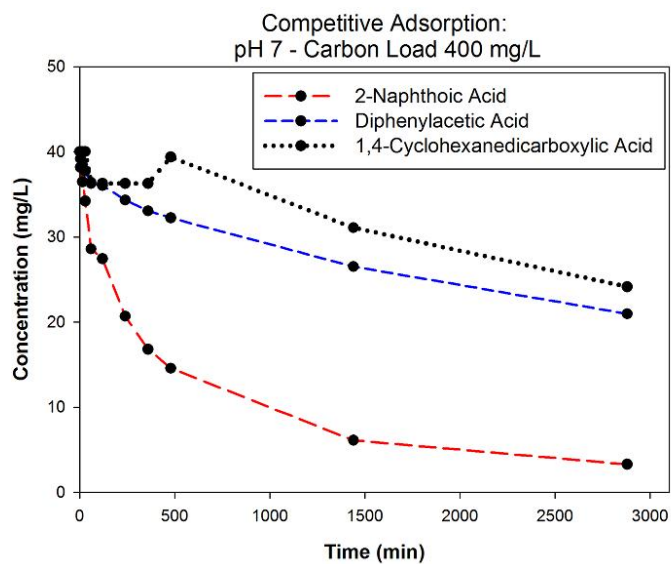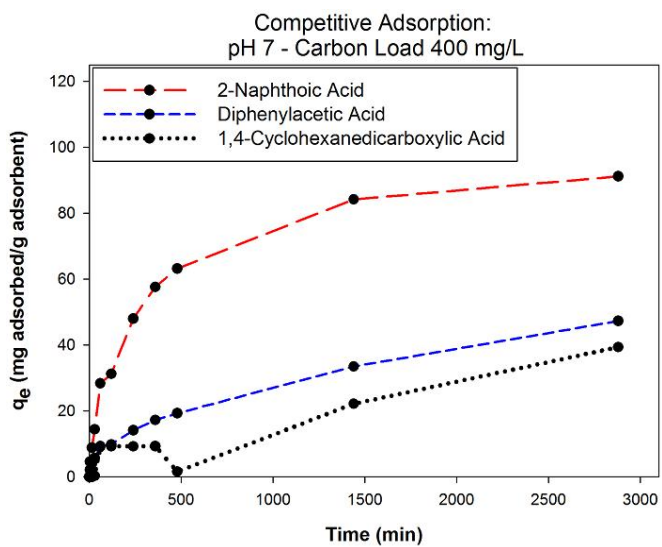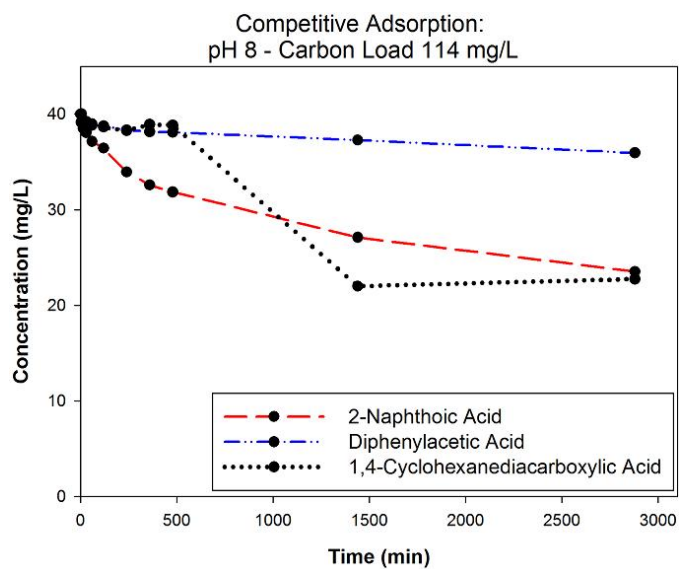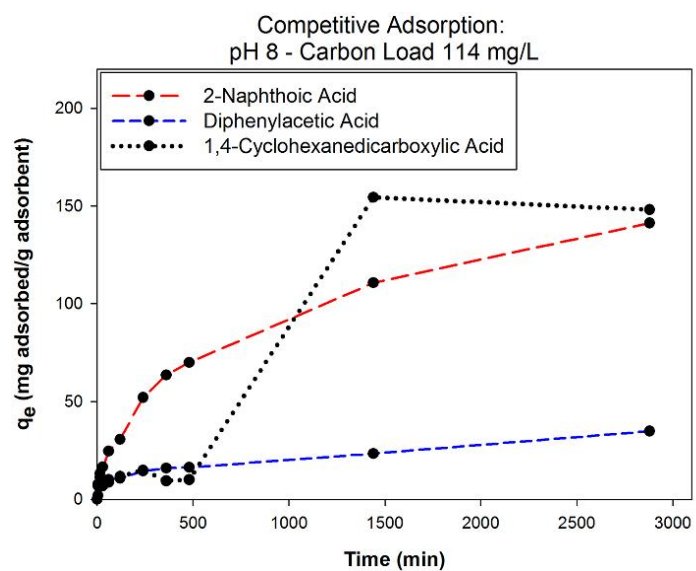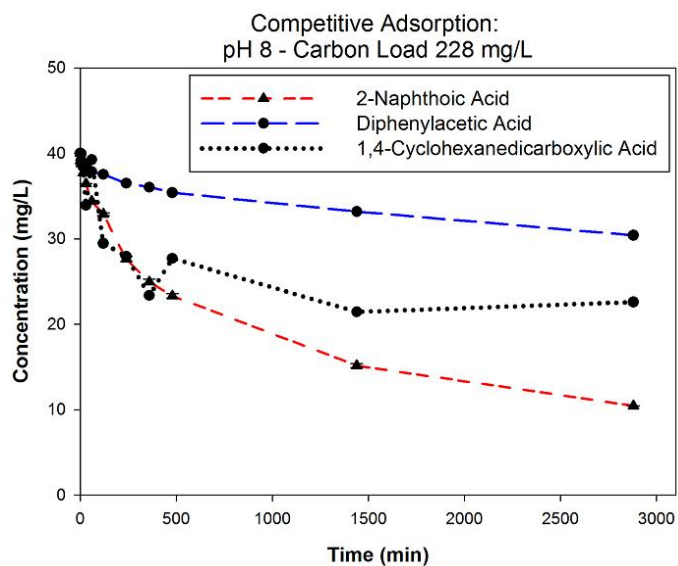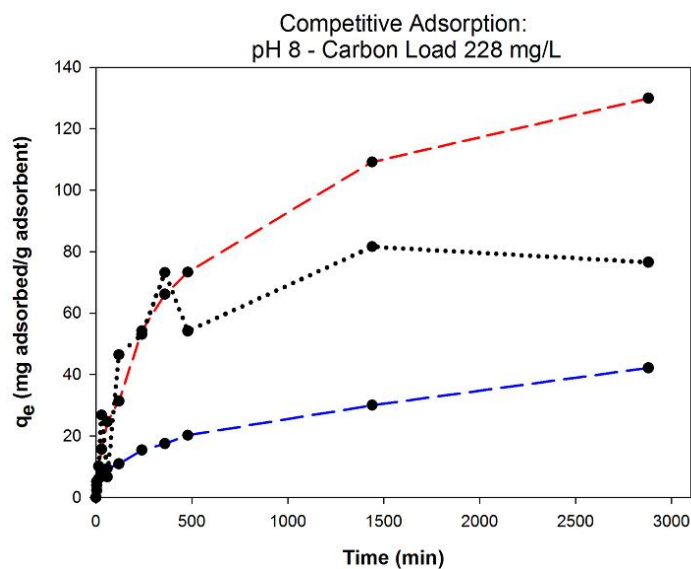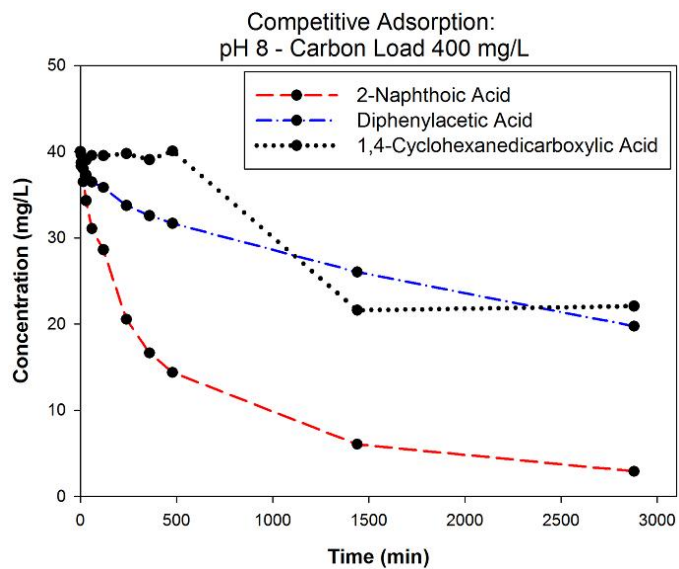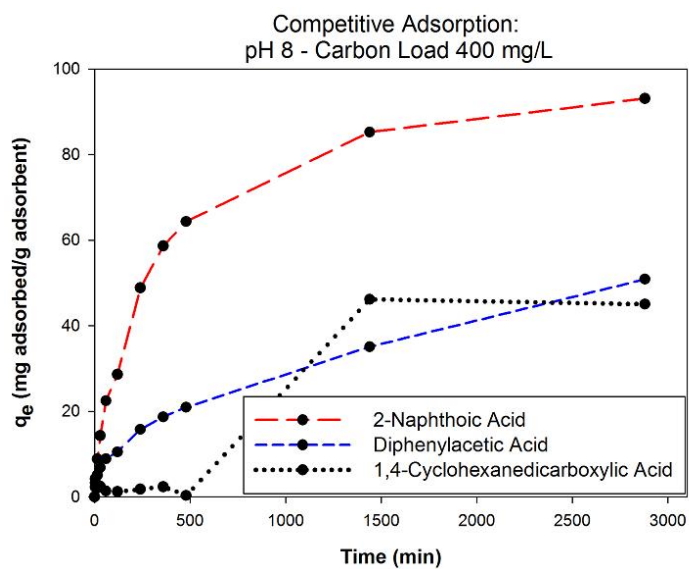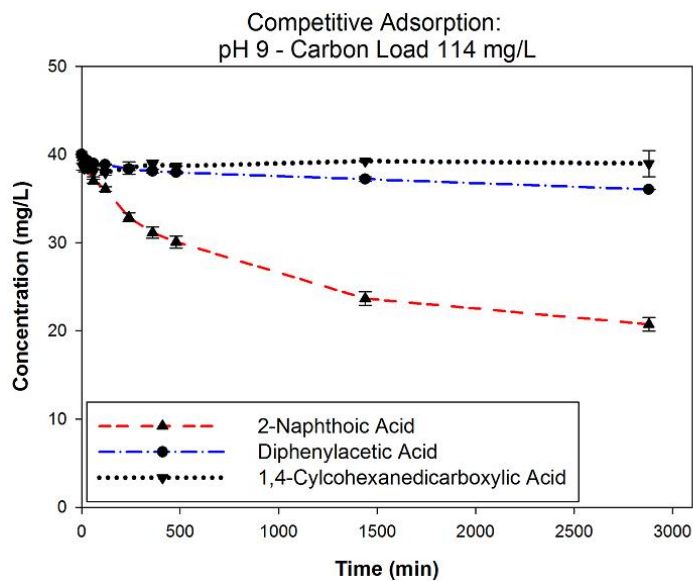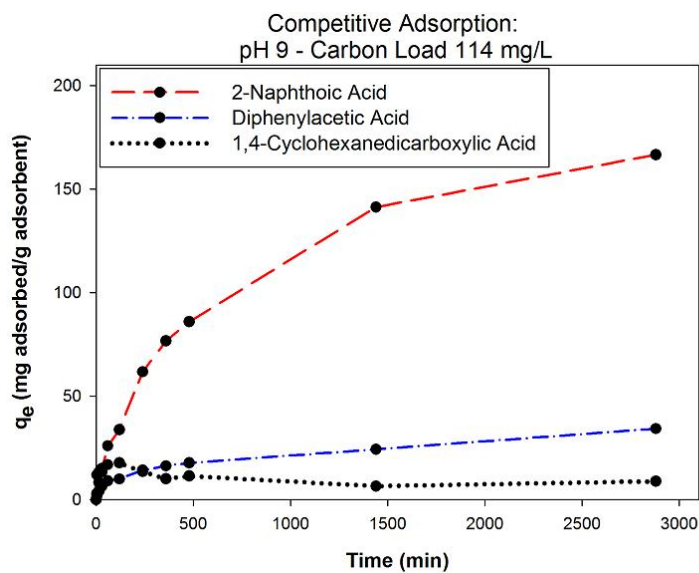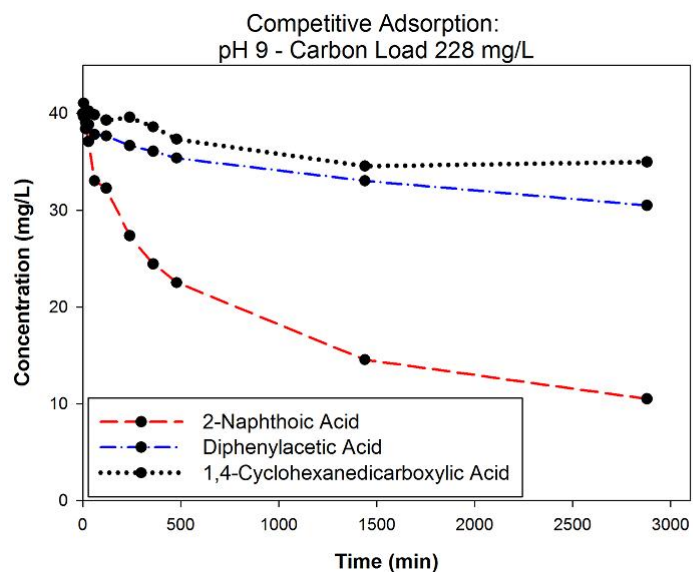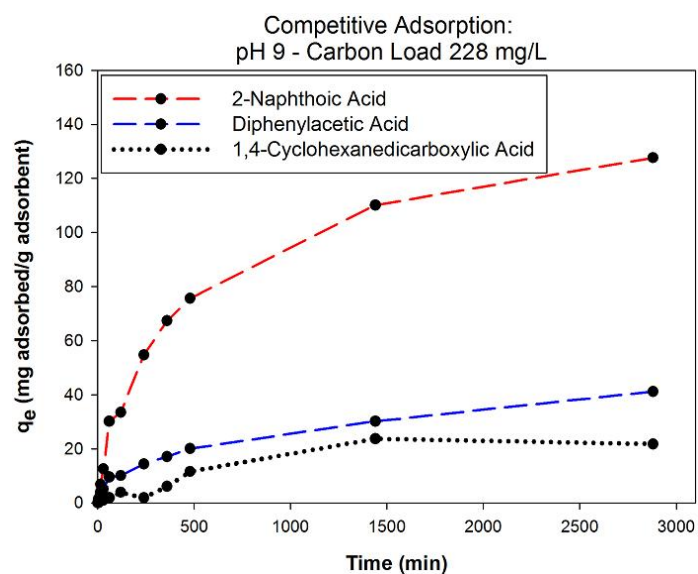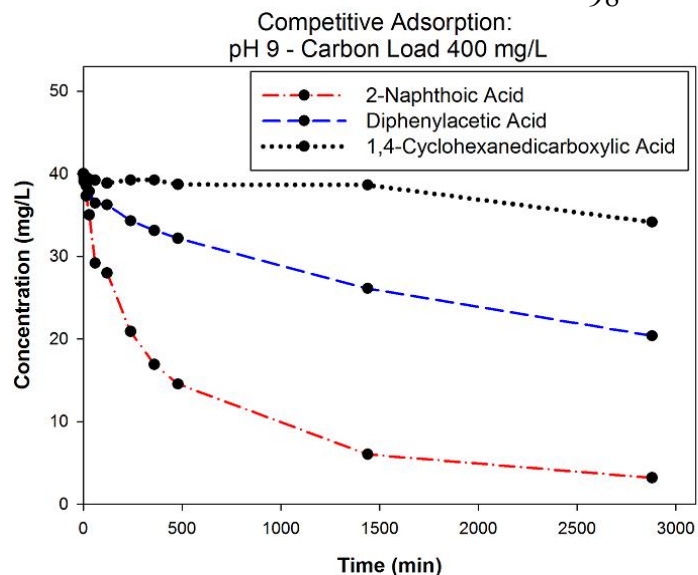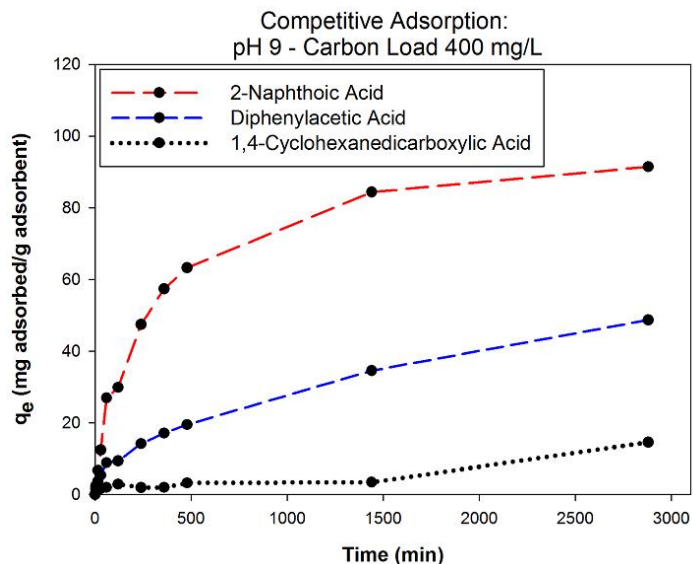**Figure A - 4: Multi-component adsorption pH 9**

References:

[1]   Canadian Association of Petroleum Producers, "Upstream Dialogue; The Facts On: Oil Sands," 2013.

[2]   J. Masliyah, Z. Zhou, and Z. Xu, "Understanding water based bitumen extraction from Athabasca oil sands," *Cnadian J. Chem. Eng.*, vol. 82, no. 4, pp. 628–654, 2004.

[3]   P. Birn, Kevin; Khanna, "A Discussion Paper On The Oil Sands: Challenges And Opportunities," Ottawa, Canada, 2010.

[4]   J. V Headley, K. M. Peru, M. H. Mohamed, R. a Frank, J. W. Martin, R. R. O. Hazewinkel, D. Humphries, N. P. Gurprasad, L. M. Hewitt, D. C. G. Muir, D. Lindeman, R. Strub, R. F. Young, D. M. Grewer, R. M. Whittal, P. M. Fedorak, D. a Birkholz, R. Hindle, R. Reisdorph, X. Wang, K. L. Kasperski, C. Hamilton, M. Woudneh, G. Wang, B. Loescher, A. Farwell, D. G. Dixon, M. Ross, a D. S. Pereira, E. King, M. P. Barrow, B. Fahlman, J. Bailey, D. W. McMartin, C. H. Borchers, C. H. Ryan, N. S. Toor, H. M. Gillis, L. Zuin, G. Bickerton, M. Mcmaster, E. Sverko, D. Shang, L. D. Wilson, and F. J. Wrona, "Chemical fingerprinting of naphthenic acids and oil sands process waters-A review of analytical methods for environmental samples.," *J. Environ. Sci. Health. A. Tox. Hazard. Subst. Environ. Eng.*, vol. 48, no. 10, pp. 1145–63, Jan. 2013.

[5]   D. W. Schindler, "Unravelling the complexity of pollution by the oil sands industry.," *Proc. Natl. Acad. Sci. U. S. A.*, vol. 111, no. 9, pp. 3209–10, Mar. 2014.

[6]   F. S. Azad, J. Abedi, and S. Iranmanesh, "Removal of naphthenic acids using adsorption process and the effect of the addition of salt.," *J. Environ. Sci. Health. A. Tox. Hazard. Subst. Environ. Eng.*, vol. 48, no. 13, pp. 1649–54, Jan. 2013.

[7]   F. M. Holowenko, M. D. MacKinnon, and P. M. Fedorak, "Methanogens and sulfate-reducing bacteria in oil sands fine tailings waste.," *Can. J. Microbiol.*, vol. 46, no. 10, pp. 927–37, Oct. 2000.

[8]   S. Solomon, D. Qi, M. Manning, M. Marquis, K. Averyt, M. M. B. Tignor, Z. Chen, and H. J. LeRoy Miller, "IPCC, 2007: Climate Change 2007: The Physical Science Basis," Cambridge, United Kingdom and New York, NY, USA, 2007.

[9]   Alberta Chamber of Resources, "Oil Sands Technology Roadmap: Unlocking The Potential," Edmonton, Alberta, 2004.

[10]   BGC Engineering Inc. & Norwest Corporation, "Oil Sands Tailings Technology Deployment Roadmap Project Report – Volume 2," Calgary, Alberta, 2012.

[11]   R. J. Chalaturnyk, J. Don Scott, and B. Özüm, "Management of Oil Sands Tailings," *Pet. Sci. Technol.*, vol. 20, no. 9–10, pp. 1025–1046, Jan. 2002.

[12] J. S. Clemente and P. M. Fedorak, "A review of the occurrence, analyses, toxicity, and biodegradation of naphthenic acids.," *Chemosphere*, vol. 60, no. 5, pp. 585–600, Jul. 2005.

[13] K. A. Clark and D. S. Pasternack, "Hot Water Separation of Bitumen from Alberta Bituminous Sand," *Ind. Eng. Chem.*, pp. 1410–1416, 1932.

[14] "Directive 074 : Tailings Performance Criteria and Requirements for Oil Sands Mining Schemes Directive 074," Calgary, Alberta, 2009.

[15] E. W. Allen, "Process water treatment in Canada's oil sands industry: II. A review of emerging technologies," *J. Environ. Eng. Sci.*, vol. 7, no. 5, pp. 499–524, Sep. 2008.

[16] Y. J. Kim, "Canada ' s Oil Sands : Strategic Decisions to Make Canada an Energy Superpower by," University of Waterloo, 2010.

[17] W. Zubot, M. D. MacKinnon, P. Chelme-Ayala, D. W. Smith, and M. Gamal El-Din, "Petroleum coke adsorption as a water management option for oil sands process-affected water.," *Sci. Total Environ.*, vol. 427–428, pp. 364–72, Jun. 2012.

[18] R. M. R. Zamora, R. Schouwenaars, A. D. Moreno, and G. Buitrón, "Production of activated carbon from petroleum coke and its application in water treatment for the removal of metals and phenol," *Water Sci. Technol.*, vol. 42, pp. 119–126, 2000.

[19] C. C. Small, A. C. Ulrich, and Z. Hashisho, "Adsorption of Acid Extractable Oil Sands Tailings Organics onto Raw and Activated Oil Sands Coke," *J. Environ. Eng.*, vol. 138, no. August, pp. 833–840, 2012.

[20] B. Sarkar, "Adsorption of Single-ring Model Naphthenic Acid from Oil Sands Tailings Pond Water Using Petroleum Coke-Derived Activated Carbon," 2013.

[21] M. Yuan, S. Tong, S. Zhao, and C. Q. Jia, "Adsorption of polycyclic aromatic hydrocarbons from water using petroleum coke-derived porous carbon.," *J. Hazard. Mater.*, vol. 181, no. 1–3, pp. 1115–20, Sep. 2010.

[22] M. Gamal El-Din, H. Fu, N. Wang, P. Chelme-Ayala, L. Pérez-Estrada, P. Drzewicz, J. W. Martin, W. Zubot, and D. W. Smith, "Naphthenic acids speciation and removal during petroleum-coke adsorption and ozonation of oil sands process-affected water.," *Sci. Total Environ.*, vol. 409, no. 23, pp. 5119–25, Nov. 2011.

[23] E. W. Allen, "Process water treatment in Canada's oil sands industry: I. Target pollutants and treatment objectives," *J. Environ. Eng. Sci.*, vol. 7, no. 2, pp. 123–138, Mar. 2008.

[24] M. R. van den Heuvel, M. Power, M. D. MacKinnon, T. Van Meer, E. P. Dobson, and D. G. Dixon, "Effects of oil sands related aquatic reclamation on yellow perch (Perca flavescens). I. Water quality characteristics and yellow perch physiological and population responses," *Can. J. Fish. Aquat. Sci.*, vol. 56, no. 7, pp. 1213–1225, Jul. 1999.

[25] R. a Frank, K. Fischer, R. Kavanagh, B. K. Burnison, G. Arsenault, J. V Headley, K. M. Peru, G. Van Der Kraak, and K. R. Solomon, "Effect of carboxylic acid content on the acute toxicity of oil sands naphthenic acids.," *Environ. Sci. Technol.*, vol. 43, no. 2, pp. 266–71, Jan. 2009.

[26] V. V Rogers, M. Wickstrom, K. Liber, and M. D. MacKinnon, "Acute and subchronic mammalian toxicity of naphthenic acids from oil sands tailings.," *Toxicol. Sci.*, vol. 66, no. 2, pp. 347–55, Apr. 2002.

[27] D. M. Grewer, R. F. Young, R. M. Whittal, and P. M. Fedorak, "Naphthenic acids and other acid-extractables in water samples from Alberta: what is being measured?," *Sci. Total Environ.*, vol. 408, no. 23, pp. 5997–6010, Nov. 2010.

[28] J. A. Brient, P. J. Wessner, and M. N. Doyle, "Naphthenic acids," *Kirk-Othmer Encyclopedia of Chemical Technology*. John Wiley & Sons, pp. 1–10, 1955.

[29] M. P. Barrow, L. A. Mcdonnell, X. Feng, J. Walker, and P. J. Derrick, "Determination of the Nature of Naphthenic Acids Present in Crude Oils Using Nanospray Fourier Transform Ion Cyclotron Resonance Mass Spectrometry : The Continued Battle Against Corrosion," *Anal. Chem.*, vol. 75, no. 4, pp. 860–866, 2003.

[30] R. Hindle, M. Noestheden, K. Peru, and J. Headley, "Quantitative analysis of naphthenic acids in water by liquid chromatography-accurate mass time-of-flight mass spectrometry.," *J. Chromatogr. A*, vol. 1286, pp. 166–74, Apr. 2013.

[31] J. V. Headley, K. M. Peru, B. Fahlman, A. Colodey, and D. W. McMartin, "Selective solvent extraction and characterization of the acid extractable fraction of Athabasca oils sands process waters by Orbitrap mass spectrometry," *Int. J. Mass Spectrom.*, vol. 345–347, pp. 104–108, Jul. 2013.

[32] C. E. West, A. G. Scarlett, J. Pureveen, E. W. Tegelaar, and S. J. Rowland, "Abundant naphthenic acids in oil sands process-affected water: studies by synthesis, derivatisation and two-dimensional gas chromatography/high-resolution mass spectrometry.," *Rapid Commun. Mass Spectrom.*, vol. 27, no. 2, pp. 357–65, Jan. 2013.

[33] J. V Headley, M. P. Barrow, K. M. Peru, B. Fahlman, R. a Frank, G. Bickerton, M. E. McMaster, J. Parrott, and L. M. Hewitt, "Preliminary fingerprinting of Athabasca oil sands polar organics in environmental samples using electrospray ionization Fourier transform ion cyclotron resonance mass spectrometry.," *Rapid Commun. Mass Spectrom.*, vol. 25, no. 13, pp. 1899–909, Jul. 2011.

[34] M. P. Barrow, M. Witt, J. V Headley, and K. M. Peru, "Athabasca oil sands process water: characterization by atmospheric pressure photoionization and electrospray ionization fourier transform ion cyclotron resonance mass spectrometry.," *Anal. Chem.*, vol. 82, no. 9, pp. 3727–35, May 2010.

[35] B. Zhao, R. Currie, and H. Mian, "Catalogue of Analytical Methods for Naphthenic Acids Related to Oil Sands Operations," 2012.

[36] J. V Headley and M. P. Barrow, "Mass Spectrometric Characterization Of Naphthenic Acids In Environmental Samples: A Review," *Mass Spectrom. Rev.*, no. 28, pp. 121–134, 2009.

[37] K. Qian, W. K. Robbins, C. a. Hughey, H. J. Cooper, R. P. Rodgers, and A. G. Marshall, "Resolution and Identification of Elemental Compositions for More than 3000 Crude Acids in Heavy Petroleum by Negative-Ion Microelectrospray High-Field Fourier Transform Ion Cyclotron Resonance Mass Spectrometry," *Energy & Fuels*, vol. 15, no. 6, pp. 1505–1511, Nov. 2001.

[38] E. K. Quagraine, H. G. Peterson, and J. V. Headley, "In Situ Bioremediation of Naphthenic Acids Contaminated Tailing Pond Waters in the Athabasca Oil Sands Region—Demonstrated Field Studies and Plausible Options: A Review," *J. Environ. Sci. Heal. Part A*, vol. 40, no. 3, pp. 685–722, Jan. 2005.

[39] A. C. Scott, M. D. MacKinnon, and P. M. Fedorak, "Naphthenic acids in athabasca oil sands tailings waters are less biodegradable than commercial naphthenic acids.," *Environ. Sci. Technol.*, vol. 39, no. 21, pp. 8388–94, Nov. 2005.

[40] R. A. Frank, "Naphthenic acids: identification of structural properties that influence acute toxicity," The University of Guelph, 2008.

[41] A. Zhang, Q. Ma, K. Wang, Y. Tang, and W. A. Goddard, "Improved Processes to Remove Naphthenic Acids," Pasadena, 2005.

[42] B. Wang, Y. Wan, Y. Gao, M. Yang, and J. Hu, "Determination and characterization of oxy-naphthenic acids in oilfield wastewater.," *Environ. Sci. Technol.*, vol. 47, no. 16, pp. 9545–54, Aug. 2013.

[43] C. Leishman, E. E. Widdup, D. M. Quesnel, G. Chua, L. M. Gieg, M. a Samuel, and D. G. Muench, "The effect of oil sands process-affected water and naphthenic acids on the germination and development of Arabidopsis.," *Chemosphere*, vol. 93, no. 2, pp. 380–7, Oct. 2013.

[44] T.-W. Yen, W. P. Marsh, M. D. MacKinnon, and P. M. Fedorak, "Measuring naphthenic acids concentrations in aqueous environmental samples by liquid chromatography," *J. Chromatogr. A*, vol. 1033, no. 1, pp. 83–90, Apr. 2004.

[45] D. Jones, A. G. Scarlett, C. E. West, and S. J. Rowland, "Toxicity of individual naphthenic acids to Vibrio fischeri.," *Environ. Sci. Technol.*, vol. 45, no. 22, pp. 9776–82, Nov. 2011.

[46] M. Nodwell, "On the Interactions between Naphthenic Acids and Inorganic Minerals," The University of British Columbia, 2011.

[47] S. J. Rowland, A. G. Scarlett, D. Jones, C. E. West, and R. a Frank, "Diamonds in the rough: identification of individual naphthenic acids in oil sands process water.," *Environ. Sci. Technol.*, vol. 45, no. 7, pp. 3154–9, Apr. 2011.

[48]   J. Peng, J. V Headley, and S. L. Barbour, "Adsorption of single-ring model naphthenic acids on soils," *NRC Res. Press*, vol. 1426, pp. 1419–1426, 2002.

[49]   N. A. Lange, *Lange's Handbook of Chemistry*. McGraw-Hill Inc.,US, 1979.

[50]   V. V Rogers, K. Liber, and M. D. MacKinnon, "Isolation and characterization of naphthenic acids from Athabasca oil sands tailings pond water.," *Chemosphere*, vol. 48, no. 5, pp. 519–27, Aug. 2002.

[51]   M. H. Mohamed, L. D. Wilson, J. V Headley, and K. M. Peru, "Screening of oil sands naphthenic acids by UV-Vis absorption and fluorescence emission spectrophotometry.," *J. Environ. Sci. Health. A. Tox. Hazard. Subst. Environ. Eng.*, vol. 43, no. 14, pp. 1700–5, Dec. 2008.

[52]   M. R. van den Heuvel, M. Power, J. Richards, M. MacKinnon, and D. G. Dixon, "Disease and gill lesions in yellow perch (Perca flavescens) exposed to oil sands mining-associated waters.," *Ecotoxicol. Environ. Saf.*, vol. 46, no. 3, pp. 334–41, Jul. 2000.

[53]   K. V Thomas, K. Langford, K. Petersen, a J. Smith, and K. E. Tollefsen, "Effect-directed identification of naphthenic acids as important in vitro xeno-estrogens and anti-androgens in North sea offshore produced water discharges.," *Environ. Sci. Technol.*, vol. 43, no. 21, pp. 8066–71, Nov. 2009.

[54]   L. E. Peters, M. MacKinnon, T. Van Meer, M. R. van den Heuvel, and D. G. Dixon, "Effects of oil sands process-affected waters and naphthenic acids on yellow perch (Perca flavescens) and Japanese medaka (Orizias latipes) embryonic development.," *Chemosphere*, vol. 67, no. 11, pp. 2177–83, May 2007.

[55]   C. Leishman, E. Widdup, D. Quesnel, G. Chua, L. M. Gieg, M. A. Samuel, and D. G. Muench, "The effect of oil sands process-affected water and naphthenic acids on the germination and development of Arabidopsis," *Chemosphere*, vol. 93, no. 2, pp. 380–7, Oct. 2013.

[56]   S. J. Rowland, C. E. West, D. Jones, A. G. Scarlett, R. a Frank, and L. M. Hewitt, "Steroidal aromatic 'naphthenic acids' in oil sands process-affected water: structural comparisons with environmental estrogens.," *Environ. Sci. Technol.*, vol. 45, no. 22, pp. 9806–15, Nov. 2011.

[57]   B. J. . Fuhr, D. E. Rose, and D. . Taplin, "Catalogue of Technologies for Reducing the Environmental Impact of Fine Tailings from Oil Sand Processing," 1993.

[58]   T. Simieritsch, J. Obad, and S. Dyer, "Tailings Plan Review — An Assessment of Oil Sands Company Submissions for Compliance with ERCB Directive 074: Tailings Performance Criteria and Requirements for Oil Sands Mining Schemes," Drayton valley, Alberta, 2009.

[59]   A. Janfada, "A Laboratory Evaluation Of The Sorption Of Oil Sands Naphthenic Acids On Soils," University of Saskatchewan, 2007.

[60] A. Janfada, J. V Headley, K. M. Peru, and S. L. Barbour, "A laboratory evaluation of the sorption of oil sands naphthenic acids on organic rich soils.," *J. Environ. Sci. Health. A. Tox. Hazard. Subst. Environ. Eng.*, vol. 41, no. 6, pp. 985–97, Jan. 2006.

[61] N. Adhoum and L. Monser, "Removal of phthalate on modified activated carbon: application to the treatment of industrial wastewater," *Sep. Purif. Technol.*, no. 38, pp. 233–239, 2004.

[62] J. H. Kwon and L. D. Wilson, "Surface-modified activated carbon with β-cyclodextrin-Part II. Adsorption properties.," *J. Environ. Sci. Health. A. Tox. Hazard. Subst. Environ. Eng.*, vol. 45, no. 13, pp. 1793–803, Nov. 2010.

[63] B. Dalmacija, E. Karlovic, Z. Tamas, and D. Miskovic, "Purification of high-salinity wastewater by activated sludge process," *Water Res.*, vol. 30, no. 2, pp. 295–298, 1996.

[64] D. Gallup, E. Isacoff, and D. Smith, "Use of Ambersorb® carbonaceous adsorbent for removal of BTEX compounds from oil field produced water," *Environ. Prog.*, vol. 15, no. 3, pp. 197–203, 1996.

[65] Y. Aldegs, M. Elbarghouthi, A. Elsheikh, and G. Walker, "Effect of Solution pH, Ionic Strength, and Temperature on Adsorption Behavior of Reactive Dyes on Activated Carbon," *Dye. Pigment.*, vol. 77, no. 1, pp. 16–23, 2008.

[66] D. Schimmel, K. C. Fagnani, J. B. O. Santos, M. A. S. D. Barros, and E. A. Silva, "Adsorption of Turquoise Blue QG Reactive Dye on Commercial Activated Carbon in a Batch Reactor: Kinetic and Equilibrium Studies," *Brazilian J. Chem. Eng.*, vol. 27, no. 02, pp. 289–298, 2010.

[67] O. Hamdaoui and E. Naffrechoux, "Modeling of adsorption isotherms of phenol and chlorophenols onto granular activated carbon. Part I. Two-parameter models and equations allowing determination of thermodynamic parameters.," *J. Hazard. Mater.*, vol. 147, no. 1–2, pp. 381–94, Aug. 2007.

[68] H. . Boehm, "Surface Oxides on Carbon and their Analysis: A critical Assessment," *Carbon N. Y.*, vol. 40, no. 2, pp. 145–149, Feb. 2002.

[69] G. Muller, C. J. Radke, and J. M. Prausnitz, "Adsorption of Weak Organic Electrolytes from Aqueous Solution on Activated Carbon. Effect of pH," *J. Phys. Chem.*, vol. 84, no. 4, pp. 369–376, 1980.

[70] J. Rivera-Utrilla, I. Bautista-Toledo, M. A. Ferro-Garcia, and C. Moreno-Castilla, "Activated carbon surface modifications by adsorption of bacteria and their effect on aqueous lead adsorption," *J. Chem. Technol. Biotechnol.*, vol. 76, no. 12, pp. 1209–1215, Dec. 2001.

[71] G. Newcombea, R. Hayes, and M. Drikas, "Granular activated carbon: importance of surface properties in the adsorption of naturally occurring organics," *Coilloids Surfaces A Physicochem. Eng. Asp.*, vol. 78, pp. 65–71, 1993.

[72] C. H. Giles, D. Smith, and A. Huitson, "A general treatment and classification of the solute adsorption isotherm. I. Theoretical," *J. Colloid Interface Sci.*, vol. 47, no. 3, pp. 755–765, Jun. 1974.

[73] C. Tien, *Adsorption Calculations and Modeling*. Newton: Butterworth-Heinemann, 1994.

[74] C. H. Giles, T. H. MacEwan, S. N. Nakhwa, and D. Smith, "Studies in Adsorption. Part XI.* A System of Classification of Solution Adsorption Isotherms, and its Use in Diagnosis of Adsorption Mechanisms and in Measurement of Specific Surface Areas of Solids.," *J. Chem. Soc.*, pp. 3973–3993, 1960.

[75] G. Limousin, J.-P. Gaudet, L. Charlet, S. Szenknect, V. Barthès, and M. Krimissa, "Sorption isotherms: A review on physical bases, modeling and measurement," *Appl. Geochemistry*, vol. 22, no. 2, pp. 249–275, Feb. 2007.

[76] K. Y. Foo and B. H. Hameed, "Insights into the modeling of adsorption isotherm systems," *Chem. Eng. J.*, vol. 156, no. 1, pp. 2–10, Jan. 2010.

[77] B. Boulinguiez, P. Le Cloirec, and D. Wolbert, "Revisiting the Determination of Langmuir Parameters - Application to Tetrahydrothiophene Adsorption Onto Activated Carbon," *Langmuir*, vol. 24, no. 13, pp. 6420–6424, Jun. 2008.

[78] D. D. Do, *Adsorption Analysis: Equilibria and Kinetics*. London: Imperial College Press, 1998, pp. 26–31.

[79] W. Plazinski, W. Rudzinski, and A. Plazinska, "Theoretical models of sorption kinetics including a surface reaction mechanism: a review.," *Adv. Colloid Interface Sci.*, vol. 152, no. 1–2, pp. 2–13, Nov. 2009.

[80] R.-L. Tseng, F.-C. Wu, and R.-S. Juang, "Characteristics and applications of the Lagergren's first-order equation for adsorption kinetics," *J. Taiwan Inst. Chem. Eng.*, vol. 41, no. 6, pp. 661–669, Nov. 2010.

[81] S. Azizian, "Kinetic Models of Sorption: A Theoretical Analysis," *J. Colloid Interface Sci.*, vol. 276, no. 1, pp. 47–52, Aug. 2004.

[82] G. Blanchard, M. Maunaye, and G. Martin, "Removal of Heavy Metals from Waters by Means of Natural Zeolites," *Water Res.*, vol. 18, no. 12, pp. 1501–1507, 1984.

[83] B. Noroozi and G. A. Sorial, "Applicable models for multi-component adsorption of dyes: A review," *J. Environ. Sci.*, vol. 25, no. 3, pp. 419–429, Mar. 2013.

[84] Y.-S. Kim, Y. Choi, and W. Lee, "Extraction Equilibria and Solvent Sublation for Determination of Ultra Trace Bi(III), In(III) and Tl(III) in Water Samples by Ion-Pairs of Metal-2-Naphthoate Complexes and Tetrabutylammonium Ion," *Bull. Chem. SOC.*, vol. 23, no. 10, pp. 1381–1388, 2002.

[85]   A. M. Brown, "A Step-by-Step Guide to Non-Linear Regression Analysis of Experimental Data Using a Microsoft Excel Spreadsheet.," *Comput. Methods Programs Biomed.*, vol. 65, no. 3, pp. 191–200, Jun. 2001.

[86]   Y.-S. Ho, "Selection of Optimum Sorption Isotherm," *Carbon N. Y.*, vol. 42, no. 10, pp. 2115–2116, 2004.

[87]   Y. Al-Degs, M. A. M. Khraisheh, S. J. Allen, and M. N. Ahmad, "Effect Of Carbon Surface Chemistry On The Removal Of Reactive Dyes From Textile," *Pergamon*, vol. 34, no. 3, pp. 927–935, 2000.

Curriculum Vitae

Name:	Alfredo Martinez Iglesias

Post-secondary Education and Degrees:

John Abbott College
Pure and Applied Sciences & Certificate in Environmental Studies
Montréal, Québec, Canada
2005-2007, DCS

Concordia University
Bachelor of Mechanical Engineering
Specialization in Thermo-fluid and Propulsion
Montréal, Québec, Canada
2008-2012

The University of Western Ontario
Masters of Chemical Engineering
London, Ontario, Canada
2012-2014

Honours and Awards:

Dean's List Faculty of Engineering at Concordia University
2011-2012
NSERC Undergraduate Research Award
2012
NSERC Undergraduate Research Award
2011

Publications:

E. Farvardin, M. Johnson, H. Alaee, A. Martinez, and A. Dolatabadi. "Comparative Study of Biodiesel and Diesel Jets in Gaseous Crossflow." Journal of Propulsion and Power, (2013).

Presentations:

A. Martinez Iglesias*, H. Seyedy Niasar, M. Ray, C. Xu; "Adsorption of Naphthenic Acids from Synthetic Oil Sands Tailings Water"; Poster presented at Western Research Bridges conference, London, Canada, 2014. Awarded 2nd place: for best presentation.

A. Martinez Iglesias*, D. Li, M. Siriwardhana, C. Lira, F. Berruti, C. Briens;"Upgrading & Separation of Pyrolysis Bio-oils for Integration with Petroleum Fuels"; Poster presented at the Annual General Meeting of BioFuelNet, Montreal, Canada, 2013.